UNDERSTANDING THE MECHANISM OF mTOR INHIBITION IN HUMAN HERPES VIRUS-8 ASSOCIATED MALIGNANCIES

Debasmita Roy

A dissertation submitted to the faculty of University of North Carolina at Chapel Hill in partial fulfillment of the requirements for the degree of Doctor of Philosophy in the Curriculum of Genetics and Molecular Biology.

Chapel Hill

2011

Approved by:

Dirk P. Dittmer

Adrienne D. Cox

Blossom A. Damania

William F. Marzluff

Kristy L. Richards

ABSTRACT

DEBASMITA ROY: Understanding the Mechanism of mTOR Inhibition in Human Herpes Virus-8 Associated Malignancies

(Under the direction of Dirk P. Dittmer)

In this dissertation, I have attempted to characterize the molecular features of Primary Effusion Lymphoma (PEL) and Kaposi's Sarcoma (KS) that render them addicted to the PI3K-mTOR pathway. PEL and KS constitute two signature diseases caused by Human Herpes Virus-8 (HHV8), or Kaposi's Sarcoma-associated Herpes Virus (KSHV), in immunocompromised individuals. KS is a cancer of endothelial cell origin and PEL a Diffuse-Large B-cell Lymphoma (DLBCL). We treated PEL cell lines *in vitro* and *in vivo* to show that sensitivity to Rapamycin, the major mTOR kinase inhibitor, is in part mediated by inhibition of interleukins: IL6 and IL10 (Sin, SH., Roy, D., et al.). We demonstrated that Phosphatase and Tensin homolog on chromosome-10 (PTEN), the major PI3K-mTOR negative regulator, is phosphorylated at Serine 380, in both PEL and KS. Reports in the literature have shown that phosphorylation at this residue results in a closed, inactive conformation of PTEN. This led us to speculate that unlike other cancers PTEN is inactivated not genetically, but via post-translational phosphorylation, in PEL and KS (Roy and Dittmer, in revision). Further, using the Affymetrix 6.0 SNP array we associated deletions in common fragile site tumor suppressor genes: FHIT and WWOX

with PEL. We correlated EBV-negative PEL with increased genomic instability compared to EBV-positive (Roy et al., in revision). Using a newly developed L1T2 cell line we demonstrated efficacy of Rapamycin against KS-like tumors in mice. We showed that Rapamycin inhibited secretion of Vascular Endothelial Growth Factor (VEGF) *in vitro*, which translated into defective tumor vasculature and angiogenesis *in vivo*. Unlike treatment with chemotherapeutic Doxorubicin, Rapamycin did not increase tumor apoptosis. We noted that Rapamycin alone is more tumor inhibitory than in combination with Doxorubicin. This led us to speculate that tumorigenesis of KS is more dependent on optimal tumor microenvironment than tumor cell proliferation. Lastly, we conducted an AIDS Malignancy Consortium (AMC) study of Rapamycin in AIDS-associated KS. We noted partial response or stable disease in all the patients. Molecular analysis showed that we could target mTOR kinase activity in patients without adversely affecting their AIDS (Krown, SE, Roy, D et. al. in submission). These data collectively suggest that mTOR inhibition can be an effective therapeutic in transplant- and AIDS-associated HHV8 malignancies.

To my family

Without your unconditional love and steadfast support I would not be standing at this threshold of life. I thank you for giving me the courage to follow my dreams and for always believing in me.

To my parents, for gently guiding me through life and inspiring me every step of the way; my grandmother, for teaching me to always focus on the good in this world; and, my little sister, who has been my motivation and shining star through it all….

I dedicate this success to you!

"The family is one of nature's masterpieces."

~ George Santayana

ACKNOWLEDGEMENTS

I sincerely express my gratitude towards my mentor, Dr. Dirk Dittmer, for giving me this opportunity to work in his lab and all my committee members: Drs. Blossom Damania, Adrienne Cox, Bill Marzluff and Kristy Richards for their guidance through the years. I am particularly thankful to Dirk for putting his faith in my abilities and allowing me to chart my own course through the various projects in lab. I would like to send special thanks to Adrienne, for not only being the chair of my thesis committee but also for the career counseling during the time we spent working together in the Cell and Molecular Biology training program. I'd like to thank Dr. Sharon Milgram, my mentor during the first year of graduate school for introducing me to process of scientific thinking and Dr. Robert Duronio, director of the curriculum in Genetics and Molecular Biology (GMB), my parent program for all his patience and guidance.

I thank all members of the UNC-GMB, Microbiology & Immunology programs and Interdisciplinary program in Biomedical Sciences (IBMS) for their assistance through the years. It is their dedication and hard work that provides us with the infrastructure upon which graduate education is built.

Last but not the least, I am indebted to all my dear friends, especially the ones I made during my time in graduate school for being my family here. In particular, I'd like

to thank Alaina Garland. When I met her as my IBMS class mate I had never imagined she is my sister, who was simply born on the other side of the world. All these people have stood by me through many joys and tears, embracing me each time with a caring hug and helping me get back on my feet. Their steadfast support, encouragement and zest for life have made these trying years of graduate school not only easier but also truly enjoyable.

Through my years at UNC, I have learned that it takes a lot of people and effort to make science happen and I am privileged to have been a part of it.

TABLE OF CONTENTS

LIST OF FIGURES

FIGURE

LIST OF TABLES

TABLE

CHAPTER I

INTRODUCTION

There has been an increasing prevalence of human cancers in the past few decades, leading us to further our understanding of the various oncogenic triggers of this complex family of malignancies. Infectious agents, especially viruses, comprise a significant fraction (nearly 20%) of the causal agents of all cancers (Pagano et al., 2004). Thus, understanding the manipulation of cellular machinery and processes by viral agents can significantly contribute towards a better understanding of human cancers. Over time several viruses have been investigated for their tumorigenic and transforming potential. In this thesis, I have attempted to better understand the progression of tumorigenesis caused by Human Herpes Virus-8 (HHV-8), also known as Kaposi's Sarcoma Herpesvirus (KSHV). Specifically, I have examined the Phospho-Inositol-3-Kinase (PI3K)- mammalian Target Of Rapamycin (mTOR) signaling pathway in KSHV-infected cells and how inhibition of this pathway results in tumor regression.

Kaposi's Sarcoma-associated Herpes Virus

KSHV is a member of the γ-Herpes family, specifically of the rhadinovirus genus (Damania, 2004b), as shown in figure I.1, panel A. It is closely related to Herpesvirus Saimiri (HVS) and Epstein-Barr Virus (EBV), also known as HHV-4. KSHV is strictly a human virus but it has tropism for an array of cell types: endothelial cells, B-cells and monocytes. The KSHV genome seems to be highly evolutionarily conserved with less than 0.4% variation between two independent viral isolates. This sequence variability, around the internal- and terminal-repeat regions, is not sufficient to sub-classify the virus into different genotypic strains. To date, two major variants have been categorized: the Prominent (P) and Minor (M) alleles (Ganem, 2010).

KSHV is the causative agent for three malignancies: Kaposi's Sarcoma (KS) (Chang et al., 1994), a cancer of endothelial cell origin and two lymphoproliferative disorders, Primary Effusion Lymphoma (PEL) (Cesarman et al., 1995) and Multicentric Castleman's Disease (MCD) (Soulier et al., 1995).

Kaposi's Sarcoma

Dr. Moritz Kaposi, a Hungarian dermatologist, identified KS in the late 19th century. He described the disease as cutaneous lesions, primarily seen in older Mediterranean men (Kaposi, 1872). Since then, KS has been seen in other settings and thereby sub-classified into: Classical, African-endemic, AIDS-associated and Transplant-associated KS. Classical KS includes the type originally described by Dr. Kaposi. The African-endemic form is mainly seen in children born with HIV infection in sub-Saharan Africa, but already existed before the emergence of HIV. The last two, AIDS- and

Transplant-associated KS, have become more prevalent in since the 1980s along with the AIDS epidemic and the increasing prevalence of transplantation that has accompanied the progress of medicine (Ganem, 2006). Association of KSHV infection with KS was established nearly a century after Dr. Kaposi's initial description of the disease. Using differential representation analysis, Chang et al. showed the presence of HVS-like DNA in nearly 100% of the KS biopsies isolated from HIV+ patients and coined the new virus KSHV (Chang et al., 1994).

Based on the histological presentation, KS lesions can be categorized as: Patch, Plaque and Nodular (figure I.2, panel A). Patch lesions are the earliest detectable dermal foci, which progress to plaque stage and eventually to nodular masses. From the earliest stages, KS lesions appear red to the naked eye. As it progresses to later stages, it becomes darker, almost a violet red color, indicative of the neovascularization and angiogenesis that is distinctive of KS. Unlike traditional cancers, in KS this crucial process of blood vessel formation is believed to begin prior to the formation of a palpable tumorigenic mass. Upon infection, the endothelial cells undergo a morphological change, losing their normal shape to take on an elongated spindle morphology that is diagnostically associated with KS (figure I.2, panel B) (Ganem, 2010).

Multicentric Castleman's Disease

MCD is a rare polyclonal hyperplasia, where there is an expansion of the germinal centers together with proliferation of endothelial cells within a specific lymph node. It is characterized by increased human interleukin-6 (IL-6) production that results in the systemic symptoms of the disease. Based on its histology, it can be sub-classified into

hyaline vascular and plasma cell types. When diagnosed in an immune-competent setting, there is 50% association of MCD with KSHV, but in HIV+, immune-compromised patients the association is much higher, nearly 100%. Given its rarity, MCD is a relatively poorly understood disease (Soulier et al., 1995; Waterston and Bower, 2004).

Primary Effusion Lymphoma

PEL, on the other hand, is a monoclonal neoplasia characterized by accumulation of fluid in the serious cavities of the body: the pleural, peritoneal and pericardial cavities. Although PEL is mainly associated with immune-compromised HIV+ patients, it has also been diagnosed in post-transplant patients on immunosuppressants. At presentation, the majority of PEL lack any solid tissue involvement, however a third of the cases may extravasate to non-serous sites. Although classified as a diffuse-large B-cell lymphoma (DLBCL), PEL cells express an array of non-B-cell plasma-cell markers. It is believed to be an expansion of post-germinal center terminally differentiated B-lymphocytes (Carbone et al., 2009; Chadburn et al., 2004; Nador et al., 1996). In addition to KSHV, PEL is often co-infected with EBV, another γ-Herpesvirus closely related to KSHV. However, the contribution of the individual herpesviruses to PEL pathogenesis remains to be determined.

KSHV Genome

KSHV is a relatively large double-stranded DNA virus, approximately 165kb in length (figure I.1, panel C). It was initially mapped by Russo et. al. from BC1 cells, a KSHV-positive, EBV-negative, PEL cell line. The central 140kb low GC-content region (L-DNA) encodes for 81 open reading frames (ORFs), 66 of which show high sequence

homology to HVS, and 5 internal repeat regions comprising the long unique region (LUR) (Russo et al., 1996). The LUR is surrounded by multiple shorter (~801 bp) highly repetitive high GC-content DNA (H-DNA) comprising the terminal repeats (TR). Molecular mimicry is a typical feature of oncogenic viruses and KSHV encodes an array of viral homologs of cellular proteins involved in cell cycle regulation, apoptosis and other signal transduction pathways as discussed below.

KSHV Life Cycles: Lytic vs. Latent

Analogous to other herpesviruses, KSHV can maintain a lytic or latent state of infection (figure I.1, panel B). Following *de novo* infection, KSHV invokes the latency program to evade immune detection and establish persistent infection. Upon establishing latency, the linear viral genome circularizes and KSHV is maintained in the host cells as a viral episome. This viral episome is tethered to the host chromosome via its Latency-associated Nuclear Antigen (LANA) protein, thereby allowing dissemination from mother to daughter cells following cell cycle division (Ballestas et al., 1999). LANA is a large protein consisting of a highly acidic central repeat domain, a basic DNA binding C-terminal domain, which recognizes the TR of KSHV, and a chromatin binding N-terminus that interacts with histone H2A-2B (Barbera et al., 2006; Schwam et al., 2000). In addition to being the defining latency protein, LANA has been implicated in KSHV-associated tumorigenesis that has been discussed in 'KSHV-associated Molecular Piracy'.

During latency, a very small subset of viral genes is expressed, all from the latency locus: LANA, viral homologs of Cyclin-D (vCyclin) and Flice-inhibitory protein

(vFLIP), Kaposin-A, -B and -C and a cluster of viral microRNAs (miRNAs) (figure I.1, panel C). In latently infected B-cells, a second locus encoding a viral homolog of Interferon Regulatory Factor -3 (vIRF3), also referred to as LANA2, is expressed and can inhibit cellular interferon induction (Rivas et al., 2001).

Transition from latency to lytic replication is triggered by the key lytic protein: Replication and Transcription Activator (RTA) (Sun et al., 1998). As LANA is considered a marker for latency, RTA constitutes the hallmark for lytic infection. RTA induces expression of specific lytic genes like viral homologs of Interleukin-6 (vIL6) and cellular G-protein coupled receptor (vGPCR) and the KSHV-specific protein K1. Although vIL6 was initially indentified as a lytic gene, recently it has been shown to be present in a sub-population of latently infected B-cells. It is detectable in a large fraction of B cell in MCD. Unlike other oncogenic herpesviruses, KSHV lytic proteins are also believed to contribute to KSHV-induced transformation. This is based on the observation that treatment of HIV patients with Ganciclovir, which specifically inhibits lytic viral replication, for Cytomegalovirus (CMV) infection led to reduced KS (Martin et al., 1999).

KSHV-associated Molecular Piracy

As mentioned earlier, KSHV encodes viral homologs of various cellular proteins and can post-transcriptionally as well as post-translationally regulate their function. KSHV can interfere with normal host cellular signaling via LANA, vCyclin and vFLIP during latency and vIL6, vGPCR and K1 upon lytic reactivation, as illustrated in figure I.3, panels A and B, respectively (Damania, 2004a; Jarviluoma and Ojala, 2006; Verma and Robertson, 2003).

LANA

LANA is the signature latency protein of KSHV. In fact, the presence of LANA antibodies is used as a serological test for KSHV infection. It was shown by Kedes et. al. using immunofluorescence (IFA) staining that the characteristic speckled dot pattern of LANA are exclusively in the nuclei of infected cells (figure I.2) (Kedes et al., 1997). Figure I.2, panel C and E show staining for LANA in L1T2 and BCBL1, KSHV-infected endothelial and B-cells, respectively. Panel D represents LANA staining in a primary patient biopsy (at 100X magnification) and panel F shows LANA in a PEL cell xenograft tumor in mice (at 400X magnification), in each case exclusively staining the nuclei. LANA has been shown to interact with key cellular proteins such as p53, Rb and GSK3β, thereby regulating apoptosis, cell cycle progression and β-catenin-mediated expression of pro-proliferative signals. It was shown by Friborg that LANA is capable of physically binding to p53, thereby inhibiting its transcription and pro-apoptotic functions (Chen et al., 2010; Friborg et al., 1999). This together with the fact that p53 is in its wild type state in the majority of KSHV-infected cells, activating p53 by agents such as Doxorubicin and

Nutlin provide a novel therapeutic approach (Petre et al., 2007; Sarek et al., 2007). LANA is also capable of interacting with Rb and serves as a cofactor in initiating transcription from E2F-responsive promoters to result in cell cycle progression (An et al., 2005). Additionally, LANA can modulate the Wnt signaling pathway by interacting with GSK3β, causing it to translocate to the nucleus and stabilize β-catenin (Fujimuro and Hayward, 2003). Normally, β-catenin is phosphorylated by GSK3β and targeted for proteasomal degradation. LANA inhibits this degradation resulting in induction of genes like Cyclin-D, c-myc and c-jun, thereby by promoting proliferation. Thus, LANA can both inhibit apoptosis via p53, and induce proliferation, by cooperating with Rb and/or β-catenin, to mediate tumorigenesis.

vCyclin and vFLIP

In addition to LANA, viral homologs of cellular proteins, vCyclin and vFLIP, can also modulate apoptosis and cell cycle progression during latency. vFLIP acts via NFκB-mediated signaling (Carbone et al., 2009; Guasparri et al., 2004). It activates IκB Kinase to phosphorylate IκB, thereby releasing NFκB to translocate to the nucleus and induce transcription of NFκB responsive genes, many of which are anti-apoptotic. vCyclin on the other hand is capable of activating Cyclin-dependent kinase 6 (CDK-6) at the G1/S-transition phase resulting in the progression of the cell cycle through S-phase (Laman et al., 2001). Additionally, vCyclin has been shown to phosphorylate Rb (GoddenKent et al., 1997) and inactivate STAT3, thereby promoting growth and degradation of p27 (Kip), further deregulating the G1/S-phase checkpoint (Jarviluoma et al., 2004).

vIL6

vIL6 is the KSHV viral homolog of pro-inflammatory cytokine Interleukin-6 (Nicholas et al., 1997). Cellular IL6 specifically binds its high-affinity glycoprotein (gp)-80 receptor and low-affinity gp130 transducer molecule to activate Jak-Stat signaling. In contrast, vIL6 can directly activate gp130 independently of gp80 to form a constitutively active signaling cascade (Damania, 2004a; Molden et al., 1997; Wan et al., 1999). It has further been shown that in addition to KSHV-infected cells, vIL6 also protects heterologous cells from the anti-viral effects of Interferon-alpha (IFNα) (Chatterjee et al., 2002). This suggests that vIL6 can not only substitute for cellular IL6 but also act as an autocrine factor for PEL and surrounding uninfected cells in the tumor microenvironment to promote proliferation.

vGPCR

The viral homolog of cellular G-protein coupled receptor, vGPCR, is a lytic protein tightly associated with KSHV-induced oncogenic transformation. vGPCR has been shown to have high sequence homology to the cellular receptor for IL8 (Cesarman et al., 1996; Guo et al., 1997). However, unlike cellular IL8 receptor, vGPCR is capable of inducing signaling in the absence of ligand binding (Arvanitakis et al., 1997). vGPCR can activate key molecules like phosphoinositide-3-Kinase (PI3K) and phospholipase C (PLC) to mediate signaling via protein kinase B (PKB/Akt), Mitogen-associated protein kinase (MAPK) and protein kinase C (PKC) (Montaner, 2007). These in turn result in enhanced expression of key pro-inflammatory factors like IL6, IL8 and major growth inducers like Vascular Endothelial Growth Factor (VEGF) (Bais et al., 1998; Sodhi et al., 2000). Review of these effects on cellular signaling strongly suggests that vGPCR plays a key role in KSHV-induced tumorigenesis in B-cells and endothelial cells alike.

KSHV K1

K1 is encoded in the first open reading frame and classified as a lytic protein. Given its proximity to the TR, K1 shows a high degree of amino acid variability that is reflected in its extracellular domain while maintaining a well-conserved C-terminal cytoplasmic tail. One of the key features of the C-tail is the presence of the immuno-receptor tyrosine-based activation motif (ITAM) that has been shown to activate NFκB, calcium mobilization and tyrosine phosphorylation, all events associated with lymphocyte activation. Specifically, it is capable of phosphorylating key signal transduction molecules such as Akt, p85 and Syk, all of which are involved in B-cell receptor (BCR) signaling. Expression of K1 has been shown to activate NFκB and induce pro-inflammatory cytokines together with expression of VEGF and Matrix Metalloprotease (MMP)-9. Last, but not least, like vIL6 and vGPCR, K1 is constitutively active and can signal in absence of ligand binding, contrary to other ITAM receptors (Damania, 2004a; Tomlinson and Damania, 2004; Wang et al., 2004).

KSHV viral microRNAs

MicroRNAs (miRNAs) are small non-coding RNAs ranging in size between 20-24 nucleotides and are involved in post-transcriptional gene silencing. They are short endogenous hairpin RNAs that can bind to the 3'-untranslated region (UTR) of its target mRNA to regulate protein translation. miRNAs are transcribed in the nucleus by RNA pol II and processed by miRNA machinery proteins Drosha and Dicer to produce the mature miRNA. miRNAs recognize their target mRNAs based on a short 'seed sequence' match found in the 3'UTR of the mRNA and given the short length of their sequence,

each miRNA can bind to and regulate hundreds of different target mRNAs. Functionally, a perfect match leads to mRNA degradation while partial complementarity results in translational inhibition.

Despite their short lengths, miRNAs constitute important phylogenetic markers and are found in essentially all biological species, including viruses. Therefore, it was not surprising to discover that KSHV encodes a set of viral miRNAs, but more interestingly, that they are all clustered in the latency locus. There are 12 KSHV pre-miRNAs, designated miR-K1 through miR-K12 (figure I.1, panel C), that give rise to 17 mature miRNAs (Cai et al., 2005). Where ten of these map to the intronic region of Kaposin, two of them (miR-K10 and -K12) are located in the coding region and 3'UTR of the gene, and can be induced by RTA. Our lab has shown that all 12 KSHV pre-miRNAs are expressed in latently infected endothelial and B-cells (modeling KS and PEL respectively) and cellular oncogenic and tumor suppressor miRNAs are up- and down-regulated, respectively, in PEL (O'Hara et al., 2009a; O'Hara et al., 2008; O'Hara et al., 2009b).

In the context of targeting cellular mRNAs, it has been shown in the literature that miR-K12-11 has 100% seed sequence homology to cellular miR-155, which is upregulated in lymphomas and plays a critical role in B-cell development (Gottwein et al., 2007; Skalsky et al., 2007). Recently, it was shown that miR-K12-10 protected KSHV-infected cells from apoptosis and pro-inflammatory signals, by inhibiting expression of cytokines, specifically IL8 and MCP1 (Abend et al., 2010). Qin et. al. made the observation that KSHV miR-K12-3 and K12-7 induce cytokines IL6 and IL10, both of which have been deemed critical in KSHV-associated malignancies (Qin et al., 2010).

Although the roles of the majority of KSHV miRNAs in KSHV pathogenesis remain to be elucidated, reports in the literature thus far suggest that they play important roles in tumorigenesis.

Models of Study for KSHV-associated Malignancies

KS

Several groups have been working on establishing a robust *in vitro* model to study KS. Where it is relatively simple to obtain primary patient biopsy displaying the classic KSHV-infection markers, it has been particularly challenging to propagate cells from biopsies in culture. While at the time of tissue procurement the majority of the cells are latently infected with KSHV and express LANA, over time the viral episome and LANA expression is lost. At present there exists no KS-tumor derived permanent cell line that is KSHV positive. Table IV.1 outlines the currently available *in vitro* models of KS (Albini et al., 1997; An et al., 2006; Flore et al., 1998; Grundhoff and Ganem, 2004; Herndier et al., 1994; Lagunoff et al., 2002; Mutlu et al., 2007; Wang and Damania, 2008). The majority of the cell lines were established from *de novo* infection of endothelial cells. Only two cell lines were explanted from primary KS biopsies from HIV-negative male patients: SLK and KS-IMM. Cytogenetic and immunophenotypic analysis showed that although SLK cells do not harbor the viral episome, they maintain spindle cell morphology and form KS-like tumors in mice (Herndier et al., 1994). KS-IMM on the other hand, was shown to harbor karyotypic abnormalities such as tetraploidy and hypertriploidy and despite the absence of spindle cells, KS-IMM cells form highly vascular KS-like tumors in mice. Of the infected endothelial cell lines, only two clones: E1 and L1 (An et al., 2006), derived from *de novo* infection of telomerase immortalized human vein endothelial cells (TIVE), have maintained the viral episome and expressed LANA without selection. Unlike KSHV-infected primary human vein endothelial cells (HUVEC) (Wang and Damania, 2008) or telomerase-immortalized dermal microvascular

endothelial cells (TIME) (Lagunoff et al., 2002), both E1 and L1-TIVE cells can form solid tumors in SCID mice.(An et al., 2006) Additionally, our lab has established a new cell line: L1T2, by explanting L1-TIVE tumors and selecting for cells in culture with proliferative advantage [Roy et. al. unpublished data]. Compared to L1-TIVE cells, L1T2 show a higher percentage of LANA-positive cells and more robust tumor growth in mice.

PEL

In contrast to KS, there are several well-characterized cell lines for PEL that grow *in vitro* and *in vivo*. As shown in table III.1, these cell lines represent an array of PEL isolates from different sources with varying EBV and HIV infection status as well as genetic differences in their p53 and PTEN status, two of the most commonly mutated tumor suppressor genes. They all express LANA and KSHV can be reactivated in culture from these cells, albeit with differing efficiency. Given the dearth of available KS cell lines, PEL constitutes the primary tissue culture model system to study KSHV pathogenesis. To study the interplay of KSHV-positive cells in the tumor microenvironment, we have established a xenograft tumor mouse model. KSHV-infected cells suspended in growth-factor reduced Matrigel™ and injected sub-cutaneously into SCID mice form localized solid tumors, which allows us to assess the effect of drug treatment on the tumor growth in an *in vivo* setting (Sin et al., 2007; Staudt et al., 2004).

The Cesarman group has developed a second xenograft model of PEL. In Keller et. al. they reported formation of PEL-like tumors in NOD/SCID mice injected intra-peritoneally with BC-3 cells suspended in PBS. The injected animals were weighed once a week and a gain of more than 10% body weight in a week's time was assessed as tumor

formation. Additionally, they injected mice with BC-3 cells expressing luciferase and using *in vivo* imaging detected bioluminescence, indicative of PEL-associated ascites accumulation (Keller et al., 2000).

In an attempt to further understand the role LANA may play towards PEL pathogenesis, our lab generated a transgenic mouse model where LANA is expressed under the regulation of its native promoter exclusively in the B-cells. It was observed that these animals exhibit splenic follicular hyperplasia along with increased germinal center formation. Although there was an increase in the incidence of lymphomas, they were distinct from the PEL type. This led the hypothesis that although LANA may be capable of B-cell activation and provide the trigger for lymphomagenesis, additional cues are required for PEL pathogenesis (Fakhari et al., 2006).

PI3K-mTOR Signaling

The Phosphatidyl-Inositol-3-Kinase (PI3K) comprise a large family of lipid kinases that regulate proliferation, differentiation, motility and cell survival, all of which are critical in the process of oncogenesis. PI3K can be further divided into three sub-classes: Class I, II and III based on their structure, regulation and most importantly their *in vitro* lipid substrates. They are heterodimeric in composition, consisting of p85 regulatory and p110 catalytic subunits. PI3K activation is initiated by binding of growth factors and other ligands to receptor tyrosine kinases (RTK) like Insulin Growth Factor Receptor (IGFR) and Epidermal Growth Factor Receptor (EGFR) at the cell membrane. The Src Homology (SH)-2 domain on the p85 subunit interacts with RTKs to recruit PI3K to the membrane where the p110α subunit can phosphorylate the intermediate messenger phosphatidylinositide-4,5-bi-phosphate (PIP_2) to phosphatidyl-inositide-3,4,5-tri-phosphate (PIP_3) (figure I.4, inset) (Vivanco and Sawyers, 2002).

PIP_3 is responsible for the recruitment of PI3K-dependent kinase (PDK)-1 and its effector protein Akt, also known as protein kinase B (PKB). This recruitment is mediated by the interaction of PIP_3 with the pleckstrin homology (PH)-domain of Akt. At the membrane, Akt is phosphorylated by PDK1, specifically at Threonine 308 (T308), which is also used as a marker for activated PI3K signaling. However, it has been noted that Akt is also phosphorylated at Serine 473 (S473) by a second elusive kinase, PDK2, which has only recently been suggested to be mTOR Complex 2 (mTORC2) (figure I.4) (Sabatini, 2006; Sarbassov et al., 2005).

Upon activation, Akt activates mTOR, one of its key downstream effectors, either directly by phosphorylating at Serine 2448 (S2448), or indirectly via disrupting the Tuberous Sclerosis (TSC)-1/2 complex to release the small G-protein Ras-homolog enriched in brain (Rheb) to activate mTOR (Inoki et al., 2003; Inoki et al., 2002). Rheb-mediated activation of mTOR involves disruption of the interaction between mTOR and FK-506 binding protein 38 (FKBP38), an endogenous cellular inhibitor of mTOR (Bai et al., 2007). This releases mTOR to interact with FKBP12 to form the enzymatic mTOR complex. mTOR can either form a Rapamycin sensitive mTOR:Raptor (mTORC1)(Kim et al., 2002) or Rapamycin insensitive mTOR:Rictor (mTORC2) (Sarbassov et al., 2005) complex. Of note is that inhibition by Rapamycin is mediated only after formation of Rapamycin:FKBP12 complex that can then interact with mTOR. Both mTORC1 and mTORC2 involve another component, GβL, which stimulates the kinase activity and has been shown to be critical for maintaining an active signaling cascade (Kim et al., 2003).

mTORC1 phosphorylates p70S6-Kinase (Isotani et al., 1999) and 4-Eukaryotic Binding Protein 1 (4EBP1) (Hara et al., 1997), two of its major downstream targets. Both these proteins have been shown to play important roles in regulating protein translation. Upon phosphorylation, 4EBP1 dissociates from eukaryotic initiation factor 4E (eIF4E) to allow for 5'-cap dependent mRNA translation. eIF4E has been shown to be crucial in the regulation of cancer gene transcripts such as c-Myc and Cyclin-D1, both containing highly structured 5'-ends. p70S6-Kinase on the other hand, phosphorylates ribosomal protein S6 (S6R) and thus activates 5'-terminal oligopyrimidine tract (5'-TOP) mediated translation. These mRNA primarily encode for ribosomal proteins and components of the translational machinery (Levy et al., 1991), thus allowing mTOR to regulate the overall

translational state of the cell. Specifically in the case of KSHV infection, we will show that the mTOR-regulated downstream mRNAs include: VEGF, IL6 and IL10 (Figure I.3).

It was shown by the Sabatini group that mTORC2 constitutes a feedback loop capable of phosphorylating Akt, at S473 residue, and thus mTORC2 has also been designated PDK2. It has further been suggested that given mTORC2's insensitivity to Rapamycin, over a prolonged period of Rapamycin treatment there is increased accumulation of mTORC2 resulting in hyper-activation of other Akt-regulated downstream targets like MAP-kinase instead of mTORC1 to promote growth. This feedback loop is seen most consistently in epithelial cell cancer cell lines and to a lesser degree in clinical studies. However, there are contradicting reports and further studies need to be conducted to determine the exact effect of Rapamycin treatment on mTORC2 (Carracedo et al., 2008; O'Reilly et al., 2006; Pollizzi et al., 2009; Sarbassov et al., 2006; Sarbassov et al., 2005; Tamburini et al., 2008; Zeng et al., 2007; Zitzmann et al., 2010).

The key event in propagating the PI3K-Akt signal from the plasma membrane to the cytoplasm is regulated by PIP_3. There exists the negative regulator, Phosphatase and Tensin homolog on chromosome 10 (PTEN), which targets the pathway at the PIP_3 formation step. PTEN is a lipid phosphatase capable of reversing PIP_3 to PIP_2, thereby putting the brakes on early in the signal transduction pathway (Stambolic et al., 1998). Accordingly, it is not surprising that PTEN has been classified as a tumor suppressor and shown to be genetically deleted in the majority of glioblastomas (GBMs). Its absence is also associated with particularly poor prognosis (Cloughesy et al., 2008; Cully et al., 2006; Stambolic et al., 1998). Another cellular point where this signal transduction is negatively regulated is by members of the TSC-1/2 complex that have also been

classified as tumor suppressors. TSC1, also known as hamartin, and TSC2, or tuberin, were identified as familial mutations associated with tuberous sclerosis complex (TSC). TSC is an autosomal dominant tumor syndrome characterized by the occurrence of benign tumors in multiple organs. The C-terminal domain of TSC-2 shows GAP (GTP-ase Activating Protein) activity towards small GTP-ase Rheb that positively regulates mTOR. When in complex, TSC-2 prevents activation of mTOR by promoting formation of Rheb:GDP as opposed to the active Rheb:GTP state (Huang and Manning, 2008; Inoki et al., 2003). Thus, genetic deletions and mutations or post-translational silencing of either PTEN or the TSC complex by KSHV can hyperactivate the mTOR signaling pathway.

IL6, IL10, VEGF and PI3K Interplay

IL6, IL10 and VEGF constitute a subset of signaling molecules believed to play a particularly significant role in KSHV pathogenesis. Where IL6 and VEGF represent pro-inflammatory and growth-inducing factors, respectively, IL10 is an anti-inflammatory cytokine. In the context of KS, given its highly vascular and angiogenic nature, it is not surprising that these tumors express elevated levels of VEGF and their corresponding receptors. In the context of PEL, high expression of VEGF is slightly less intuitive, but considering the increased vascular permeability allowing for ascites accumulation and the clinical observation that a fraction of PEL patients go onto developing disseminated solid tumors, it can be reasoned that increased VEGF together with its receptors may promote these symptoms. Given the hypoxic environment that PEL thrives in, it is not surprising that it has adapted mechanisms that allow for optimal growth in a demanding environment (Gasperini and Tosato, 2009; Zebrowski et al., 1999).

As for the cytokines, given their pro- and anti-inflammatory functions, it can be hypothesized that where IL10 allows the virus to evade immune surveillance following infection, IL6 allows for recruitment of uninfected cells and thus promotes de novo infection. The presence of a viral homolog of cellular IL6 and its capacity to function independently of the cellular IL6 receptor further supports the notion that IL6 is important for KSHV to establish a persistent and productive infection. Previous studies in our lab have revealed that Rapamycin-mediated growth inhibition of PEL is accompanied by reduced expression of both IL6 and IL10. Both IL6 and IL10 are required for PEL cell growth (Drexler et al., 1999; Jones et al., 1999).

Various groups have proposed the regulation of VEGF and other angiogenic factors by PI3K-mTOR. VEGF, like c-Myc and Cyclin-D1, has a highly structured 5'-end (Konicek et al., 2008) and has been shown to be concomitantly overexpressed with eIF4E (Yang et al., 2007), a downstream effector of mTOR. Additionally, it can also be indirectly regulated either via Myc or mTOR regulation of HIF1-α. Myc has been shown to be involved in regulation of VEGF in B-cells (Mezquita et al., 2005). Specifically, in KSHV-infected B-cells, Myc has increased stability (Bubman et al., 2007) leading us to speculate its involvement in VEGF expression in PEL. Hypoxia-inducible factor 1-alpha (HIF1-α), is a transcription factor involved in VEGF expression and has been shown to be regulated by mTOR in a different tumor, renal cell carcinoma (Toschi et al., 2008). Currently there are no studies directly associating regulation of IL-6 and IL-10 with mTOR.

Drugs Targeting PI3K-mTOR Pathway

Rapamycin is one of the key inhibitors of the PI3K-mTOR signaling pathway. An anti-fungal, it initially came into prominence as a potent immunosuppressant and has frequently been used in solid transplant recipients, especially renal transplants (Baker et al., 1978; Eng et al., 1984; Heitman et al., 1991). Subsequently, it was reported that Rapamycin also exhibited strong anti-tumor activity (Houchens et al., 1983). This posed a very interesting conundrum as to how the same agent can act both in an immune-suppressive and anti-tumorigenic manner.

Structurally, Rapamycin first interacts with cytosolic FKBP12, to induce a conformational change that allows for Rapamycin:FKBP12 complex to interact with and inhibit mTORC1 (Brown et al., 1994; Sabatini et al., 1994). Interestingly, Cyclosporin A (CsA), another structurally similar immunosuppressant, does not have any anti-tumor potential; in fact CsA has been shown to aggravate tumor phenotype in mice. A third popular immunosuppressant in the clinic is FK506 (Kino et al., 1987), also known as Tacrolimus. Structurally, FK506 and Rapamycin are distinct from each other. However, they interact with the same intermediate FKBP12 to form complexes that have different cellular targets. The FK506:FKBP12 complex interacts with and inhibits Calcineurin mediated signaling, as does the CsA:Cyclophilin complex (Quesniaux et al., 1988). Rapamycin:FKBP12 on the other hand interacts with and inhibits mTORC1. Despite their different intermediates, from the immunomodulatory stand point all three inhibitors--Rapamycin, CsA and FK506--inhibit IL2 mediated activation and proliferation of T-lymphocytes. While Rapamycin inhibits response to IL2, Calcineurin inhibitors (CsA and FK506) block the production of IL2 all together (Abraham and Wiederrecht, 1996; Dumont et al., 1994; Fruman et al., 1995).

Being an anti-proliferative agent, Rapamycin is particularly beneficial as an immunosuppressant in transplant recipients since a significant portion of these patients develop iatrogenic KS. Stallone et al. found that Rapamycin is efficacious against renal transplant associated KS while maintaining the organ graft. They showed that patients initially on CsA developed KS-like lesions, which upon biopsy were shown to be KSHV-positive. Additionally, these patients expressed high levels of VEGF and its corresponding receptors indicative of angiogenesis: a signature feature of KS tumors. Upon switching from CsA to Rapamycin, there was a complete regression of lesions and compared to pre-treatment, there was a significant reduction in phosphorylated levels of Akt (Stallone et al., 2005). Further, compared to the Calcineurin inhibitors (CsA and FK506), Rapamycin has relatively low levels of toxicity, especially towards the kidneys, making it a very popular immunosuppressant.

One of the downsides of Rapamycin treatment involves the dosing scheme required to establish the clinically effective trough levels of the drug in the blood stream. Since the popularity of Rapamycin escalated, several improved derivatives, including Temsirolimus (CCI-779) and Everolimus (RAD-001) (Sedrani et al., 1998), have been introduced. While they maintain the same basic molecular structure and mechanism of inhibition, these derivatives have improved bioavailability and metabolic stability. The Food and Drug Administration (FDA) has approved Temsirolimus for Renal Cell Carcinoma (RCC) and Everolimus for advanced kidney cancers and organ rejection prophylaxis. Among the Calcineurin inhibitors, FK506 has been more popular than CsA. Akin to Rapamycin, analogs of FK506 include Ascomycin and Pimecrolimus, used to treat autoimmune skin disorders and atopic dermatitis respectively. However, none of

these derivatives have been evaluated in terms of their effect on KS or KSHV infection in general.

Given the prevalence of KS in AIDS patients, in addition to dosing concerns, the interaction of Rapamycin with the anti-retroviral therapy (ART) administered to these patients presents another area of concern. Protease Inhibitors (PI) and Non-Nucleoside Reverse Transcriptase Inhibitor (NNRTI) constitute the two primary arms of ART. Whereas PI is an inhibitor of the hepatic Cytochrome P450-3A4 (CYP450) metabolizing enzyme system, NNRTIs are themselves substrates for processing by CYP450. CYP450 enzymes comprise the major family of the drug metabolizing and bioactivation system. The effects of concomitant administration of either PI or NNRTI with immunosuppressants has been investigated in the setting of AIDS-associated transplants. Patients on PI together with Calcineurin or mTOR inhibitors require markedly reduced doses of immunosuppressants to achieve trough levels. On the other hand, patients on NNRTI require increased dosing that is closely monitored to avoid the risk of drug toxicity (Frassetto et al., 2007; Marfo and Greenstein, 2009). Currently, much of the effort in understanding drug-drug interactions between ART and immunosuppressants focuses on the context of transplant-associated rather than of the use of mTOR inhibitors as anti-tumorigenic agents against systemic AIDS-associated KS.

Inhibition of mTOR in PEL

In the Sin, SH, Roy, D, et al. report we showed that Rapamycin is efficacious against PEL *in vitro* as well as in our *in vivo* xenograft model. We established that this inhibition of growth is primarily mediated by down regulation of IL6 and IL10. We propose that IL6 and IL10 form an autocrine feedback loop to activate PI3K signaling in PEL thus making them addicted to the mTOR signaling cascade. Further, presence of the viral IL6 homolog lends credence to the presence of our proposed IL6r-dependent signaling loop. However, the exact effect of Rapamycin treatment, or otherwise inhibition of mTOR, on viral IL6 expression needs to be evaluated. Given that viral IL6 can signal independently of gp80 receptor it is further interesting to evaluate whether viral IL6 can compensate for inhibition of cellular IL6. Previous data from our lab has shown that Rapamycin treatment does not affect transcription of the KSHV genome. Therefore, it could be speculated that upon inhibition of cellular IL6 by Rapamycin, the virus can upregulate expression of viral IL6 as a compensatory mechanism for sustained signaling through the PI3K signaling cascade. Although initially identified as a lytic gene product, viral IL6 has subsequently been detected at low levels through latency further suggesting that it may play a regulator and compensator role throughout the viral life cycle. Still within the limits of our analysis, we did not detect a change in vIL6 mRNA levels in PEL upon rapamycin exposure.

Although we demonstrated that Rapamycin treatment inhibits secreted levels and expression in tumor of both IL6 and IL10, the exact mechanism of this down regulation is unclear. To eliminate a secretion defect, unpublished data from our lab has shown that decrease in intra-cellular levels of IL6 and IL10 is equivalent to the secreted levels.

mTOR is primarily involved in translation regulation. Therefore, it can be hypothesized that both cytokines are inhibited at the post-transcriptional level. However, there is a possibility that Rapamycin treatment of PEL cells results in reduced expression of a key transcription factor that in turn regulates expression of IL6 and IL10.

We further showed that the Rapamycin mediated inhibition is a cell cycle arrest where majority of the PEL cells were arresting in G_1-phase, as expected of a cytostatic drug. Others have shown that Rapamycin can induce autophagy in PEL cells (Lee et al., 2009). It would be interesting to investigate whether inhibition of mTOR by Rapamycin or other inhibitors preferentially selects for one vs. another mode of growth restriction. It is evident that KSHV induces hyper-activation of the PI3K-mTOR pathway and successfully hijacks it to initiate an autocrine signaling loop the promote proliferation. In majority of solid tumors showing sensitivity to Rapamycin PTEN is either deleted or mutated resulting in lack of protein expression. However, it remains unclear as to what role PTEN plays in KSHV mediated addiction to PI3K-mTOR signaling cascade.

FIGURES

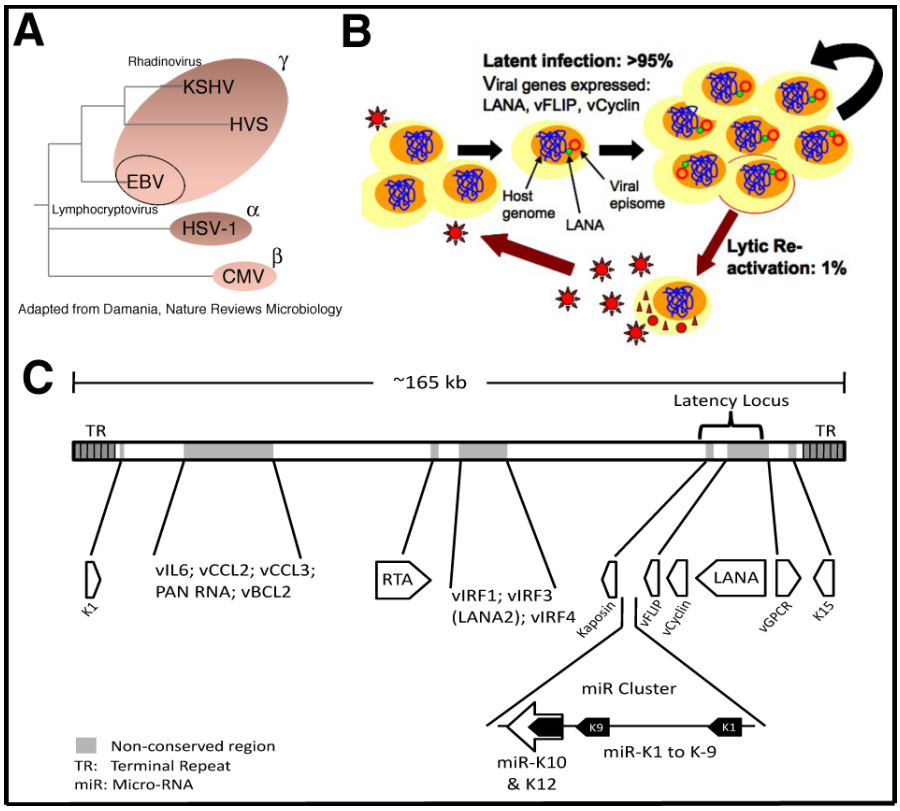

Figure I.1: KSHV Virus Panel A represents the phylogenetic tree of Herpes viruses denoting KSHV to be a rhadinovirus closely related to HVS and EBV in the γ-herpes family. Panel B shows the lytic and latent replication cycles the virus can exist in illustrating in green the latency protein LANA that tethers the viral episome, in red, to the host chromosome of latently infected cells. Panel C illustrates the layout of the KSHV genome, with the terminal repeats (TR) at the ends and the conserved and unique regions in white and grey, respectively.

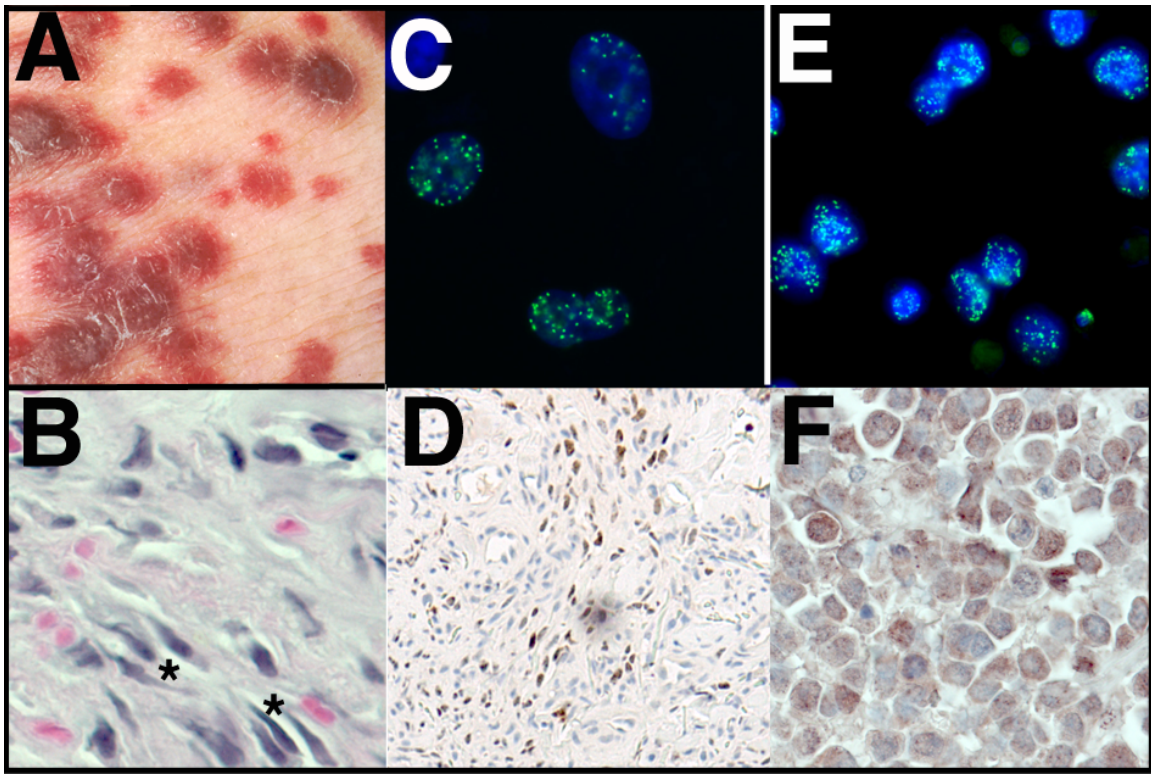

Figure I.2: Clinical Histology of KS and PEL Panel A is a snap-shot of patch and plaque lesions as seen on a patient. Panel B is a Hematoxylin-Eosin stain showing the spindle cells (marked with a black asterisk) that are characteristic to KS lesions. Panels C and E are immunofluorescence staining for LANA showing the typical punctate pattern in KS and PEL cells in culture, respectively. Panels D and F are immunohistochemical staining for LANA in patient biopsy sample and mouse xenograft tumor, respectively. Again we note that the staining is restricted exclusively to the nuclei of the cells.

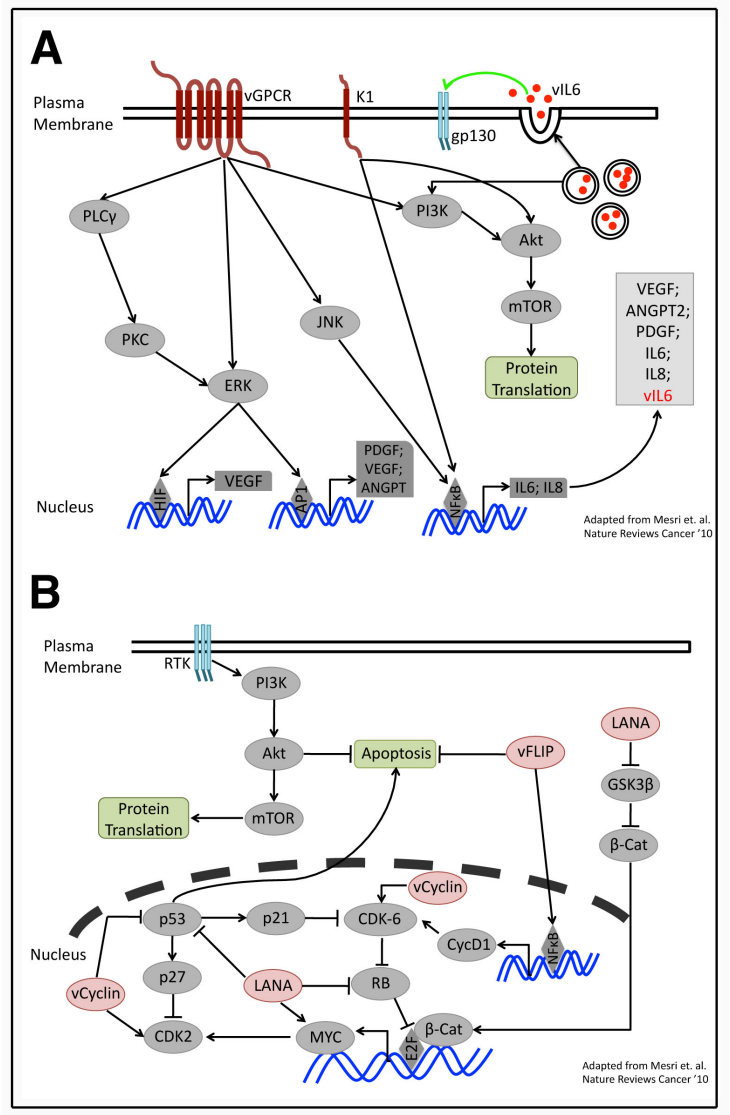

Figure I.3: Molecular Piracy of Cellular Signaling by KSHV Panel A represents the lytic life cycle where viral-GPCR is capable of inducing signaling via PI3K, PKC and NKκB; K1 via Akt and NFκB, in addition to B-cell receptor signaling in general; and viral-IL6 shown to activate PI3K and Stat3 (via gp130). Panel B represents the latency arm to show that within the cytoplasm, LANA is capable of inhibiting p53, Rb and GSK3β; viral-Cyclin activates CDK-2, -6 while inhibiting p53; and viral-FLIP activates NFκB while inhibiting apoptosis.

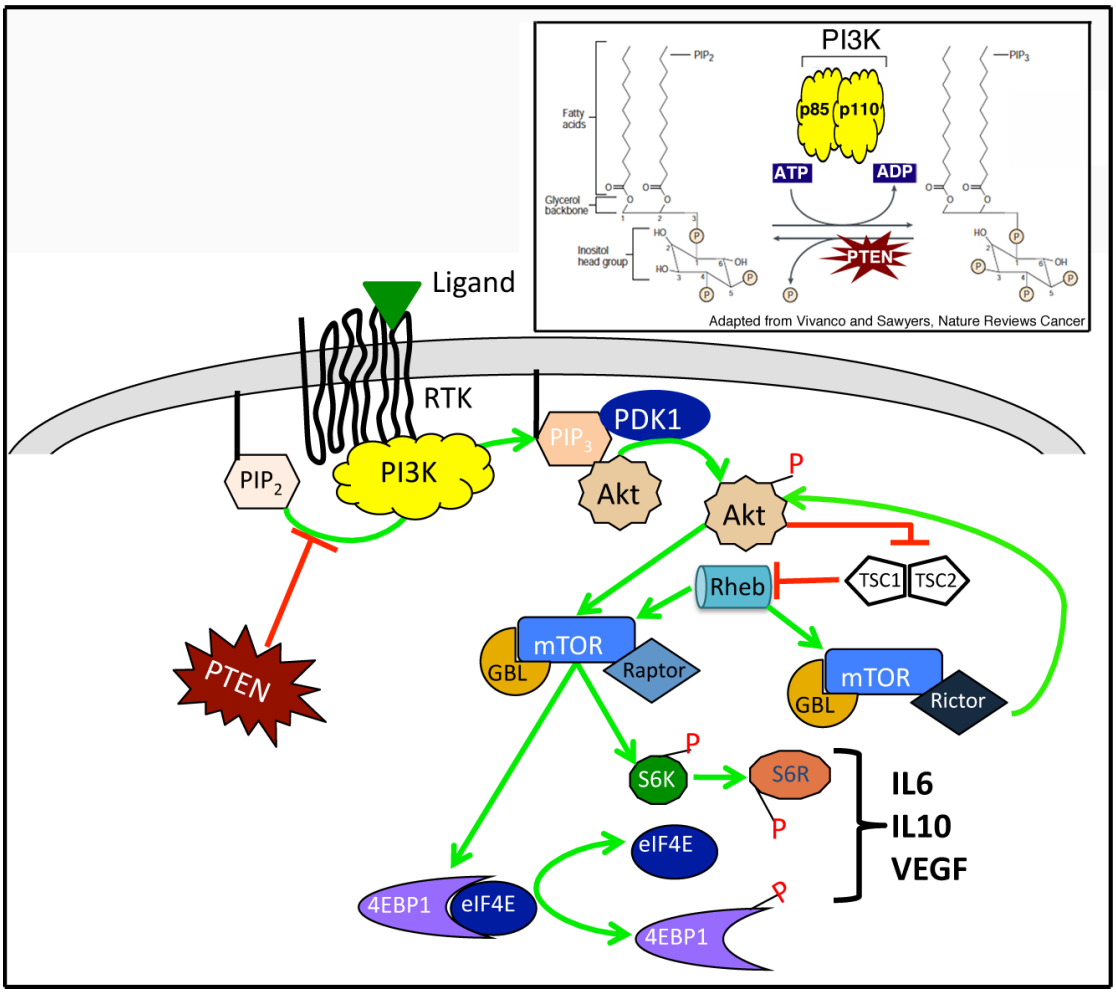

Figure I.4: PI3K-mTOR Signaling Pathway The inset box represents the structural components of PI3-Kinase and its target phospho-lipids. The signaling cascade shows the different pro-growth (PI3K, Akt, mTOR, Rheb, S6K, S6R, eIF4e) and tumor suppressor components (PTEN, TSC1-TSC2, 4EBP1). The green arrows indicate activating changes and the red denotes inhibition. The cell surface ligand can be anything from VEGF to vIL6 and the Receptor Tyrosine Kinase (RTK) can either be cellular or viral receptors.

REFERENCES

Abend, J.R., Uldrick, T., and Ziegelbauer, J.M. (2010). Regulation of tumor necrosis factor-like weak inducer of apoptosis receptor protein (TWEAKR) expression by Kaposi's sarcoma-associated herpesvirus microRNA prevents TWEAK-induced apoptosis and inflammatory cytokine expression. J Virol *84*, 12139-12151.

Abraham, R.T., and Wiederrecht, G.J. (1996). Immunopharmacology of rapamycin. Annu Rev Immunol *14*, 483-510.

Albini, A., Paglieri, I., Orengo, G., Carlone, S., Aluigi, M.G., DeMarchi, R., Matteucci, C., Mantovani, A., Carozzi, F., Donini, S.*, et al.* (1997). The beta-core fragment of human chorionic gonadotrophin inhibits growth of Kaposi's sarcoma-derived cells and a new immortalized Kaposi's sarcoma cell line. AIDS *11*, 713-721.

An, F.Q., Compitello, N., Horwitz, E., Sramkoski, M., Knudsen, E.S., and Renne, R. (2005). The latency-associated nuclear antigen of Kaposi's sarcoma-associated herpesvirus modulates cellular gene expression and protects lymphoid cells from p16 INK4A-induced cell cycle arrest. J Biol Chem *280*, 3862-3874.

An, F.Q., Folarin, H.M., Compitello, N., Roth, J., Gerson, S.L., McCrae, K.R., Fakhari, F.D., Dittmer, D.P., and Renne, R. (2006). Long-Term-Infected Telomerase-Immortalized Endothelial Cells: a Model for Kaposi's Sarcoma-Associated Herpesvirus Latency In Vitro and In Vivo. J Virol *80*, 4833-4846.

Arvanitakis, L., Geras-Raaka, E., Varma, A., Gershengorn, M.C., and Cesarman, E. (1997). Human herpesvirus KSHV encodes a constitutively active G-protein-coupled receptor linked to cell proliferation. Nature *385*, 347-350.

Bai, X., Ma, D., Liu, A., Shen, X., Wang, Q.J., Liu, Y., and Jiang, Y. (2007). Rheb activates mTOR by antagonizing its endogenous inhibitor, FKBP38. Science *318*, 977-980.

Bais, C., Santomasso, B., Coso, O., Arvanitakis, L., Raaka, E.G., Gutkind, J.S., Asch, A.S., Cesarman, E., Gershengorn, M.C., Mesri, E.A.*, et al.* (1998). G-protein-coupled receptor of Kaposi's sarcoma-associated herpesvirus is a viral oncogene and angiogenesis activator [see comments] [published erratum appears in Nature 1998 Mar 12;392(6672):210]. Nature *391*, 86-89.

Baker, H., Sidorowicz, A., Sehgal, S.N., and Vezina, C. (1978). Rapamycin (AY-22,989), a new antifungal antibiotic. III. In vitro and in vivo evaluation. J Antibiot (Tokyo) *31*, 539-545.

Ballestas, M.E., Chatis, P.A., and Kaye, K.M. (1999). Efficient persistence of extrachromosomal KSHV DNA mediated by latency- associated nuclear antigen. Science *284*, 641-644.

Barbera, A.J., Chodaparambil, J.V., Kelley-Clarke, B., Joukov, V., Walter, J.C., Luger, K., and Kaye, K.M. (2006). The nucleosomal surface as a docking station for Kaposi's sarcoma herpesvirus LANA. Science *311*, 856-861.

Brown, E.J., Albers, M.W., Shin, T.B., Ichikawa, K., Keith, C.T., Lane, W.S., and Schreiber, S.L. (1994). A mammalian protein targeted by G1-arresting rapamycin-receptor complex. Nature *369*, 756-758.

Bubman, D., Guasparri, I., and Cesarman, E. (2007). Deregulation of c-Myc in primary effusion lymphoma by Kaposi's sarcoma herpesvirus latency-associated nuclear antigen. Oncogene *26*, 4979-4986.

Cai, X., Lu, S., Zhang, Z., Gonzalez, C.M., Damania, B., and Cullen, B.R. (2005). Kaposi's sarcoma-associated herpesvirus expresses an array of viral microRNAs in latently infected cells. Proc Natl Acad Sci U S A *102*, 5570-5575.

Carbone, A., Cesarman, E., Spina, M., Gloghini, A., and Schulz, T.F. (2009). HIV-associated lymphomas and gamma-herpesviruses. Blood *113*, 1213-1224.

Carracedo, A., Ma, L., Teruya-Feldstein, J., Rojo, F., Salmena, L., Alimonti, A., Egia, A., Sasaki, A.T., Thomas, G., Kozma, S.C.*, et al.* (2008). Inhibition of mTORC1 leads to MAPK pathway activation through a PI3K-dependent feedback loop in human cancer. J Clin Invest *118*, 3065-3074.

Cesarman, E., Chang, Y., Moore, P.S., Said, J.W., and Knowles, D.M. (1995). Kaposi's sarcoma-associated herpesvirus-like DNA sequences in AIDS-related body-cavity-based lymphomas. N Engl J Med *332*, 1186-1191.

Cesarman, E., Nador, R.G., Bai, F., Bohenzky, R.A., Russo, J.J., Moore, P.S., Chang, Y., and Knowles, D.M. (1996). Kaposi's sarcoma-associated herpesvirus contains G protein-coupled receptor and cyclin D homologs which are expressed in Kaposi's sarcoma and malignant lymphoma. J Virol *70*, 8218-8223.

Chadburn, A., Hyjek, E., Mathew, S., Cesarman, E., Said, J., and Knowles, D.M. (2004). KSHV-positive solid lymphomas represent an extra-cavitary variant of primary effusion lymphoma. Am J Surg Pathol *28*, 1401-1416.

Chang, Y., Cesarman, E., Pessin, M.S., Lee, F., Culpepper, J., Knowles, D.M., and Moore, P.S. (1994). Identification of herpesvirus-like DNA sequences in AIDS-associated Kaposi's sarcoma. Science *266*, 1865-1869.

Chatterjee, M., Osborne, J., Bestetti, G., Chang, Y., and Moore, P.S. (2002). Viral IL-6-induced cell proliferation and immune evasion of interferon activity. Science *298*, 1432-1435.

Chen, W., Hilton, I.B., Staudt, M.R., Burd, C.E., and Dittmer, D.P. (2010). Distinct p53, p53:LANA, and LANA complexes in Kaposi's Sarcoma--associated Herpesvirus Lymphomas. J Virol *84*, 3898-3908.

Cloughesy, T.F., Yoshimoto, K., Nghiemphu, P., Brown, K., Dang, J., Zhu, S., Hsueh, T., Chen, Y., Wang, W., Youngkin, D., *et al.* (2008). Antitumor activity of rapamycin in a Phase I trial for patients with recurrent PTEN-deficient glioblastoma. PLoS Med *5*, e8.

Cully, M., You, H., Levine, A.J., and Mak, T.W. (2006). Beyond PTEN mutations: the PI3K pathway as an integrator of multiple inputs during tumorigenesis. Nat Rev Cancer *6*, 184-192.

Damania, B. (2004a). Modulation of Cell Signaling Pathways by Kaposi's Sarcoma-Associated Herpesvirus (KSHVHHV-8). Cell Biochem Biophys *40*, 305-322.

Damania, B. (2004b). Oncogenic gamma-herpesviruses: comparison of viral proteins involved in tumorigenesis. Nat Rev Microbiol *2*, 656-668.

Drexler, H.G., Meyer, C., Gaidano, G., and Carbone, A. (1999). Constitutive cytokine production by primary effusion (body cavity- based) lymphoma-derived cell lines. Leukemia *13*, 634-640.

Dumont, F.J., Kastner, C., Iacovone, F., Jr., and Fischer, P.A. (1994). Quantitative and temporal analysis of the cellular interaction of FK-506 and rapamycin in T-lymphocytes. J Pharmacol Exp Ther *268*, 32-41.

Eng, C.P., Sehgal, S.N., and Vezina, C. (1984). Activity of rapamycin (AY-22,989) against transplanted tumors. J Antibiot (Tokyo) *37*, 1231-1237.

Fakhari, F.D., Jeong, J.H., Kanan, Y., and Dittmer, D.P. (2006). The latency-associated nuclear antigen of Kaposi sarcoma-associated herpesvirus induces B cell hyperplasia and lymphoma. J Clin Invest *116*, 735-742.

Flore, O., Rafii, S., Ely, S., O'Leary, J.J., Hyjek, E.M., and Cesarman, E. (1998). Transformation of primary human endothelial cells by Kaposi's sarcoma- associated herpesvirus. Nature *394*, 588-592.

Frassetto, L.A., Browne, M., Cheng, A., Wolfe, A.R., Roland, M.E., Stock, P.G., Carlson, L., and Benet, L.Z. (2007). Immunosuppressant pharmacokinetics and dosing modifications in HIV-1 infected liver and kidney transplant recipients. Am J Transplant *7*, 2816-2820.

Friborg, J., Jr., Kong, W., Hottiger, M.O., and Nabel, G.J. (1999). p53 inhibition by the LANA protein of KSHV protects against cell death. Nature *402*, 889-894.

Fruman, D.A., Wood, M.A., Gjertson, C.K., Katz, H.R., Burakoff, S.J., and Bierer, B.E. (1995). FK506 binding protein 12 mediates sensitivity to both FK506 and rapamycin in murine mast cells. Eur J Immunol *25*, 563-571.

Fujimuro, M., and Hayward, S.D. (2003). The latency-associated nuclear antigen of Kaposi's sarcoma-associated herpesvirus manipulates the activity of glycogen synthase kinase-3beta. J Virol *77*, 8019-8030.

Ganem, D. (2006). KSHV infection and the pathogenesis of Kaposi's sarcoma. Annu Rev Pathol *1*, 273-296.

Ganem, D. (2010). KSHV and the pathogenesis of Kaposi sarcoma: listening to human biology and medicine. J Clin Invest *120*, 939-949.

Gasperini, P., and Tosato, G. (2009). Targeting the mammalian target of Rapamycin to inhibit VEGF and cytokines for the treatment of primary effusion lymphoma. Leukemia *23*, 1867-1874.

GoddenKent, D., Talbot, S.J., Boshoff, C., Chang, Y., Moore, P., Weiss, R.A., and Mittnacht, S. (1997). The cyclin encoded by Kaposi's sarcoma-associated herpesvirus stimulates cdk6 to phosphorylate the retinoblastoma protein and histone H1. J Virol *71*, 4193-4198.

Gottwein, E., Mukherjee, N., Sachse, C., Frenzel, C., Majoros, W.H., Chi, J.T., Braich, R., Manoharan, M., Soutschek, J., Ohler, U*., et al.* (2007). A viral microRNA functions as an orthologue of cellular miR-155. Nature *450*, 1096-1099.

Grundhoff, A., and Ganem, D. (2004). Inefficient establishment of KSHV latency suggests an additional role for continued lytic replication in Kaposi sarcoma pathogenesis. J Clin Invest *113*, 124-136.

Guasparri, I., Keller, S.A., and Cesarman, E. (2004). KSHV vFLIP is essential for the survival of infected lymphoma cells. J Exp Med *199*, 993-1003.

Guo, H.G., Browning, P., Nicholas, J., Hayward, G.S., Tschachler, E., Jiang, Y.W., Sadowska, M., Raffeld, M., Colombini, S., Gallo, R.C*., et al.* (1997). Characterization of a chemokine receptor-related gene in human herpesvirus 8 and its expression in Kaposi's sarcoma. Virology *228*, 371-378.

Hara, K., Yonezawa, K., Kozlowski, M.T., Sugimoto, T., Andrabi, K., Weng, Q.P., Kasuga, M., Nishimoto, I., and Avruch, J. (1997). Regulation of eIF-4E BP1 phosphorylation by mTOR. J Biol Chem *272*, 26457-26463.

Heitman, J., Movva, N.R., and Hall, M.N. (1991). Targets for cell cycle arrest by the immunosuppressant rapamycin in yeast. Science *253*, 905-909.

Herndier, B.G., Werner, A., Arnstein, P., Abbey, N.W., Demartis, F., Cohen, R.L., Shuman, M.A., and Levy, J.A. (1994). Characterization of a human Kaposi's sarcoma cell line that induces angiogenic tumors in animals. Aids *8*, 575-581.

Houchens, D.P., Ovejera, A.A., Riblet, S.M., and Slagel, D.E. (1983). Human brain tumor xenografts in nude mice as a chemotherapy model. Eur J Cancer Clin Oncol *19*, 799-805.

Huang, J., and Manning, B.D. (2008). The TSC1-TSC2 complex: a molecular switchboard controlling cell growth. Biochem J *412*, 179-190.

Inoki, K., Li, Y., Xu, T., and Guan, K.L. (2003). Rheb GTPase is a direct target of TSC2 GAP activity and regulates mTOR signaling. Genes Dev *17*, 1829-1834.

Inoki, K., Li, Y., Zhu, T., Wu, J., and Guan, K.L. (2002). TSC2 is phosphorylated and inhibited by Akt and suppresses mTOR signalling. Nat Cell Biol *4*, 648-657.

Isotani, S., Hara, K., Tokunaga, C., Inoue, H., Avruch, J., and Yonezawa, K. (1999). Immunopurified mammalian target of rapamycin phosphorylates and activates p70 S6 kinase alpha in vitro. J Biol Chem *274*, 34493-34498.

Jarviluoma, A., Koopal, S., Rasanen, S., Makela, T.P., and Ojala, P.M. (2004). KSHV viral cyclin binds to p27KIP1 in primary effusion lymphomas. Blood *104*, 3349-3354.

Jarviluoma, A., and Ojala, P.M. (2006). Cell signaling pathways engaged by KSHV. Biochim Biophys Acta *1766*, 140-158.

Jones, K.D., Aoki, Y., Chang, Y., Moore, P.S., Yarchoan, R., and Tosato, G. (1999). Involvement of interleukin-10 (IL-10) and viral IL-6 in the spontaneous growth of Kaposi's sarcoma herpesvirus-associated infected primary effusion lymphoma cells. Blood *94*, 2871-2879.

Kaposi, M. (1872). Idiopathisches multiples Pigmentsarkom der Haut. Arch Dermatol Syph *4*, 265–273.

Kedes, D., H. , Lagunoff, M., Renne, R., and Ganem, D. (1997). Identification of the gene encoding the major latency-associated nuclear antigen of the Kaposi's sarcoma-associated herpesvirus. Journal of Clinical Investigation *100*, 2606-2610.

Keller, S.A., Schattner, E.J., and Cesarman, E. (2000). Inhibition of NF-kappaB induces apoptosis of KSHV-infected primary effusion lymphoma cells. Blood *96*, 2537-2542.

Kim, D.H., Sarbassov, D.D., Ali, S.M., King, J.E., Latek, R.R., Erdjument-Bromage, H., Tempst, P., and Sabatini, D.M. (2002). mTOR interacts with raptor to form a nutrient-sensitive complex that signals to the cell growth machinery. Cell *110*, 163-175.

Kim, D.H., Sarbassov, D.D., Ali, S.M., Latek, R.R., Guntur, K.V., Erdjument-Bromage, H., Tempst, P., and Sabatini, D.M. (2003). GbetaL, a positive regulator of the rapamycin-sensitive pathway required for the nutrient-sensitive interaction between raptor and mTOR. Mol Cell *11*, 895-904.

Kino, T., Hatanaka, H., Miyata, S., Inamura, N., Nishiyama, M., Yajima, T., Goto, T., Okuhara, M., Kohsaka, M., Aoki, H.*, et al.* (1987). FK-506, a novel immunosuppressant isolated from a Streptomyces. II. Immunosuppressive effect of FK-506 in vitro. J Antibiot (Tokyo) *40*, 1256-1265.

Konicek, B.W., Dumstorf, C.A., and Graff, J.R. (2008). Targeting the eIF4F translation initiation complex for cancer therapy. Cell Cycle *7*, 2466-2471.

Lagunoff, M., Bechtel, J., Venetsanakos, E., Roy, A.M., Abbey, N., Herndier, B., McMahon, M., and Ganem, D. (2002). De novo infection and serial transmission of Kaposi's sarcoma-associated herpesvirus in cultured endothelial cells. J Virol *76*, 2440-2448.

Laman, H., Coverley, D., Krude, T., Laskey, R., and Jones, N. (2001). Viral cyclin-cyclin-dependent kinase 6 complexes initiate nuclear DNA replication. Mol Cell Biol *21*, 624-635.

Lee, J.S., Li, Q., Lee, J.Y., Lee, S.H., Jeong, J.H., Lee, H.R., Chang, H., Zhou, F.C., Gao, S.J., Liang, C.*, et al.* (2009). FLIP-mediated autophagy regulation in cell death control. Nat Cell Biol *11*, 1355-1362.

Levy, S., Avni, D., Hariharan, N., Perry, R.P., and Meyuhas, O. (1991). Oligopyrimidine tract at the 5' end of mammalian ribosomal protein mRNAs is required for their translational control. Proc Natl Acad Sci U S A *88*, 3319-3323.

Marfo, K., and Greenstein, S. (2009). Antiretroviral and immunosuppressive drug-drug interactions in human immunodeficiency virus-infected liver and kidney transplant recipients. Transplant Proc *41*, 3796-3799.

Martin, D.F., Kuppermann, B.D., Wolitz, R.A., Palestine, A.G., Li, H., and Robinson, C.A. (1999). Oral ganciclovir for patients with cytomegalovirus retinitis treated with a ganciclovir implant. Roche Ganciclovir Study Group [see comments]. N Engl J Med *340*, 1063-1070.

Mezquita, P., Parghi, S.S., Brandvold, K.A., and Ruddell, A. (2005). Myc regulates VEGF production in B cells by stimulating initiation of VEGF mRNA translation. Oncogene *24*, 889-901.

Molden, J., Chang, Y., You, Y., Moore, P.S., and Goldsmith, M.A. (1997). A Kaposi's sarcoma-associated herpesvirus-encoded cytokine homolog (vIL- 6) activates signaling through the shared gp130 receptor subunit. J Biol Chem *272*, 19625-19631.

Montaner, S. (2007). Akt/TSC/mTOR activation by the KSHV G protein-coupled receptor: emerging insights into the molecular oncogenesis and treatment of Kaposi's sarcoma. Cell Cycle *6*, 438-443.

Mutlu, A.D., Cavallin, L.E., Vincent, L., Chiozzini, C., Eroles, P., Duran, E.M., Asgari, Z., Hooper, A.T., La Perle, K.M., Hilsher, C.*, et al.* (2007). In Vivo-Restricted and Reversible Malignancy Induced by Human Herpesvirus-8 KSHV: A Cell and Animal Model of Virally Induced Kaposi's Sarcoma. Cancer Cell *11*, 245-258.

Nador, R.G., Cesarman, E., Chadburn, A., Dawson, D.B., Ansari, M.Q., Sald, J., and Knowles, D.M. (1996). Primary effusion lymphoma: a distinct clinicopathologic entity associated with the Kaposi's sarcoma-associated herpes virus. Blood *88*, 645-656.

Nicholas, J., Ruvolo, V.R., Burns, W.H., Sandford, G., Wan, X., Ciufo, D., Hendrickson, S.B., Guo, H.G., Hayward, G.S., and Reitz, M.S. (1997). Kaposi's sarcoma-associated human herpesvirus-8 encodes homologues of macrophage inflammatory protein-1 and interleukin-6. Nat Med *3*, 287-292.

O'Hara, A.J., Chugh, P., Wang, L., Netto, E.M., Luz, E., Harrington, W.J., Dezube, B.J., Damania, B., and Dittmer, D.P. (2009a). Pre-micro RNA signatures delineate stages of endothelial cell transformation in Kaposi sarcoma. PLoS Pathog *5*, e1000389.

O'Hara, A.J., Vahrson, W., and Dittmer, D.P. (2008). Gene alteration and precursor and mature microRNA transcription changes contribute to the miRNA signature of primary effusion lymphoma. Blood *111*, 2347-2353.

O'Hara, A.J., Wang, L., Dezube, B.J., Harrington, W.J., Jr., Damania, B., and Dittmer, D.P. (2009b). Tumor suppressor microRNAs are underrepresented in primary effusion lymphoma and Kaposi sarcoma. Blood *113*, 5938-5941.

O'Reilly, K.E., Rojo, F., She, Q.B., Solit, D., Mills, G.B., Smith, D., Lane, H., Hofmann, F., Hicklin, D.J., Ludwig, D.L.*, et al.* (2006). mTOR inhibition induces upstream receptor tyrosine kinase signaling and activates Akt. Cancer Res *66*, 1500-1508.

Pagano, J.S., Blaser, M., Buendia, M.A., Damania, B., Khalili, K., Raab-Traub, N., and Roizman, B. (2004). Infectious agents and cancer: criteria for a causal relation. Semin Cancer Biol *14*, 453-471.

Petre, C.E., Sin, S.H., and Dittmer, D.P. (2007). Functional p53 signaling in Kaposi's sarcoma-associated herpesvirus lymphomas: implications for therapy. J Virol *81*, 1912-1922.

Pollizzi, K., Malinowska-Kolodziej, I., Stumm, M., Lane, H., and Kwiatkowski, D. (2009). Equivalent benefit of mTORC1 blockade and combined PI3K-mTOR blockade in a mouse model of tuberous sclerosis. Mol Cancer *8*, 38.

Qin, Z., Kearney, P., Plaisance, K., and Parsons, C.H. (2010). Pivotal advance: Kaposi's sarcoma-associated herpesvirus (KSHV)-encoded microRNA specifically induce IL-6 and IL-10 secretion by macrophages and monocytes. J Leukoc Biol *87*, 25-34.

Quesniaux, V.F., Schreier, M.H., Wenger, R.M., Hiestand, P.C., Harding, M.W., and Van Regenmortel, M.H. (1988). Molecular characteristics of cyclophilin-cyclosporine interaction. Transplantation *46*, 23S-28S.

Rivas, C., Thlick, A.E., Parravicini, C., Moore, P.S., and Chang, Y. (2001). Kaposi's sarcoma-associated herpesvirus LANA2 is a B-cell-specific latent viral protein that inhibits p53. J Virol *75*, 429-438.

Russo, James J., Bohenzky, Roy A., Chien, M.-C., Chen, J., Yan, M., Maddalena, D., Parry, J.P., Peruzzi, D., Edelman, Isidore S., Chang, Y.*, et al.* (1996). Nucleotide

sequence of the Kaposi sarcoma-associated herpesvirus (HHV8). Proceedings of the National Academy of Science USA *93*, 14862-14867.

Sabatini, D.M. (2006). mTOR and cancer: insights into a complex relationship. Nat Rev Cancer *6*, 729-734.

Sabatini, D.M., Erdjument-Bromage, H., Lui, M., Tempst, P., and Snyder, S.H. (1994). RAFT1: a mammalian protein that binds to FKBP12 in a rapamycin-dependent fashion and is homologous to yeast TORs. Cell *78*, 35-43.

Sarbassov, D.D., Ali, S.M., Sengupta, S., Sheen, J.H., Hsu, P.P., Bagley, A.F., Markhard, A.L., and Sabatini, D.M. (2006). Prolonged rapamycin treatment inhibits mTORC2 assembly and Akt/PKB. Mol Cell *22*, 159-168.

Sarbassov, D.D., Guertin, D.A., Ali, S.M., and Sabatini, D.M. (2005). Phosphorylation and regulation of Akt/PKB by the rictor-mTOR complex. Science *307*, 1098-1101.

Sarek, G., Kurki, S., Enback, J., Iotzova, G., Haas, J., Laakkonen, P., Laiho, M., and Ojala, P.M. (2007). Reactivation of the p53 pathway as a treatment modality for KSHV-induced lymphomas. J Clin Invest *117*, 1019-1028.

Schwam, D.R., Luciano, R.L., Mahajan, S.S., Wong, L., and Wilson, A.C. (2000). Carboxy terminus of human herpesvirus 8 latency-associated nuclear antigen mediates dimerization, transcriptional repression, and targeting to nuclear bodies. J Virol *74*, 8532-8540.

Sedrani, R., Cottens, S., Kallen, J., and Schuler, W. (1998). Chemical modification of rapamycin: the discovery of SDZ RAD. Transplant Proc *30*, 2192-2194.

Sin, S.H., Roy, D., Wang, L., Staudt, M.R., Fakhari, F.D., Patel, D.D., Henry, D., Harrington, W.J., Jr., Damania, B.A., and Dittmer, D.P. (2007). Rapamycin is efficacious against primary effusion lymphoma (PEL) cell lines in vivo by inhibiting autocrine signaling. Blood *109*, 2165-2173.

Skalsky, R.L., Samols, M.A., Plaisance, K.B., Boss, I.W., Riva, A., Lopez, M.C., Baker, H.V., and Renne, R. (2007). Kaposi's Sarcoma-associated Herpesvirus Encodes an Ortholog of miR-155. J Virol.

Sodhi, A., Montaner, S., Patel, V., Zohar, M., Bais, C., Mesri, E.A., and Gutkind, J.S. (2000). The Kaposi's sarcoma-associated herpes virus G protein-coupled receptor up-regulates vascular endothelial growth factor expression and secretion through mitogen-activated protein kinase and p38 pathways acting on hypoxia-inducible factor 1alpha. Cancer Res *60*, 4873-4880.

Soulier, J., Grollet, L., Oksenhendler, E., Cacoub, P., Cazals-Hatem, D., Babinet, P., d'Agay, M.F., Clauvel, J.P., Raphael, M., Degos, L.*, et al.* (1995). Kaposi's sarcoma-associated herpesvirus-like DNA sequences in multicentric Castleman's disease. Blood *86*, 1276-1280.

Stallone, G., Schena, A., Infante, B., Di Paolo, S., Loverre, A., Maggio, G., Ranieri, E., Gesualdo, L., Schena, F.P., and Grandaliano, G. (2005). Sirolimus for Kaposi's sarcoma in renal-transplant recipients. N Engl J Med *352*, 1317-1323.

Stambolic, V., Suzuki, A., de la Pompa, J.L., Brothers, G.M., Mirtsos, C., Sasaki, T., Ruland, J., Penninger, J.M., Siderovski, D.P., and Mak, T.W. (1998). Negative regulation of PKB/Akt-dependent cell survival by the tumor suppressor PTEN. Cell *95*, 29-39.

Staudt, M.R., Kanan, Y., Jeong, J.H., Papin, J.F., Hines-Boykin, R., and Dittmer, D.P. (2004). The tumor microenvironment controls primary effusion lymphoma growth in vivo. Cancer Res *64*, 4790-4799.

Sun, R., Lin, S.F., Gradoville, L., Yuan, Y., Zhu, F., and Miller, G. (1998). A viral gene that activates lytic cycle expression of Kaposi's sarcoma-associated herpesvirus. Proc Natl Acad Sci U S A *95*, 10866-10871.

Tamburini, J., Chapuis, N., Bardet, V., Park, S., Sujobert, P., Willems, L., Ifrah, N., Dreyfus, F., Mayeux, P., Lacombe, C.*, et al.* (2008). Mammalian target of rapamycin (mTOR) inhibition activates phosphatidylinositol 3-kinase/Akt by up-regulating insulin-like growth factor-1 receptor signaling in acute myeloid leukemia: rationale for therapeutic inhibition of both pathways. Blood *111*, 379-382.

Tomlinson, C.C., and Damania, B. (2004). The K1 protein of Kaposi's sarcoma-associated herpesvirus activates the Akt signaling pathway. J Virol *78*, 1918-1927.

Toschi, A., Lee, E., Gadir, N., Ohh, M., and Foster, D.A. (2008). Differential dependence of hypoxia-inducible factors 1 alpha and 2 alpha on mTORC1 and mTORC2. J Biol Chem *283*, 34495-34499.

Verma, S.C., and Robertson, E.S. (2003). Molecular biology and pathogenesis of Kaposi sarcoma-associated herpesvirus. FEMS Microbiol Lett *222*, 155-163.

Vivanco, I., and Sawyers, C.L. (2002). The phosphatidylinositol 3-Kinase AKT pathway in human cancer. Nat Rev Cancer *2*, 489-501.

Wan, X., Wang, H., and Nicholas, J. (1999). Human herpesvirus 8 interleukin-6 (vIL-6) signals through gp130 but has structural and receptor-binding properties distinct from those of human IL-6. J Virol *73*, 8268-8278.

Wang, L., and Damania, B. (2008). Kaposi's sarcoma-associated herpesvirus confers a survival advantage to endothelial cells. Cancer Res *68*, 4640-4648.

Wang, L., Wakisaka, N., Tomlinson, C.C., DeWire, S.M., Krall, S., Pagano, J.S., and Damania, B. (2004). The Kaposi's sarcoma-associated herpesvirus (KSHV/HHV-8) K1 protein induces expression of angiogenic and invasion factors. Cancer Res *64*, 2774-2781.

Waterston, A., and Bower, M. (2004). Fifty years of multicentric Castleman's disease. Acta Oncol *43*, 698-704.

Yang, S.X., Hewitt, S.M., Steinberg, S.M., Liewehr, D.J., and Swain, S.M. (2007). Expression levels of eIF4E, VEGF, and cyclin D1, and correlation of eIF4E with VEGF and cyclin D1 in multi-tumor tissue microarray. Oncol Rep *17*, 281-287.

Zebrowski, B.K., Yano, S., Liu, W., Shaheen, R.M., Hicklin, D.J., Putnam, J.B., Jr., and Ellis, L.M. (1999). Vascular endothelial growth factor levels and induction of permeability in malignant pleural effusions. Clin Cancer Res *5*, 3364-3368.

Zeng, Z., Sarbassov dos, D., Samudio, I.J., Yee, K.W., Munsell, M.F., Ellen Jackson, C., Giles, F.J., Sabatini, D.M., Andreeff, M., and Konopleva, M. (2007). Rapamycin derivatives reduce mTORC2 signaling and inhibit AKT activation in AML. Blood *109*, 3509-3512.

Zitzmann, K., Ruden, J., Brand, S., Goke, B., Lichtl, J., Spottl, G., and Auernhammer, C.J. (2010). Compensatory activation of Akt in response to mTOR and Raf inhibitors - a rationale for dual-targeted therapy approaches in neuroendocrine tumor disease. Cancer Lett *295*, 100-109.

CHAPTER II

PHOSPHATASE AND TENSIN HOMOLOG ON CHROMOSOME 10 (PTEN) IS INACTIVATED BY PHOSPHORYLATION IN PRIMARY EFFUSION LYMPHOMA AND KAPOSI'S SARCOMA

Debasmita Roy and Dirk P. Dittmer

This work is under revision for publication at American Journal of Pathology

ABSTRACT

Primary Effusion Lymphoma (PEL) is a non-Hodgkin B-cell lymphoma that is driven by Kaposi sarcoma associated herpesvirus (KSHV) and uniquely sensitive to mTOR, PI3K and Akt inhibitors. Yet, the basis of this addiction to the mTOR pathway remains to be elucidated. The phosphatase and tensin homolog on Chromosome 10 (PTEN) controls the first step in the PI3K/Akt/mTOR pathway and is genetically inactivated in many solid tumors. I found an absence of germline PTEN mutations or de-localization in PEL. However, consistent hyperphosphorylation at Serine 380 of PTEN, which has previously been shown to be an inactivating modification, was detected in culture and tumor xenografts. I also evaluated a tissue microarray of Kaposi sarcoma primary biopsies and observed high levels of PTEN expression. Introduction of PTEN into PEL inhibited colony formation in soft agar verifying functionally the dependence of PEL on PI3K signaling. This was also true for PEL cell lines that carried mutant p53. Activating PTEN in these cancers may yield a new treatment strategy for PEL, KS and similar, PTEN wild-type lymphomas.

INTRODUCTION

Primary Effusion Lymphoma (PEL) was initially identified as an AIDS associated non-Hodgkin's lymphoma with poor prognosis(Cesarman et al., 1995a). PEL also occurs in non-AIDS patients, specifically transplant recipients on immune suppressive drugs (Dotti et al., 1999; Matsushima et al., 1999). PEL is tightly associated with Kaposi's Sarcoma-associated Herpes Virus (KSHV) infection (Dotti et al., 1999; Matsushima et al., 1999; Nador et al., 1996). KSHV, also known as Human Herpes Virus 8 (HHV8), is a human virus with a primary tropism for B cells and endothelial cells. In addition to KSHV, PEL cells can be co-infected with Epstein Barr Virus (EBV) (Horenstein et al., 1997).

KSHV is also the causative agent of Kaposi's Sarcoma (KS), a tumor of endothelial cell lineage. KS is characteristically found in AIDS patients, but is also detected in other settings of immune suppression such as solid organ transplant recipients (Chang et al., 1994). Stallone et al. reported on transplant patients who developed KS. Upon switching from cyclosporine to the equally potent immunosuppressant, Sirolimus™/ Rapamycin, the lesions regressed (Stallone et al., 2005). Since then multiple reports have repeated this experience. Rapamycin binds to and inhibits the activity of mammalian target of Rapamycin complex-1 (mTORC1) (Kahan, 2001).

mTORC1 is a downstream effector of the phosphatidylinositol-3-kinase (PI3K) signaling cascade. Phosphorylation of receptor tyrosine kinases (RTKs) result in activation of the p110 catalytic subunit of PI3K, which then phosphorylates membrane associated phospholipid phosphatidylinositol (3,4-) biphosphate (PIP_2) to phosphatidylinositol(3,4,5-)triphosphate (PIP_3). PIP_3 then recruits Akt to the plasma

membrane. Akt is phosphorylated at Serine 473 by mTOR-Complex 2 (mTORC2) as well as by PI3K-dependent kinase 1 (PDK1) at Threonine 308. Activated Akt then phosphorylates downstream targets, with mTORC1 being one of the key effectors (Cully et al., 2006; Hay, 2005; Sabatini, 2006; Stambolic et al., 1998; Vivanco and Sawyers, 2002).

It was previously reported that Rapamycin inhibits PEL in culture, in a mouse model and in a patient (Sin et al., 2007). The reason for mTORC1 activity in PEL is the subject of research. KSHV proteins may activate mTORC1 through cellular receptor engagement (by vIL6), or PI3K activation (by viral proteins like vGPCR and K1)(Damania, 2004; Montaner, 2007; Tomlinson and Damania, 2004). Here I examined whether in addition to viral factors, host genetic aberrations in the phosphatase and tensin homolog on Chromosome 10 (PTEN) contributed to PI3K/Akt/mTORC signaling.

PTEN can revert PIP_3 to PIP_2 and thereby counteracts the activation of Akt by PDK1 (Carrasco et al., 2006; Cloughesy et al., 2008; Cully et al., 2006; Hyun et al., 2000; Li et al., 1997; Neshat et al., 2001; Sarbassov et al., 2006; Stambolic et al., 1998; Steelman et al., 2008). PTEN is located on chromosome 10, specifically 10q23, and frequently mutated in human cancers (Carrasco et al., 2006; Cloughesy et al., 2008; Hyun et al., 2000; Li et al., 1997; Neshat et al., 2001; Stambolic et al., 1998; Steelman et al., 2008). Ectopic expression of PTEN in tumor cells results in cell cycle arrest or apoptosis (Chang et al., 2008; Liu et al., 2007). PTEN exists either in a hypo- or hyper-phosphorylated state corresponding to its active (open) and inactive (closed) enzymatic states, respectively. PTEN expression and PTEN phosphorylation status thus serve as markers for PTEN activity.

MATERIALS AND METHODS:

Cell culture B-cell lines were cultured in RPMI 1640 or DMEM supplemented with 100 μg/ml streptomycin sulphate, 100 U/ml penicillin G (Life Technologies, Carlsbad, CA, USA), 2 mM L-glutamine, 0.05 mM 2-mercaptoethanol, 0.075% sodium bicarbonate, 1 U/ml IL-6 (PeproTech Inc. Rock Hill, NJ, USA) and 10% FBS at 37°C in 5% CO_2. Cell lines used are listed in Table II.1.(Arvanitakis et al., 1996; Ben-Bassat et al., 1977; Boshoff et al., 1998; Brander et al., 2000; Cannon et al., 2000; Cesarman et al., 1995b; Ghosh et al., 2003; Guasparri et al., 2004; Katano et al., 1999; Komanduri et al., 1996; Menezes et al., 1975)

Sequencing Genomic DNA was isolated using the Wizard Genomic DNA Purification kit (Promega Co. Madison, WI, USA). PCR amplification was performed using GoTaq™ PCR master mix (Promega Co., Madison, WI). Specific primers, flanking individual exons, used from (Carrasco et al., 2006; van Hattem et al., 2008) are listed in Table II.2. The amplified fragments were subjected to Sanger sequencing.

Immunoblot Analysis 1-5 x 10^6 cells were analyzed by Western-Blot as described previously (Sin et al., 2007) For cell fractionation I used the ProteoExtract® Subcellular Proteome Extraction Kit (EMD Chemicals Inc., NJ, USA) as per manufacturer's protocol. The primary antibodies were Rabbit anti-PTEN, Rabbit anti-phospho-PTEN (S380) (Cell Signaling, MA, USA)) diluted 1:1000 in blocking solution; horseradish-peroxidase conjugated secondary antibody (Vector Labs, Burlingame, CA, USA) diluted 1:5000. I used HRP-conjugated anti-actin mAb (Abcam Inc., Cambridge, MA, USA) at 1:10,000 dilution or mouse anti-β-actin (Sigma Aldrich, Inc., St Louis,

MO, USA) at 1:3000. Ratio of phosphorylated to total PTEN was quantified using ImageJ (v10.2) analysis software.

Immunofluorescence. Cells were cultured overnight on glass coverslips in 6-well plates (Falcon-BD Biosci. Inc, San Jose, CA, USA). They were then washed in PBS followed by protocol for immune fluorescence as described (Chen et al., 2010). Primary antibodies used include: rabbit anti-PTEN, rabbit anti-phospho-PTEN (S380) (Cell Signaling, MA) diluted 1:100 and mouse anti-LANA (Novocastra Lab Ltd., Newcastle, UK), diluted 1:600. Images were taken on LEICA DM4000B fluorescence microscope (Leica, Heidelberg, Germany) equipped with a 63/1.4-0.6 numerical aperture (NA) objective and a Q-Imaging Retiga 2000RV camera. Raw single microscopy images were deconvoluted using Simple PCI™ (Hamamatsu Corp., Sewickley, PA, USA) 2D Blind Deconvolution that iteratively applies AutoQuant Imaging (Media Cybernetics, Inc. Bethesda, MD, USA) proprietary algorithm to remove blur and generate high clarity images, stored as tiff files.

Immunohistochemistry Solid tumors were removed from SCID mice injected sub-cutaneously with BC-1 cells in growth factor-reduced Matrigel™ as per published.(Sin et al., 2007) Primary KS biopsy Tissue MicroArray (TMA) was obtained from the AIDS Cancer Specimen Resource (ACSR). All sections were processed as per our prior publications(Sin et al., 2007; Staudt et al., 2004) using following primary antibodies: Rab anti-total PTEN at 1:100 dil (Cell Signaling, Boston, MA), Rab anti-phospho-PTEN Serine 380 at 1:50 dil. (Millipore Co., Billerica, MA) and Rab anti-phospho-Akt Threonine 308 at 1:50 dil. (Cell Signaling, Boston, MA). Sections were imaged using a LEICA DM LA histology microscope (Leica, Heidelberg, Germany)

equipped with a 10/0.25 numerical aperture (NA) or a 40/0.75 NA N plan objective and Leica DPC 480 camera. Images were stored as TIFF files under Mac OS X10.5.

Growth Suppression Assay The human PTEN cDNA, pORF_hPTEN, was obtained from InvivoGen Inc. (San Diego, CA, USA) and cloned into pMONO-blasti-mcs (InvivoGen Inc., CA) under control of the constitutive ferritin promoter to yield pMONO-blasti-hPTEN. The construct was verified by restriction analysis and two independent clones, #1 and #7, (pDD1540 and pDD1541 respectively) were used for further analysis. pMONO-blasti-mcs carries the Blasticidin™ selection marker. DNA was introduced into PEL cells by nucleofection, as per manufacturer's protocol (Lonza, Switzerland). The cells were nucleofected and recovered in complete media overnight before plating them in 0.3% on an 0.5% soft agar in complete RPMI media supplemented with 6 ug/ml of Blasticidin (selection marker) and growth was assessed 2-3 weeks later. In the case of endothelial SLK cells, cells were transfected using SuperFect Transfection Reagent (Qiagen Inc., Valencia, CA, USA) following manufacturer's protocol and plated on 10 cm dishes. Colonies were allowed to form over a period of two weeks and stained with 200x Magic Stain (3g Crystal Violet and 0.8 g Ammonium Oxalate in 20%ethanol) diluted to ~10x in water and counted.

RESULTS

The PTEN gene is wild type in PEL

To determine whether PEL carry gross genomic abnormalities at the PTEN locus, each of the nine exons of the PTEN gene (Figure II.1, panel A) was amplified individually from ten PEL and two non-PEL lymphoma cell lines. This represents almost

all PEL cells lines that can successfully grow in culture. These PEL cell lines form tumors in immune deficient mice ((Sin et al., 2007; Staudt et al., 2004) and Roy unpublished). Figure II.1, panel B is a representative gel showing the presence of all nine exons in BCBL-1 cells. I was unable to find gross deletions of any of the PTEN exons in any of the ten independent PEL. Further, I performed Affymetrix 500K SNP and gene copy number analysis for these PEL and did not detect any loss of heterozygosity associated amplifications or deletions associated with the PTEN locus (data not shown).

Next, individual PTEN exons were sequenced for each PEL cell line. With the exception of BC-1, I was unable to detect any aberrations in the genomic sequence (data submitted to genbank, Submission ID 1367943). In BC-1, I detected a base pair transversion mutation, G1282C resulting in an Arginine (R) to Threonine (T) (R84T) change at the amino acid level. Taken together, I concluded that genetic aberrations of PTEN are infrequent in PEL.

The PTEN protein is expressed and hyper-phosphorylated in PEL

There are reports in the literature suggesting epigenetic silencing of PTEN in cancer (Carrasco et al., 2006; Parsons, 2004). Thus I wanted to determine whether PTEN mRNA and protein itself was expressed in PEL. Using RT-PCR PTEN mRNA was shown to be present in all of the PEL cell lines (data not shown) thereby eliminating the possibility of promoter silencing.

Next, I used Western Blot analysis to detect phosphorylated (Serine 380) and total PTEN protein. PTEN protein was detectable at the appropriate molecular weight (~54kDa) in every PEL cell lines at similar levels to those observed in HEK293 positive

control cells. Figure II.1, panel C shows a representative blot comprising majority of the cell lines, including BC-1. Phosphorylated PTEN (Ser380) was also detected in all PEL (Figure II.1, panel D). As negative control I used PTEN null BJAB cells (Sarbassov et al., 2006). To investigate the localization of PTEN, immunofluorescence staining was used. Independent of its phosphorylation status, PTEN, stained in green, was found both in the nucleus and cytoplasm (Figure II.1, panel E). I used KSHV-LANA staining in red as a positive nuclear control (Kedes et al., 1997). LANA was distributed in the characteristic nuclear speckles (Figure II.1, panel E). There was no co-localization between PTEN and LANA, irrespective of PTEN phosphorylation status.

PTEN becomes inactive upon phosphorylation at Serine 380 thereby unable to dephosphorylate PIP_3 to PIP_2 (Vivanco and Sawyers, 2002). A scattered distribution of phosphorylated PTEN (Ser380), shown in green, (Figure II.1, panel F) was observed. Analogous to our previous Western-Blot analysis, comparable levels of phosphorylated to total PTEN were detected. This is consistent with our hypothesis that PTEN is inactivated via phosphorylation in PEL. Localization of PTEN also determines its cellular function (Chung and Eng, 2005). To verify our immunofluorescence data, I used immunoblot analysis of cell fractions (data not shown). Both PTEN and phospho-PTEN were detected in the same compartments. Irrespective of the localization of PTEN, I always detected comparable amounts of phosphorylated and total PTEN.

Phospho-PTEN is readily detectable in PEL xenograft tumors

To test the hypothesis that the phosphorylation status of PTEN is maintained within a more demanding, less nutrient-rich, tumor microenvironment the expression of

phospho-PTEN in established PEL tumor graft models was assessed using immunohistochemistry (Boshoff et al., 1998; Picchio et al., 1997; Staudt et al., 2004). Sections of PEL xenograft tumors were stained for total (Figure II.2, panels B, F) and phospho-PTEN (Figure II.2, panels D, H). Phospho-PTEN was expressed in every tumor cell. The staining pattern of total PTEN matched that of phospho-PTEN (Figure II.2) and there was no evidence of heterogeneity. Figure II.2, panels A, C, E and G, represent no antibody controls that show the absence of staining for both total and phosphorylated PTEN. This demonstrates that the high phosphorylation status of PTEN is not a result of optimal (10% serum) growth conditions, but that it is maintained even as PEL grow in the much more demanding xenograft microenvironment.

Expression of PTEN reduces of colony formation in PEL

To test the hypothesis that inactive PTEN contributes to hyperactivation of Akt and PEL proliferation, human PTEN (hPTEN) was ectopically expressed in PEL and evaluated its effect on cell growth. If PEL evolved downstream mutations (e.g. activating mutations in Akt) to be resistant to the activity of PTEN, continued growth would be expected. Instead, PTEN reduced colony formation in soft agar as determined independently in three distinct PEL cell lines (BC1, BCBL1, BCP1) with varying p53 mutant status (Petre et al., 2007). Figure II.3 shows a representative experiment where fewer colonies were formed by PTEN overexpressing BCP1 cells (panel B) compared to vector only control (panel A). $1/10^{th}$ amount of EGFP-Max plasmid (Lonza, Switzerland) was nucleofected in tandem with vector and hPTEN plasmids, thus GFP expression was used to demonstrate equivalent efficiency of nucleofection. (Figure II.3, panels C and D

represent the bright field and fluorescence images respectively). PTEN expression upon nucleofection was verified using BJAB cells, since they lack endogenous PTEN (Figure II.3, panel E). PTEN was expressed at the appropriate molecular weight only upon nucleofection of hPTEN but not vector control. Figure II.3, panel F quantifies the inhibition of colony formation ($p \leq 0.005$ by Wilcoxon-signed Rank test) in our representative BCP1 cells. This functional assay demonstrates that the signaling components downstream of PTEN still respond to PTEN and that PTEN phosphorylation controls activation of the PI3K/Akt/mTOR pathway in PEL.

PTEN is expressed in primary KS tumor biopsies

In addition to PEL, KSHV is also the causative agent of KS, which is a tumor of endothelial cell lineage. I hypothesized that this cancer, too, would inactivate PTEN by phosphorylation. I used the SLK cell line, derived from KS biopsy, to test effect of introducing PTEN on cell growth. As with PEL a significant reduction was noted in the number of colonies formed (Figure II.3, panel F). Figure II.3, panels G, H and I, show colony formation of SLK cells upon transfection with vector or two independent plasmids expressing hPTEN, respectively.

To verify PTEN phosphorylation status in vivo, I utilized the KS Tissue Microarrays (TMA). 141 out of 176 (80%) cases stained positive for PTEN and 75 out of 130 (58%) positive for phospho-PTEN (S380). Figure II.4, panels A and B show staining for total and phospho-PTEN (S380) in three representative skin KS biopsies. Interestingly 87 out of 176 (50%) also stained positive for phosphorylated Akt (T308), i.e. many KS tumors exhibit activated Akt despite robust PTEN expression. Figure II.4 panel C, shows

staining for phosphorylated Akt, at Threonine 308, which requires PI3K activation. Where total PTEN was detected in the normal control lung sample, it did not detect positive stain for phospho-PTEN or activated Akt, as would be expected for normal cells. The skin KS is a representative sample, where PTEN, phospho-PTEN and phospho-Akt (T308) was detected in the same biopsy. No staining was observed in the no primary antibody control (figure II.4, panel D). These data support the hypothesis that analogous to PEL, in KS, the tumor suppressor PTEN is not deleted but post-translationally inactivated to allow phosphorylation of Akt.

DISCUSSION

Activation of the PI3K-Akt-mTOR signaling cascade is a defining phenotype of the KSHV-associated cancers: PEL and KS. Clinically KS (Stallone et al., 2005) as well as PEL (Henry and Dittmer, unpublished) respond to Rapamycin. Other virus-associated lymphoproliferative diseases such as EBV-associated post transplant disease (PTLD) also rely on the mTORC1 pathway (Majewski et al., 2000; Wlodarski et al., 2005) and respond to mTOR inhibitors. To activate this pathway, either a positive regulator has to be hyperactivated, or a negative regulator has to be inactivated, or both. To date most studies on PEL have concentrated on positive regulators of the PI3K-Akt-mTOR pathway. In this report, I investigated the principal negative regulator of PI3K-Akt-mTOR signaling: the tumor suppressor PTEN.

PTEN antagonizes PI3K in the first step in the PI3K-Akt-mTOR cascade, by de-phosphorylating PIP_3 back to PIP_2. Diminished PTEN activity in human cancer results in hyperactivation of the PI3K signaling pathway: a condition that has also been termed

oncogene addiction to PI3K/Akt/mTOR. In non-viral tumors PTEN is typically inactivated by mutation. The PTEN gene is deleted in many solid tumors (Wendel et al., 2006) and in about 40% of cell lines derived from prostate, endometrial and nervous system cancers (http://www.sanger.ac.uk/perl/genetics/CGP).

The situation is different in viral lymphoma. Our data show that KSHV-associated PEL invariably express high levels of PTEN protein (Figure II.1) and at the same time exhibit high levels of phosphorylated Akt (Sin et al., 2007). The same seemingly contradictory pattern of staining was observed in KS biopsies (Figure II.4). I found no evidence of point mutations in PEL cell lines, or of mis-localization. Rather PTEN appeared hyper-phosphorylated in PEL and KS. Furthermore, it was shown that ectopic expression of PTEN in PEL or KS-tumor derived cell lines inhibited colony formation (Figure II.3). This suggests that downstream mediators of the PI3K/Akt/mTOR pathway cannot override the growth inhibitory signal of PTEN in PEL and KS. This phenotype is in contrast to the behavior of cells carrying activating mutations in downstream mediators e.g. in Akt (Radu et al., 2003; Van de Sande et al., 2002).

Boulanger et al. (Boulanger et al., 2009) reported similarly in the absence of PTEN mutations in archived biopsies from PEL patients. Yet, found mutations in some of their PEL cell lines. For instance, they reported a homozygous deletion of PTEN exons 6-9 in the BCP-1 cell line, whereas PTEN protein was detectable in this cell line. Uddin et al. (Uddin et al., 2005) also detected PTEN protein in the BCP-1 cell line. Discrepancies like this are not unexpected as PEL cell lines change upon passage in culture (Roy and Dittmer, unpublished). BCP-1 is unique among PEL, since it carries homozygous mutant

p53 and would thus be expected to be less genetically stable than other PEL cell lines, all of which carry wild-type p53 (Abbott et al., 2003).

At present the identity of the kinase capable of phosphorylating PTEN in PEL remains unknown. KSHV proteins may mediate the phosphorylation of PTEN. Alternatively, Casein Kinase 2 (CK2), Glycogen Synthase Kinase 3β (GSK3β), LKB1, RhoA-associated kinase (ROCK) have all been implicated in PTEN phosphorylation (Al-Khouri et al., 2005). However, the KSHV LANA protein can bind and sequester GSK3β in the nucleus (Fujimuro and Hayward, 2003), which would eliminate GSK3β from mediating PTEN phosphorylation in PEL. Further studies are needed to elucidate the players in phosphorylation of PTEN in KSHV-associated malignancies.

What is the significance of our findings? Viral cancers express viral oncogenes. Viral lymphomas in particular express viral oncoproteins that impact the PI3K/Akt/mTOR pathway. Several KSHV proteins, such as K1 and vGPCR, activate PI3K (Damania, 2004; Montaner, 2007; Tomlinson and Damania, 2004). This would lessen the selective pressure to mutate and genetically inactivate PTEN. Epstein-Barr Virus (EBV), a closely related member of KSHV, is capable of silencing PTEN protein expression by CpG island and promoter methylation in gastric cancers (Hino et al., 2009; Kang et al., 2002), whereas no such observation has been reported for EBV-associated lymphomas. KSHV has chosen to silence PTEN protein function by constitutive phosphorylation. In addition, there are two reports of non-viral lymphomas, which also inactive PTEN post-translationally: cases of Mantle Cell Lymphoma (MCL) and some T-cell acute lymphoblastic leukemia (T-ALL) show hyperactivation of PI3K in the context of wild-type PTEN (Dal Col et al., 2008; Silva et al., 2008). What seems the default

route for viral lymphomas (post-translational or epigenetic inactivation of PTEN) is also seen in the evolution of non-viral cancers. It is intriguing that of all non-Hodgkin lymphomas only MCL shows clinical response to mTOR inhibitiors (Hess et al., 2009). If confirmed in a clinical trial I hypothesize that phospho-PTEN expression may serve as a novel biomarker for Rapamycin sensitivity of human cancers.

A key finding of this report is that expression of wild-type PTEN in PEL inhibited growth in semi-solid medium (Figure II.3). This implies that adding back PTEN can revert virus- and/or cell-induced Akt activation (Radu et al., 2003; Van de Sande et al., 2002). This result fuels the speculation that PTEN activation by small molecules may present a novel treatment modality for wild-type PTEN tumors, similar to the rationale that p53 activation by Nutlin-3 (Petre et al., 2007; Sarek et al., 2007) may present a treatment modality for post-translationally-inactivated, but genetically wild-type p53 cancers.

ACKNOWLEDGMENTS

This work was supported by NIH grant DE018304, the AIDS Malignancy Consortium (CA70058) and the Leukemia Lymphoma Society. I thank B. Damania and her lab for helpful discussion and critical reading. I apologize to our colleagues whose work could not be cited due to space limitations.

FIGURES

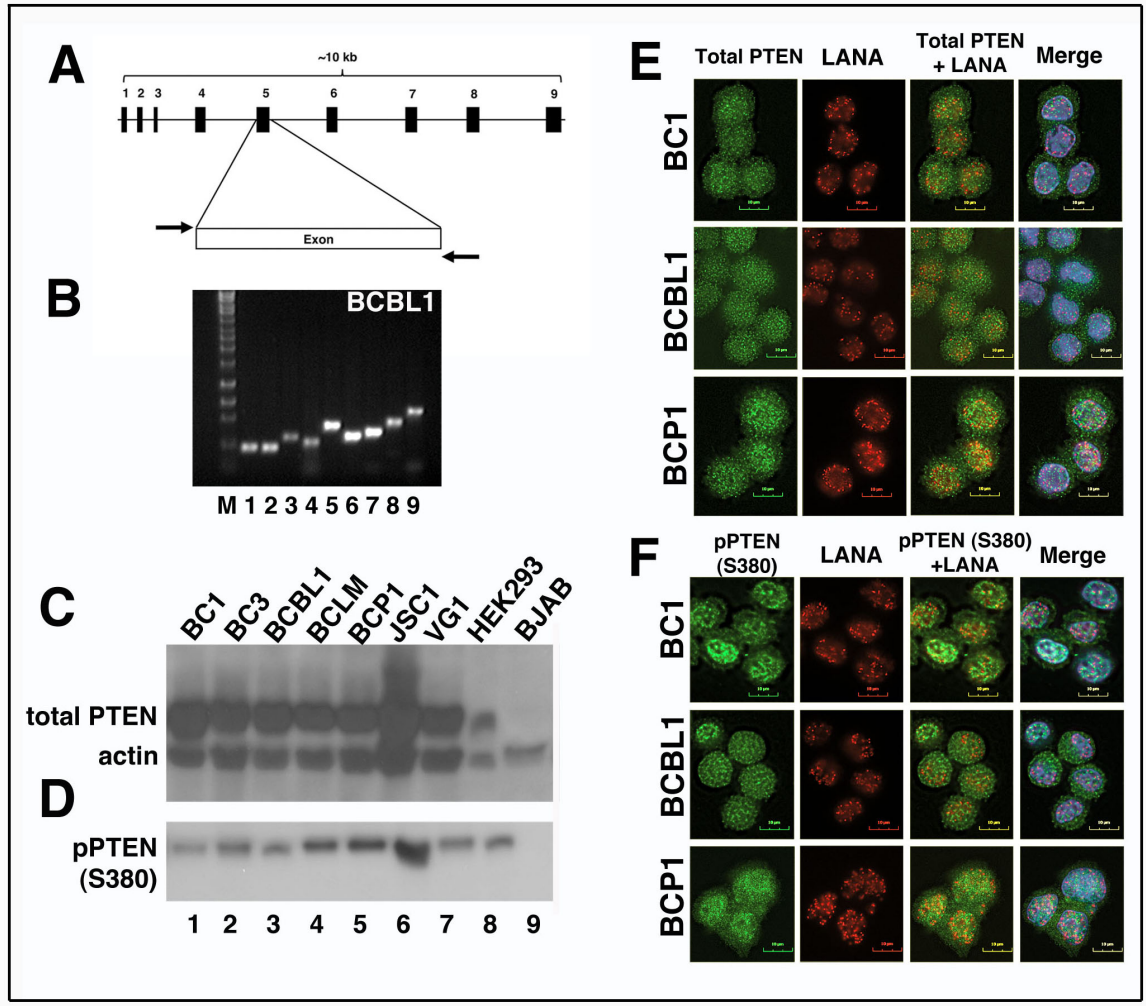

Figure II.1: Comparable levels of total and phospho-PTEN were detected in PEL in culture, localizing both to the nucleus and cytoplasm

Genomic DNA was isolated from PEL cell lines and each of the exons was amplified using specific primers, as outlined in Table II.2. Figure II.1, panel A shows a schematic of the organization of the primers used and Panel B a representative PCR gel, specifically detection of all nine exons in BCBL-1 cells.

Immunoblots were performed on protein isolated from whole cell lysate. Panel C shows the total PTEN immunoblot where beta-actin was used as loading control and Panel D shows the phosphorylated PTEN in the respective cells, equivalent amounts of protein was loaded as in Panel C.

Immunofluorescence analysis was used to verify the Immunoblot results and map the distribution of total and phosphorylated PTEN in representative PEL cells with varying p53 status. Panel E shows distribution of total PTEN throughout the nucleus and cytoplasm. We performed double IFA with total PTEN (green) and LANA (red) to note that there is no co-localization of the two even though we show presence of PTEN in the nucleus. Panel F shows the punctate distribution of phosphorylated PTEN throughout the cell, analogous to total PTEN. All cells were counterstained with DAPI (blue) for the nucleus and images were generated using different optical filters using Adobe Photoshop software suite. All images are shown at 63X magnification using oil immersion.

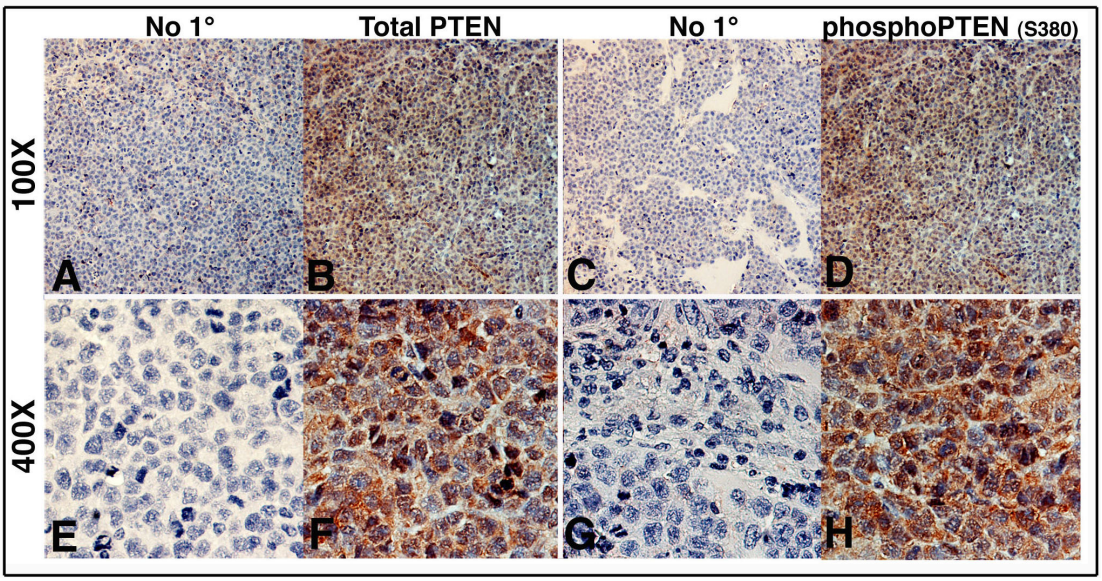

Figure II.2: Immunohistochemical analysis of PEL xenograft tumors shows similar localization of total and phospho-PTEN

BC-1 xenograft tumor sections were stained for either total or phosphorylated PTEN (red) and counterstained using hematoxylin (blue) that identifies the nucleus. Sections shown were incubated either with dilution buffer (no primary antibody) or with primary antibody (1:100 dilution) in dilution buffer. No staining, red, was observed in the no primary antibody control. Images were taken either at 100X or 400X magnification.

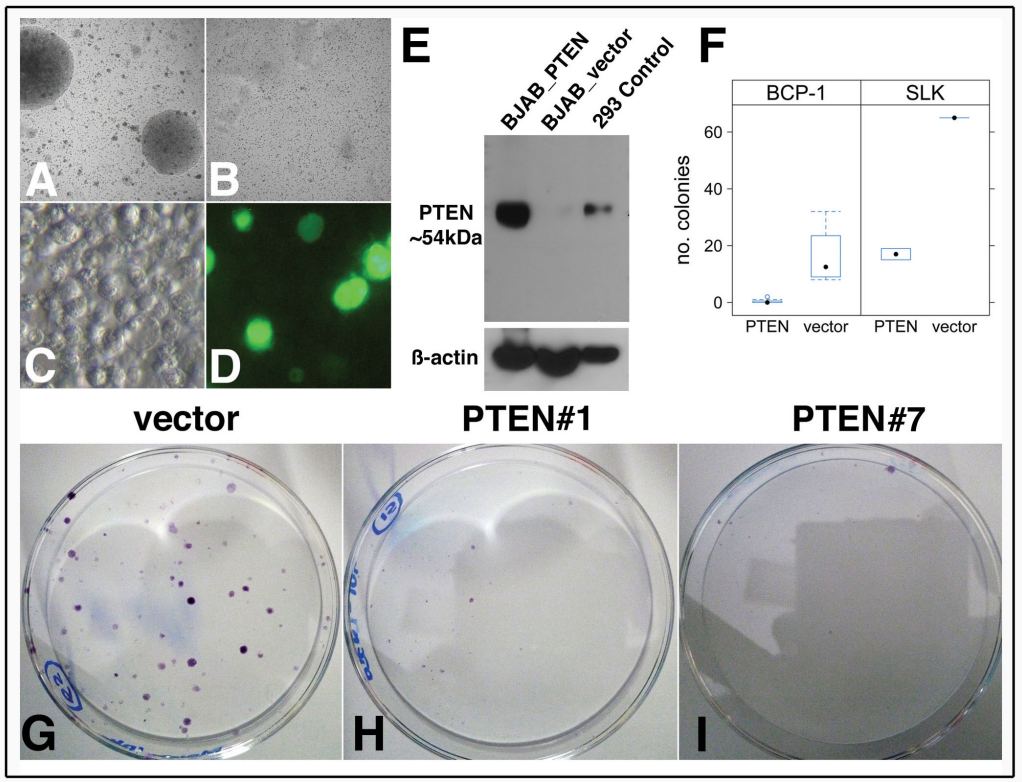

Figure II.3: Growth suppression of BCP-1 and SLK cells by exogenous PTEN

Human PTEN construct was cloned in the pMONO-blasti expression vector as outlined in the methods section and growth was monitored post-expression using colony formation assay. Panel A shows the formation of colonies in soft agar that disappear upon overexpression of PTEN in BCP-1 cells, panel B shows the huPTEN clone #1. Panels C and D represent GFP positive control for nucleofection in bright light and fluorescence fields, respectively. Panel E shows the expression of protein in PTEN null BJAB cells upon expression of the huPTEN clone #1 only and not the vector control. Panel F represents the quantification of colonies observed in both BCP-1 and SLK cells. Panels G, H and I show the inhibitory effect of colony formation upon overexpression of huPTEN, clones 1 and 7, in SLK cells over vector control.

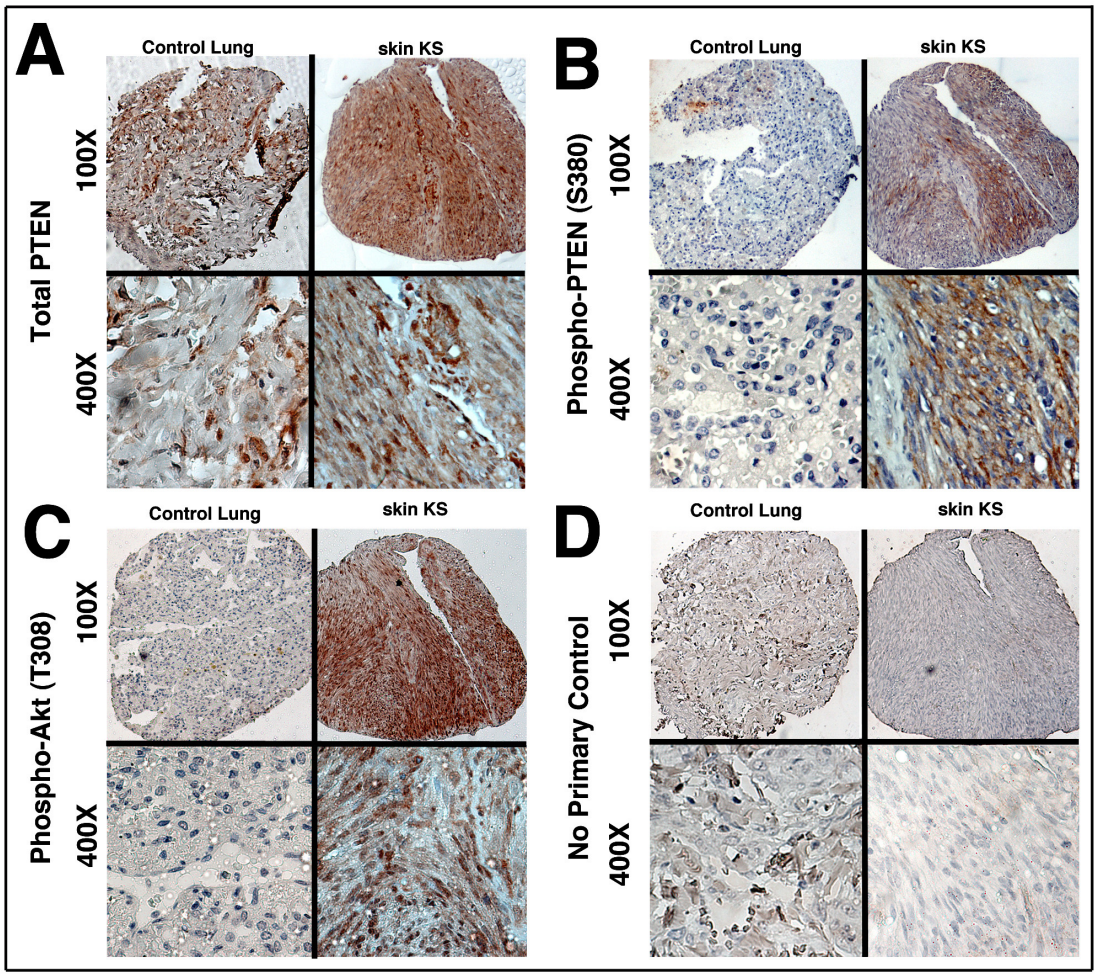

Figure II.4: Expression of total PTEN, phospho PTEN (S380) and phospho-Akt (T308) in KS primary biopsies by immunohistochemistry

Panels A, B, C and D shows the presence of total PTEN, phospho-PTEN(S380), phospho-Akt at T308 (a PI3K dependent site) and no primary antibody negative control, respectively, at 100x and 400x magnifications. The left images on each panel indicate the control lung tissue that does only stains positively for PTEN but not for phospho-PTEN(S380) or phospho-Akt (T308). The sample on the right indicates a representative biopsy where the same tissue section stained positive for total PTEN, phospho-PTEN(S380) and phospho-Akt (T308).

Table II.1: Summary of PEL Cells Lines Used in PTEN Sequencing

Cell Line	Lymphoma Type	KSHV	EBV	p53	PTEN	GenBank Accession ID	Reference for cell line
BC1	PEL	+	+	Wild type	R84T	>H.sapiens_PEL_BC1_PTEN_CDS	Cesarman, E., et. al. Blood, 1995
BC2	PEL	+	+	Wild type	Wild type	>H.sapiens_PEL_BC2_PTEN_CDS	Cesarman, E., et. al. Blood, 1995
BC3	PEL	+	-	Wild type	Wild type	>H.sapiens_PEL_BC3_PTEN_CDS	Arvanitakis, L., et. al. Blood, 1996
BC5	PEL	+	+	Wild type	Wild type	>H.sapiens_PEL_BC5_PTEN_CDS	Guasparri, I., et. al. J Exp Med, 2004
BCBL1	PEL	+	-	M246I; hetero-zygous mutation	Wild type	>H.sapiens_PEL_BCBL1_PTEN_CDS	Komanduri, K.V., et. al. J AIDS Hum Retrovirol,

							1996
BCLM	PEL	+	-	Wild type	Wild type	>H.sapiens_PEL_BCLM_PTEN_CDS	Ghosh, S.K., et. al. Blood, 2003
BCP1	PEL	+	-	S262; homo-zygous insertion	Wild type	>H.sapiens_PEL_BCP1_PTEN_CDS	Boshoff, C., et. al. Blood, 1998
BJAB	Burkitt's	-	-	Deletion; non-functional	Null	>H.sapiens_Lymphoma_BJAB_PTEN_CDS	Menezes, J., et. al. Biomedicine, 1975
DG75	Burkitt-like	-	-		Wild type	>H.sapiens_Lymphoma_DG75_PTEN_CDS	Ben-Bassat, H., et. al. Int J Can, 1977
JSC1	PEL	+	+	Wild type	Wild type	>H.sapiens_Lymphoma_JSC1_PTEN_CDS	Cannon, J.S., et. al. J Virol, 2000
TY1	PEL	+	-	S262 insertion; M246I	Wild type	>H.sapiens_Lymphoma_TY1_PTEN_CDS	Katano, H., et. al. J Med Virol, 1999
VG1	PEL	+	-	Wild type	Wild type	>H.sapiens_Lymphoma_VG1_PTEN_CDS	Brander, C., et. al. J Immunol, 2000

Table II.2: Primer Sequence and Annealing Temperature for PTEN PCR Analysis

	Forward Primer (5' → 3')	**Reverse Primer (5' → 3')**	**Annealing Temperature**
Exon 1	ATTTCCATCCTGCAG AAGAAGC	CATCCGTCTACTCCC ACGTTCT	55°C
Exon 2	AGTTTGATTGCTGCA TATTTCAGA	TCTTTTTCTGTGGCT TAGAAATCTTTT	55°C
Exon 3	ATGGTATTTGAGATT AGGAA	TGGACTTCTTGACTT AATCGGTTT	55°C
Nested Exon 4 - *Outer*	GTTAAACACAGCATA ATATGTGTCACATT	TTAAAGATAATTCT TAAAT	51°C
Nested Exon 4- *Inner*	AAAGATTCAGGCAA TGTTTGTTAGT	TGTATCTCACTCGAT AATCTGGATG	51°C
Alternate Exon 4	CATTATAAAGATTCA GGCAATG	GACAGTAAGATACA GTCTATC	58°C
Exon 5	ATCCAGTGTTTCTTT TAAATA	ATCTGTTTTCCAATA AATTCT	55°C
Exon 6	CTAATGTATATATGT TCTTAA	CTTCTAGATATGGTT AAGAAA	50°C
Exon 7	GTATATTGCTGATAT TAATCATT	ATTATAGTTCCTTAC ATGTCA	55°C
Exon 8	TTTTGGGTAAATACA	CGCACCTTTGCCCC	55°C

	TTCTT	AGAT	
Alternate Exon 8	TGTCATTTCATTTCTT TTTCTTTTC	AAGTCAACAACCCC CACAAA	56°C
Exon 9	TGTTGAACATCTTAA GAAGA	ATGACACAGCTACA CAACCTT	55°C
RT PCR for mRNA	CGAACTGGTGTAATG ATATGT	CATGAACTTGTCTTC CCGT	60°C

REFERENCES

Abbott, R.T., Tripp, S., Perkins, S.L., Elenitoba-Johnson, K.S., and Lim, M.S. (2003). Analysis of the PI-3-Kinase-PTEN-AKT pathway in human lymphoma and leukemia using a cell line microarray. Mod Pathol *16*, 607-612.

Al-Khouri, A.M., Ma, Y., Togo, S.H., Williams, S., and Mustelin, T. (2005). Cooperative phosphorylation of the tumor suppressor phosphatase and tensin homologue (PTEN) by casein kinases and glycogen synthase kinase 3beta. J Biol Chem *280*, 35195-35202.

Arvanitakis, L., Mesri, E.A., Nador, R.G., Said, J.W., Asch, A.S., Knowles, D.M., and Cesarman, E. (1996). Establishment and characterization of a primary effusion (body cavity- based) lymphoma cell line (BC-3) harboring kaposi's sarcoma-associated herpesvirus (KSHV/HHV-8) in the absence of Epstein-Barr virus. Blood *88*, 2648-2654.

Ben-Bassat, H., Goldblum, N., Mitrani, S., Goldblum, T., Yoffey, J.M., Cohen, M.M., Bentwich, Z., Ramot, B., Klein, E., and Klein, G. (1977). Establishment in continuous culture of a new type of lymphocyte from a "Burkitt like" malignant lymphoma (line D.G.-75). Int J Cancer *19*, 27-33.

Boshoff, C., Gao, S.J., Healy, L.E., Matthews, S., Thomas, A.J., Coignet, L., Warnke, R.A., Strauchen, J.A., Matutes, E., Kamel, O.W.*, et al.* (1998). Establishing a KSHV+ cell line (BCP-1) from peripheral blood and characterizing its growth in Nod/SCID mice. Blood *91*, 1671-1679.

Boulanger, E., Marchio, A., Hong, S.S., and Pineau, P. (2009). Mutational analysis of TP53, PTEN, PIK3CA and CTNNB1/beta-catenin genes in human herpesvirus 8-associated primary effusion lymphoma. Haematologica *94*, 1170-1174.

Brander, C., Suscovich, T., Lee, Y., Nguyen, P.T., O'Connor, P., Seebach, J., Jones, N.G., van Gorder, M., Walker, B.D., and Scadden, D.T. (2000). Impaired CTL recognition of cells latently infected with Kaposi's sarcoma-associated herpes virus. J Immunol *165*, 2077-2083.

Cannon, J.S., Ciufo, D., Hawkins, A.L., Griffin, C.A., Borowitz, M.J., Hayward, G.S., and Ambinder, R.F. (2000). A new primary effusion lymphoma-derived cell line yields a highly infectious Kaposi's sarcoma herpesvirus-containing supernatant [In Process Citation]. J Virol *74*, 10187-10193.

Carrasco, D.R., Fenton, T., Sukhdeo, K., Protopopova, M., Enos, M., You, M.J., Di Vizio, D., Nogueira, C., Stommel, J., Pinkus, G.S.*, et al.* (2006). The PTEN and

INK4A/ARF tumor suppressors maintain myelolymphoid homeostasis and cooperate to constrain histiocytic sarcoma development in humans. Cancer Cell *9*, 379-390.

Cesarman, E., Chang, Y., Moore, P.S., Said, J.W., and Knowles, D.M. (1995a). Kaposi's sarcoma-associated herpesvirus-like DNA sequences in AIDS-related body-cavity-based lymphomas. N Engl J Med *332*, 1186-1191.

Cesarman, E., Moore, P.S., Rao, P.H., Inghirami, G., Knowles, D.M., and Chang, Y. (1995b). In vitro establishment and characterization of two acquired immunodeficiency syndrome-related lymphoma cell lines (BC-1 and BC-2) containing Kaposi's sarcoma-associated herpesvirus-like (KSHV) DNA sequences. Blood *86*, 2708-2714.

Chang, C.J., Mulholland, D.J., Valamehr, B., Mosessian, S., Sellers, W.R., and Wu, H. (2008). PTEN nuclear localization is regulated by oxidative stress and mediates p53-dependent tumor suppression. Mol Cell Biol *28*, 3281-3289.

Chang, Y., Cesarman, E., Pessin, M.S., Lee, F., Culpepper, J., Knowles, D.M., and Moore, P.S. (1994). Identification of herpesvirus-like DNA sequences in AIDS-associated Kaposi's sarcoma. Science *266*, 1865-1869.

Chen, W., Hilton, I.B., Staudt, M.R., Burd, C.E., and Dittmer, D.P. (2010). Distinct p53, p53:LANA, and LANA complexes in Kaposi's Sarcoma--associated Herpesvirus Lymphomas. J Virol *84*, 3898-3908.

Chung, J.H., and Eng, C. (2005). Nuclear-cytoplasmic partitioning of phosphatase and tensin homologue deleted on chromosome 10 (PTEN) differentially regulates the cell cycle and apoptosis. Cancer Res *65*, 8096-8100.

Cloughesy, T.F., Yoshimoto, K., Nghiemphu, P., Brown, K., Dang, J., Zhu, S., Hsueh, T., Chen, Y., Wang, W., Youngkin, D*., et al.* (2008). Antitumor activity of rapamycin in a Phase I trial for patients with recurrent PTEN-deficient glioblastoma. PLoS Med *5*, e8.

Cully, M., You, H., Levine, A.J., and Mak, T.W. (2006). Beyond PTEN mutations: the PI3K pathway as an integrator of multiple inputs during tumorigenesis. Nat Rev Cancer *6*, 184-192.

Dal Col, J., Zancai, P., Terrin, L., Guidoboni, M., Ponzoni, M., Pavan, A., Spina, M., Bergamin, S., Rizzo, S., Tirelli, U*., et al.* (2008). Distinct functional significance of Akt and mTOR constitutive activation in mantle cell lymphoma. Blood *111*, 5142-5151.

Damania, B. (2004). Modulation of cell signaling pathways by Kaposi's sarcoma-associated herpesvirus (KSHVHHV-8). Cell Biochem Biophys *40*, 305-322.

Dotti, G., Fiocchi, R., Motta, T., Facchinetti, B., Chiodini, B., Borleri, G.M., Gavazzeni, G., Barbui, T., and Rambaldi, A. (1999). Primary effusion lymphoma after heart transplantation: a new entity associated with human herpesvirus-8. Leukemia *13*, 664-670.

Fujimuro, M., and Hayward, S.D. (2003). The latency-associated nuclear antigen of Kaposi's sarcoma-associated herpesvirus manipulates the activity of glycogen synthase kinase-3beta. J Virol *77*, 8019-8030.

Ghosh, S.K., Wood, C., Boise, L.H., Mian, A.M., Deyev, V.V., Feuer, G., Toomey, N.L., Shank, N.C., Cabral, L., Barber, G.N.*, et al.* (2003). Potentiation of TRAIL-induced apoptosis in primary effusion lymphoma through azidothymidine-mediated inhibition of NF-kappa B. Blood *101*, 2321-2327.

Guasparri, I., Keller, S.A., and Cesarman, E. (2004). KSHV vFLIP is essential for the survival of infected lymphoma cells. J Exp Med *199*, 993-1003.

Hay, N. (2005). The Akt-mTOR tango and its relevance to cancer. Cancer Cell *8*, 179-183.

Hess, G., Herbrecht, R., Romaguera, J., Verhoef, G., Crump, M., Gisselbrecht, C., Laurell, A., Offner, F., Strahs, A., Berkenblit, A.*, et al.* (2009). Phase III study to evaluate temsirolimus compared with investigator's choice therapy for the treatment of relapsed or refractory mantle cell lymphoma. J Clin Oncol *27*, 3822-3829.

Hino, R., Uozaki, H., Murakami, N., Ushiku, T., Shinozaki, A., Ishikawa, S., Morikawa, T., Nakaya, T., Sakatani, T., Takada, K.*, et al.* (2009). Activation of DNA methyltransferase 1 by EBV latent membrane protein 2A leads to promoter hypermethylation of PTEN gene in gastric carcinoma. Cancer Res *69*, 2766-2774.

Horenstein, M.G., Nador, R.G., Chadburn, A., Hyjek, E.M., Inghirami, G., Knowles, D.M., and Cesarman, E. (1997). Epstein-Barr virus latent gene expression in primary effusion lymphomas containing Kaposi's sarcoma-associated herpesvirus/human herpesvirus-8. Blood *90*, 1186-1191.

Hyun, T., Yam, A., Pece, S., Xie, X., Zhang, J., Miki, T., Gutkind, J.S., and Li, W. (2000). Loss of PTEN expression leading to high Akt activation in human multiple myelomas. Blood *96*, 3560-3568.

Kahan, B.D. (2001). Sirolimus: a comprehensive review. Expert Opin Pharmacother *2*, 1903-1917.

Kang, G.H., Lee, S., Kim, W.H., Lee, H.W., Kim, J.C., Rhyu, M.G., and Ro, J.Y. (2002). Epstein-barr virus-positive gastric carcinoma demonstrates frequent aberrant methylation of multiple genes and constitutes CpG island methylator phenotype-positive gastric carcinoma. Am J Pathol *160*, 787-794.

Katano, H., Hoshino, Y., Morishita, Y., Nakamura, T., Satoh, H., Iwamoto, A., Herndier, B., and Mori, S. (1999). Establishing and characterizing a CD30-positive cell line harboring HHV-8 from a primary effusion lymphoma. J Med Virol *58*, 394-401.

Kedes, D.H., Lagunoff, M., Renne, R., and Ganem, D. (1997). Identification of the gene encoding the major latency-associated nuclear antigen of the Kaposi's sarcoma-associated herpesvirus. J Clin Invest *100*, 2606-2610.

Komanduri, K.V., Luce, J.A., McGrath, M.S., Herndier, B.G., and Ng, V.L. (1996). The natural history and molecular heterogeneity of HIV-associated primary malignant lymphomatous effusions. J Acquir Immune Defic Syndr Hum Retrovirol *13*, 215-226.

Li, J., Yen, C., Liaw, D., Podsypanina, K., Bose, S., Wang, S.I., Puc, J., Miliaresis, C., Rodgers, L., McCombie, R.*, et al.* (1997). PTEN, a putative protein tyrosine phosphatase gene mutated in human brain, breast, and prostate cancer. Science *275*, 1943-1947.

Liu, J.L., Mao, Z., LaFortune, T.A., Alonso, M.M., Gallick, G.E., Fueyo, J., and Yung, W.K. (2007). Cell cycle-dependent nuclear export of phosphatase and tensin homologue tumor suppressor is regulated by the phosphoinositide-3-kinase signaling cascade. Cancer Res *67*, 11054-11063.

Majewski, M., Korecka, M., Kossev, P., Li, S., Goldman, J., Moore, J., Silberstein, L.E., Nowell, P.C., Schuler, W., Shaw, L.M.*, et al.* (2000). The immunosuppressive macrolide RAD inhibits growth of human Epstein-Barr virus-transformed B lymphocytes in vitro and in vivo: A potential approach to prevention and treatment of posttransplant lymphoproliferative disorders. Proc Natl Acad Sci U S A *97*, 4285-4290.

Matsushima, A.Y., Strauchen, J.A., Lee, G., Scigliano, E., Hale, E.E., Weisse, M.T., Burstein, D., Kamel, O., Moore, P.S., and Chang, Y. (1999). Posttransplantation plasmacytic proliferations related to Kaposi's sarcoma-associated herpesvirus. Am J Surg Pathol *23*, 1393-1400.

Menezes, J., Leibold, W., Klein, G., and Clements, G. (1975). Establishment and characterization of an Epstein-Barr virus (EBC)-negative lymphoblastoid B cell line (BJA-B) from an exceptional, EBV-genome-negative African Burkitt's lymphoma. Biomedicine *22*, 276-284.

Montaner, S. (2007). Akt/TSC/mTOR activation by the KSHV G protein-coupled receptor: emerging insights into the molecular oncogenesis and treatment of Kaposi's sarcoma. Cell Cycle *6*, 438-443.

Nador, R.G., Cesarman, E., Chadburn, A., Dawson, D.B., Ansari, M.Q., Sald, J., and Knowles, D.M. (1996). Primary effusion lymphoma: a distinct clinicopathologic entity associated with the Kaposi's sarcoma-associated herpes virus. Blood *88*, 645-656.

Neshat, M.S., Mellinghoff, I.K., Tran, C., Stiles, B., Thomas, G., Petersen, R., Frost, P., Gibbons, J.J., Wu, H., and Sawyers, C.L. (2001). Enhanced sensitivity of PTEN-deficient tumors to inhibition of FRAP/mTOR. Proc Natl Acad Sci U S A *98*, 10314-10319.

Parsons, R. (2004). Human cancer, PTEN and the PI-3 kinase pathway. Semin Cell Dev Biol *15*, 171-176.

Petre, C.E., Sin, S.H., and Dittmer, D.P. (2007). Functional p53 signaling in Kaposi's sarcoma-associated herpesvirus lymphomas: implications for therapy. J Virol *81*, 1912-1922.

Picchio, G.R., Sabbe, R.E., Gulizia, R.J., McGrath, M., Herndier, B.G., and Mosier, D.E. (1997). The KSHV/HHV8-infected BCBL-1 lymphoma line causes tumors in SCID mice but fails to transmit virus to a human peripheral blood mononuclear cell graft. Virology *238*, 22-29.

Radu, A., Neubauer, V., Akagi, T., Hanafusa, H., and Georgescu, M.M. (2003). PTEN induces cell cycle arrest by decreasing the level and nuclear localization of cyclin D1. Mol Cell Biol *23*, 6139-6149.

Sabatini, D.M. (2006). mTOR and cancer: insights into a complex relationship. Nat Rev Cancer *6*, 729-734.

Sarbassov, D.D., Ali, S.M., Sengupta, S., Sheen, J.H., Hsu, P.P., Bagley, A.F., Markhard, A.L., and Sabatini, D.M. (2006). Prolonged rapamycin treatment inhibits mTORC2 assembly and Akt/PKB. Mol Cell *22*, 159-168.

Sarek, G., Kurki, S., Enback, J., Iotzova, G., Haas, J., Laakkonen, P., Laiho, M., and Ojala, P.M. (2007). Reactivation of the p53 pathway as a treatment modality for KSHV-induced lymphomas. J Clin Invest *117*, 1019-1028.

Silva, A., Yunes, J.A., Cardoso, B.A., Martins, L.R., Jotta, P.Y., Abecasis, M., Nowill, A.E., Leslie, N.R., Cardoso, A.A., and Barata, J.T. (2008). PTEN posttranslational inactivation and hyperactivation of the PI3K/Akt pathway sustain primary T cell leukemia viability. J Clin Invest *118*, 3762-3774.

Sin, S.H., Roy, D., Wang, L., Staudt, M.R., Fakhari, F.D., Patel, D.D., Henry, D., Harrington, W.J., Jr., Damania, B.A., and Dittmer, D.P. (2007). Rapamycin is efficacious against primary effusion lymphoma (PEL) cell lines in vivo by inhibiting autocrine signaling. Blood *109*, 2165-2173.

Stallone, G., Schena, A., Infante, B., Di Paolo, S., Loverre, A., Maggio, G., Ranieri, E., Gesualdo, L., Schena, F.P., and Grandaliano, G. (2005). Sirolimus for Kaposi's sarcoma in renal-transplant recipients. N Engl J Med *352*, 1317-1323.

Stambolic, V., Suzuki, A., de la Pompa, J.L., Brothers, G.M., Mirtsos, C., Sasaki, T., Ruland, J., Penninger, J.M., Siderovski, D.P., and Mak, T.W. (1998). Negative regulation of PKB/Akt-dependent cell survival by the tumor suppressor PTEN. Cell *95*, 29-39.

Staudt, M.R., Kanan, Y., Jeong, J.H., Papin, J.F., Hines-Boykin, R., and Dittmer, D.P. (2004). The tumor microenvironment controls primary effusion lymphoma growth in vivo. Cancer Res *64*, 4790-4799.

Steelman, L.S., Navolanic, P.M., Sokolosky, M.L., Taylor, J.R., Lehmann, B.D., Chappell, W.H., Abrams, S.L., Wong, E.W., Stadelman, K.M., Terrian, D.M., *et al.* (2008). Suppression of PTEN function increases breast cancer chemotherapeutic drug resistance while conferring sensitivity to mTOR inhibitors. Oncogene *27*, 4086-4095.

Tomlinson, C.C., and Damania, B. (2004). The K1 protein of Kaposi's sarcoma-associated herpesvirus activates the Akt signaling pathway. J Virol *78*, 1918-1927.

Uddin, S., Hussain, A.R., Al-Hussein, K.A., Manogaran, P.S., Wickrema, A., Gutierrez, M.I., and Bhatia, K.G. (2005). Inhibition of phosphatidylinositol 3'-kinase/AKT signaling promotes apoptosis of primary effusion lymphoma cells. Clin Cancer Res *11*, 3102-3108.

Van de Sande, T., De Schrijver, E., Heyns, W., Verhoeven, G., and Swinnen, J.V. (2002). Role of the phosphatidylinositol 3'-kinase/PTEN/Akt kinase pathway in the overexpression of fatty acid synthase in LNCaP prostate cancer cells. Cancer Res *62*, 642-646.

van Hattem, W.A., Brosens, L.A., de Leng, W.W., Morsink, F.H., Lens, S., Carvalho, R., Giardiello, F.M., and Offerhaus, G.J. (2008). Large genomic deletions of SMAD4, BMPR1A and PTEN in juvenile polyposis. Gut *57*, 623-627.

Vivanco, I., and Sawyers, C.L. (2002). The phosphatidylinositol 3-Kinase AKT pathway in human cancer. Nat Rev Cancer *2*, 489-501.

Wendel, H.G., Malina, A., Zhao, Z., Zender, L., Kogan, S.C., Cordon-Cardo, C., Pelletier, J., and Lowe, S.W. (2006). Determinants of sensitivity and resistance to rapamycin-chemotherapy drug combinations in vivo. Cancer Res *66*, 7639-7646.

Wlodarski, P., Kasprzycka, M., Liu, X., Marzec, M., Robertson, E.S., Slupianek, A., and Wasik, M.A. (2005). Activation of mammalian target of rapamycin in transformed B lymphocytes is nutrient dependent but independent of Akt, mitogen-activated protein kinase/extracellular signal-regulated kinase kinase, insulin growth factor-I, and serum. Cancer Res *65*, 7800-7808.

CHAPTER III

DELETION OF TUMOR SUPPRESSOR GENES FHIT AND WWOX IS A DEFINING CHROMOSOMAL ABNORMALITY FOR PRIMARY EFFUSION LYMPHOMA

Debasmita Roy, Sang-Hoon Sin, Blossom Damania, Dirk P. Dittmer

This work is under revision for publication at Blood

ABSTRACT

Primary Effusion Lymphoma (PEL) is a Diffuse-Large B-cell Lymphoma (DLBCL) with poor prognosis. 100% of PEL carry the genome of Kaposi Sarcoma-associated herpesvirus (KSHV) and approximately half are co-infected with Epstein-Barr virus (EBV). Genomic aberrations in PEL were profiled using the Affymetrix 6.0 SNP array. This identified for the first time individual genes that are altered in PEL. 10/13 (76%) samples were deleted for the fragile site tumor suppressors: WWOX and FHIT. Alterations were also observed in the DERL1, ETV1, RASA4, TPK1, TRIM56 and VPS41 genes, which are yet to be characterized for their roles in cancer. Co-infection with EBV was associated with significantly fewer gross genomic aberrations; and PEL could be segregated into EBV positive and EBV negative clusters on the basis of host chromosome alterations. This suggests a model in which both host genetic aberrations and virus contribute to the PEL phenotype.

INTRODUCTION

Primary effusion lymphoma (PEL) is a post germinal center, diffuse-large B-cell Lymphoma (DLBCL) with poor prognosis. It is characterized by accumulation of tumor cells in the serous cavities of the body and therefore was initially referred to as body-cavity-based lymphoma (BCBL). Since then, isolated instances of solid, lymph node-associated variants have been described (Chadburn et al., 2004). Morphologically, PEL are pleiomorphic and exhibit heterogeneity in cell size and nuclear shape (Carbone et al., 2009). PEL is an acquired immuno-deficiency syndrome (AIDS) defining malignancy, and usually manifests itself in conjunction with Kaposi Sarcoma (KS). However, PEL has also been diagnosed in HIV-negative patients experiencing severe immune-suppression after organ transplantation (Carbone et al., 2009). PEL is unique histologically as well as in its expression of immunophenotypic markers, mRNA and microRNA profile (Klein et al., 2003; Nador et al., 1996; O'Hara et al., 2008; O'Hara et al., 2009). As expected for cancer cells, PEL show gross chromosome alterations (Nair et al., 2006; Ohshima et al., 2002) although to a limited extent. Genome-wide high-resolution analysis of copy number variants (CNV) and loss-of heterozygosity (LOH) has not been reported.

All PEL are infected with Kaposi's Sarcoma-associated Herpesvirus (KSHV) (Nador et al., 1996). KSHV is also the causative agent for Kaposi's Sarcoma (KS) (Chang et al., 1994) and the plasmablastic variant of Multicentric Castleman's Disease (MCD) (Soulier et al., 1995). KSHV is required for PEL survival (Godfrey et al., 2005); a subset of viral proteins as well as all viral miRNAs are consistently expressed in all PEL (Fakhari and Dittmer, 2002). Approximately half of PEL are co-infected with EBV and this results in altered host mRNA transcription compared to EBV negative PEL (Fan et

al., 2005). It has been reported that upon overexpression of a dominant negative form of the EBV EBNA2 protein, some EBV-positive PEL cease to proliferate (Mack and Sugden, 2008). However, the contribution of EBV to PEL development remains unclear as both EBV-positive and EBV-negative PEL grow equally well in culture and form tumors with equal efficiency in immune deficient mice (Sin et al., 2007; Staudt et al., 2004).

Cancer is thought to arise in a multi-step fashion, though not necessarily in a linear manner, where each step provides a selective advantage in terms of cell proliferation and cell survival in the tumor microenvironment. This leads to cancer type specific genome signatures such as the classic "Philadelphia" t(9;22)(q34;q11) translocation resulting in oncogenic BCR:ABL gene fusion in chronic myelogenous leukemia (CML). These signatures in turn provide tumor cell specific targets for therapy (eg. use of Imatinib/Gleevec™ in CML). In non-virus associated cancers, each step in this pathway involves activating or inhibitory mutations in cellular oncogenes or tumor suppressors, respectively. In virus-associated cancers, the virus contributes to one or multiple steps along this pathway, thus reducing the need for specific mutations in host oncogenes or tumor suppressor genes.

Chromosomal imbalances and genomic instability comprise a major contributing factor in malignant diseases. Unlike other lymphomas, no signature translocation or single gene mutation has been associated with PEL to date. The p53 tumor suppressor protein appears functional in PEL (Petre et al., 2007), the Myc locus un-rearranged, although the protein is unusually stable (Bubman et al., 2007), and no amplifications or deletions are reported for Bcl-2 (Nador et al., 1996), Bcl-6 (Gaidano et al., 1999), Ras

(Nador et al., 1996), the catalytic subunit of PI3K (Boulanger et al., 2009), PTEN or p16/INK4 (Boulanger et al., 2009). Therefore, the Affymetrix 6.0 Single Nucleotide Polymorphism (SNP)-based microarray was used to conduct comparative genomic hybridization (CGH). This identified PEL specific gene alterations in the fragile site tumor suppressor genes, Fragile Histidine Triad (FHIT) and WW-domain containing Oxidoreductase (WWOX), which were deleted in 11/13 (85%) and 12/13 (92%) of the samples, respectively (p-value ≤ 0.0005). In addition, I observed alterations in other key signaling pathways albeit at a lower frequency. Since a subset of PEL are co-infected with EBV in addition to KSHV, I asked whether EBV influenced overall genomic instability or was associated with genomic alterations in specific genes. EBV-negative PEL exhibited significantly increased genomic aberrations compared to EBV-positive PEL, suggesting that the presence of EBV contributes to genomic stability.

MATERIALS AND METHODS

Cell Culture The PEL and control cell lines used in the study are shown in table III.1. All cells were cultured in RPMI 1640 supplemented with 100μg/ml streptomycin sulphate, 100U/ml penicillin G (Life Technologies, Carlsbad, CA), 2mM L-glutamine, 0.05mM 2-mercaptoethanol, 0.075% sodium bicarbonate, 1 U/ml IL-6 (PeproTech Inc. Rock Hill, NJ) and 10% FBS and maintained at 37°C in 5% CO_2.

DNA Extraction and CGH Genomic DNA was extracted using the Wizard Genomic DNA Purification Kit (Promega Inc., Madison, WI) as per manufacturer's protocol. Signature profiles were obtained using the 6.0 GeneChip Human Mapping

Array that uses known human SNP markers (Affymetrix, Santa Clara, CA). Both the SNP and CNV data have been deposited in the NIH GEO Datasets archives: GSE25389.

Data Analysis All analyses were performed on data from the 6.0 GeneChip Human Mapping Arrays using the Partek® Genomics Suite v6.0 (Partek Inc., St. Louis, MO). Raw CGH data (.CEL files) were imported and adjusted for background using Robust Multi-array Average (RMA) algorithm. CNV was determined by generating *copy number* values using Genomic Segmentation algorithm with preset program parameters. LOH was determined by applying the Hidden Markov Model Region (HMM-R) detection algorithm to the raw Genotype data (.CHP) files. Our data set was compared to the 270 HapMap baseline for CNV and LOH (version 122809) available at: <http://www.affymetrix.com/support/technical/sample_data/genomewide_snp6_data.affx>. Gene lists were generated by determining regions of significance (by estimating t-statistics for each probe adjusted for multiple comparisons by MAT algorithm(Johnson et al., 2006)) in multiple samples and annotating using the NCBI Reference Sequence database. Further analysis used the R v2.11.1 statistic software environment.

Real Time Quantitative PCR Analysis Real-time quantitative PCR (qPCR) was used to verify our candidate genes. Primers were selected following criteria outlined by D'haene et. al. (D'Haene et al., 2010) from the RTprimerDb (www.rtprimerdb.org). Primer sequences used are: WWOX (For: 5'-GCAATGAAGGCAACAAAGT-3'; Rev: 5'-TTAAAAGACCTGGGGGAAT-3') FHIT (For: 5'-CCAGTGGAGCGCTTCCAT-3'; Rev: 5'-TCCACCACTGTCCCGACTCT-3'), GRID2 (For: 5'-GCATTTCAGTGTTTTGAAAATTG-3'; Rev: 5'-CCAGTCTGGGCAAACTCATT-3').

Cycling conditions were: 95°C for 10 min followed by 45 cycles of 95°C for 15 seconds and 60°C for 1 min followed by melting curve analysis on a Roche LC480 Lightcycler. All reactions were conducted in five technical replicates. Purified normal human genomic DNA (Roche Coop. Indianapolis, IN) was used as positive control and water served for non-template negative control. A standard curve was generated using serial (1:4) dilutions of human genomic DNA, starting at 8 μg/ml concentration, against the individual primers. Robust regression analysis (Rousseeuw P., 2003) was used to obtain copy number changes for each sample relative to normal diploid human DNA.

RESULTS

Genetic Signature of PEL: FHIT and WWOX

Using the high resolution Affymetrix 6.0 SNP array I assessed the genomic signatures of virtually all available PEL (Table III.1). I used cell lines, as they form a renewable resource and have been characterized phenotypically with regard to growth in culture and tumorigenicity in mice, *in vitro* and *in vivo* drug susceptibility, mRNA transcription, miRNA expression, p53 status and other markers. Although the samples displayed a high degree of variability in their genomic signatures, using Principle Component Analysis (PCA) I found that the majority of PEL (with the exception of JSC1) form a tight cluster. As expected PEL cells could easily be distinguished from non-PEL control cell lines (figure III.1, panel A) on the basis of genomic alterations.

Using PCA of only the PEL data I found that all PEL clustered together irrespective of whether they were grown in culture or as xenografts in mice. This is

represented by overlapping grey (culture) and red (xenograft) spheres in figure III.1, panel B. This demonstrated that PEL form tumors in mice, as noted in Table III.1, without acquiring additional mutations *in vivo*. This phenotype would be expected for a monoclonal tumor, as PEL is believed to be. For our detailed analysis, I excluded the samples from xenografts, to avoid the bias of repeat sampling of some PEL lines, and exclusively focused on the samples from cells in culture, including the outliers. Using only PEL –derived data for PCA afforded us the resolution to identify differences among individual PEL isolates. 10/13 PEL clustered tightly together, which reaffirmed the initial, phenotype-based classification of PEL. Three unique samples were observed: BCLM and VG1, in addition to the previously noted JSC1. I therefore concluded that BCLM, JSC1 and VG1 represent non-typical variants of PEL.

Upon analyzing the CNV markers in detail, I identified discrete regions of amplifications and deletions on each chromosome, many of which were shared in > 50% of the samples. Figure III.2, shows the heat map representation of CNV for PEL. The upper panel shows the EBV-positive and the lower EBV-negative PEL. Chromosomes 7, 8, 12 and the q-arm of chromosome 1 harbor the majority of amplifications.

The 946,000 copy number-variant specific probes that are contained in the Affymetrix 6.0 array allowed us, for the first time, to define the genomic signature exhibited by PEL at the single gene level. Table III.2 shows the individual genes with CNV in 12 of 13 PEL. This represents our most stringent cut-off. Two of these: WWOX and FHIT represent common fragile site (CFS) genes. The Glutamate Receptor Ionotrophic, Delta 2 (GRID2) that was deleted exclusively from the EBV-negative PEL samples (listed in Table III.3) is also classified as a CFS gene. CFS are regions of the

genome particularly susceptible to breaks in metaphase chromosomes. These regions are evolutionarily conserved and tend to encode for genes involved in tumor suppression, replicative stress and DNA damage repair (Durkin and Glover, 2007). FHIT, WWOX and GRID2 map to the CFS FRA3D, FRA16D and FRA4G on chromosomes 3 (p-arm), 16 (q-arm), and 4 (q-arm), respectively (Bednarek et al., 2000; Ohta et al., 1996; Rozier et al., 2004). Figure III.3 shows the detailed distribution of markers around these three sites. This demonstrated the partial or complete loss of FHIT (11/13 PEL), WWOX (12/13 PEL) and GRID2 (all in EBV-negative PEL) in an otherwise normal chromosomal setting, panels A, B and C respectively. Note that these three sites are small and contained in an otherwise normal region of the chromosome. By contrast, figure III.3, panel C shows the example of large-scale chromosomal alteration in the q-arm of chromosome 4. These large-scale rearrangements were present in more than one PEL sample, but by no means in all PEL.

Using quantitative PCR (qPCR) I verified our CNV data for the three fragile site tumor suppressor genes. Figure III.4 shows copy number loss relative to normal diploid copy number per genome on a $\log_2$ scale. Panels A, B and C represent WWOX, FHIT and GRID2 respectively. Compared to normal human DNA (labeled N) all PEL show losses of FHIT, WWOX and GRID2. These data confirmed independently the loss of WWOX and FHIT in majority of PEL cell lines, and of GRID2 in EBV-negative PEL. Loss of FHIT, WWOX and GRID2 (in EBV-negative PEL) is a defining genomic aberration in PEL.

Table III.2 also contains genes that were significantly amplified in 12/13 (92%) PEL based on the Affymetrix arrays. These are DER-like family member 1 (DERL1),

ETS translocation variant 1 (ETV1), RAS p21 activator protein 4 (RASA4), Thiamin pyrophospho-kinase 1 (TPK1), Tripartite motif containing 56 (TRIM56), and Vacuolar protein sorting-41, homolog (VPS41). Other genes were deleted or amplified in a smaller fraction of samples. Although these alterations may have biological relevance alone or in combination, the significance of these candidate alterations needs to be established in a larger series of experiments.

CNV, not LOH, distinguishes EBV-positive from EBV-negative PEL

A tally of the CNV markers further shows a significantly ($p \leq 0.05$ by t-test) greater number of amplifications in the EBV-negative group compared to the EBV-positive, figure III.5, panel A. The data for deletions mirror the trend; EBV-negative cells harbor more deletions than the EBV-positive group, figure III.5, panel B, though the level of significance was lower ($p \leq 0.1$ by t-test). Overall, using PCA, it was demonstrated that PEL formed two distinct sub-clusters as shown in figure III.5, panel C. These two distinct clusters correlate with EBV infection status, JSC1 and VG1 being the outliers.

I further mapped the CNV markers to the RefSeq database to identify specific genes. Table III.3 shows 23 genes that were most significantly altered in EBV-negative PEL. I used false-discovery rate based adjustment for multiple comparison and defined q-values ≤ 0.01 as cut off (Storey and Tibshirani, 2003). I annotated this list using GeneCards® database v3.0 <www.genecards.org> (Rebhan et al., 1997). Based on their known functions, the genes were classified into: (i) Transcriptional (CDYL, CHD1, MEF2C, RFX2, RREB1, ZEB1), (ii) Developmental (EPHA-3, -5, GRID2, HBS1L), (iii) Metabolic (ACSBG2, FUT3), (iv) Cell signaling (IKBKB, ITPR1) and (v) Cell adhesion

(CADM2, CDH9, EDIL3, LRFN5, PCDH9) molecules. The oncogene: RAF1, tumor suppressor: BRCA2, cytoskeletal regulator: ARAP2 and Major Histocompatibility Complex (MHC) receptor: HLA-DRB5, were put in their own categories.

In addition to CNV, the Affymetrix 6.0 SNP markers allowed us to interrogate LOH in PEL for the first time. LOH is indicative of allelic imbalance and can be used to assess overall genomic integrity (Kawai et al., 2000; Nunn et al., 1999; Sogame et al., 2003). Unstable genomes harbor a greater extent of LOH compared to those that are genetically stable. In PEL, the presence of allelic imbalance (LOH) did not correlate with EBV infection status. Both EBV-positive and -negative groups harbor the same degree of Copy Neutral LOH (indicative of Uniparental Disomy) and heterozygous gains or losses (data not shown). In summary, CNV (amplifications/deletions) but not LOH, separate EBV-positive from EBV-negative PEL.

DISCUSSION

In this study the genomic signature of PEL was defined at the individual gene level using Affymetrix SNP6.0 array–based CGH. The majority of the genetic changes corresponded to broad amplifications of regions of chromosome 7, 8, 12 and q-arm of 1. This first high-resolution data extends earlier low-resolution studies that have reported similar observations in a single PEL or in a smaller collection using 1st generation BAC-mid based assays (Boulanger et al., 2001; Gaidano et al., 2000; Mullaney et al., 2000; Nair et al., 2006; Ohshima et al., 2002). In addition, three fragile site tumor suppressor genes: FHIT, WWOX and GRID2 were deleted in PEL. PEL maintained the same genomic signatures whether grown in culture or as xenograft in a

SCID mouse, which is consistent with the monoclonal origin of PEL. The presence of EBV, in addition to KSHV, was associated with decreased gross genomic rearrangements.

This is the first high resolution CGH analysis of PEL. It allowed us to identify individual genes that were deleted or amplified. The two most prominent deletions were the fragile site genes: WWOX and FHIT. These have been classified as tumor suppressor genes in multiple cancers, including DLBCL (Bednarek et al., 2000; Capello et al., 2010; Deffenbacher et al., 2010; Kameoka et al., 2004; Ohta et al., 1996). Transgenic mice that lack FHIT or WWOX are more prone to developing tumors, especially those of the lymphoid origin (Aqeilan et al., 2007; Fujishita et al., 2004; Ludes-Meyers et al., 2007). Reintroduction of the respective tumor suppressor genes, ectopically or by gene therapy, restores non-tumor properties in the mice (Dumon et al., 2001; Fabbri et al., 2005; Ji et al., 1999). It is likely that in PEL, as in other DLBCL, a loss of function of these genes promotes tumorigenesis. One might even speculate that the re-introduction of FHIT or WWOX may be developed into a gene-transfer-based therapy for PEL.

I detected six non-fragile site genes that were amplified in the majority of PEL. DERL1 and ETV1 have previously been associated with viral and non-viral cancers(Jane-Valbuena et al., 2010; Lilley and Ploegh, 2004; Reid et al., 2010; Shin et al., 2008; Wang et al., 2008). DERL1 protects cells from ER-stress induced apoptosis and is over-expressed in breast cancer. In addition, DERL1 is essential for Human Cytomegalovirus (HCMV) protein US11 mediated degradation of Major Histocompatibility Complex-I products (Lilley and Ploegh, 2004). Multiple reports have demonstrated associations between solid tumors and ETV1 and alteration in ETV1 is a

prognostic marker in tumor progression (Jane-Valbuena et al., 2010; Reid et al., 2010; Shin et al., 2008). Yet, the specific biochemical function of ETV1 remains to be elucidated. The remaining high significance amplifications include Ras-p21 Activator Protein 4 (RASA4), Tyrosine Protein Kinase 1 (TPK1), Tripartite-motif containing 56 (TRIM56) and Vacuolar protein Sorting 41 homolog (VSP41). These are involved in cell signaling, metabolism and protein maturation. These data are the first to link these to oncogenesis.

PEL is believed to be monoclonal expansion of a post-GC B-cell (Carbone et al., 2009; Matolcsy et al., 1998). Immunophenotypic analysis suggests that PEL comprise a subset of plasma cells. Normally, naïve B-cells entering the GC undergo B-cell receptor (BCR) mediated differentiation/ activation to form memory and plasma cells. Those that cannot be stimulated due to lack of BCR or crippling mutations are eliminated via Fas-mediated apoptosis. However, in PEL as well as EBV-positive post-transplant associated lymphomas (PTLD), a subset of these cells escapes apoptosis and ultimately develops into lymphoma. By some account this escaping population of cells lacking function BCR is particularly susceptible to EBV infection; EBV infection not only protects them from GC- mediated apoptosis but also contributes to proliferation (Bechtel et al., 2005; Chaganti et al., 2005; Mancao et al., 2005).

Mack and Sugden reported that EBV is essential for sustained proliferation of some EBV-positive PEL in culture (Mack and Sugden, 2008) but EBV-negative PEL exhibit similar sustained proliferation in culture and tumor forming potential in mice (Sin et al., 2007). This study for the first time found a PEL phenotype that associated with EBV infection: EBV-negative PEL harbor significantly more gross genomic alterations

than EBV-positive PEL. EBV appears to facilitate host chromosomal genomic stability in PEL. This phenotype is consistent with EBV-transformed lymphoblastoid cell lines (LCLs) that retain a normal karyotype indefinitely (Johnson et al., 1981). Vaghefi et. al. suggested that for KSHV-negative AIDS lymphomas there also exists an inverse correlation between EBV infection and the number of chromosomal aberrations (Vaghefi et al., 2006). At this point it is unclear whether this is due to a direct stabilizing effect of EBV latent genes, or if the expression of EBV latent genes relieves selective pressure by modulating growth promoting pathways post-translationally, which EBV-negative PEL would need to be selected by genomic alterations. Alternatively there exists the possibility that genomic aberration is a result of EBV-negative PEL having traversed the GC (Matolcsy et al., 1998) and EBV-positive PEL not. Typically post-GC DLBCL show genomic evidence of having passed through the recombinogenic environment of the germinal center.

The contribution of EBV to PEL development has remained a matter of debate because EBV-positive and EBV-negative PEL exhibit the same tumorigenecity in mouse models and in the clinic. Based on the available evidence and our understanding of plasma cell development, multiple scenarios of PEL tumor evolution can be envisioned. Figure III.6, panel A represents the classic, Sequential scenario where naïve B-cells entering the germinal center (GC) are infected with EBV that drives them through the maturation/differentiation process and contributes to their proliferative advantage. Some of the EBV-infected B-cells subsequently acquire the PEL-defining CFS gene mutations and KSHV, which drive the malignant transformation. As these pre-PEL cells proceed to leave the GC to form PEL, it can be speculated that some of them lose the EBV episome

but acquire additional compensatory genetic mutations, by a yet undefined mechanism, to give rise to EBV-negative PEL; others never lose EBV.

The lower panel B of figure III.6 summarizes 2 additional hypotheses for PEL pathogenesis: (a) Parallel and (b) Stem cell guided. Analogous to the Sequential model, naïve B-cells in the Parallel model also traverse through the GC, but instead of pre-PEL cells being infected with EBV, one can imagine that these cells acquire the PEL-defining CFS gene mutations first. These pre-PEL CFS gene mutant cells are either infected with EBV or acquire additional genetic mutations to form PEL. The Stem cell guided model of PEL pathogenesis proposes that a PEL stem cell (PEL^S) population arises in the GC that has proliferative advantage and acquired FHIT and WWOX mutation. These cells form a self-renewing source for pre-PEL from which different PEL clones arise. Subsequently, a in the Parallel model, some of these sub-clones are infected with EBV and others acquire additional genetic mutations to form PEL. Further, it has been suggested that in addition to traversing through the GC, B-cells can differentiate into plasma cells in the extra-GC follicular region (Oracki et al., 2010). Given that the PEL defining tumor suppressors are CFS genes, it can be hypothesized that these extra-GC B-cells lose FHIT and WWOX together with acquiring genomic instability and result in PEL, without the involvement of EBV, whereas GC-derived PEL carry EBV.

In table III.3, are also noted individual genes that were correlated with EBV status. A significant number of those were involved with cell adhesion. With regards to known tumor genes, I noted amplification of Raf1 or c-Raf and deletion of the tumor suppressor gene Breast Cancer gene 2, BRAC2 in EBV-negative PEL. c-Raf is the cellular homolog of the murine leukemia viral oncogene, v-Raf-1, a serine/threonine-

specific protein kinase involved in the MAPK-ERK pathway and BRCA2 is a DNA damage repair, specifically associated with double strand breaks and homologous recombination. This is the first report associating c-Raf with PEL.

Other interesting genes that were significantly amplified in EBV-negative PEL include IKBKB, IKB Kinase-β, a key activator of NFκB, and ITPR1, Inositol-1,4,5-triphosphosphate receptor 1. NFκB has a known role in PEL tumorigenesis. It is modulated by the KSHV homolog of the cellular FLICE inhibitory protein (vFLIP) (Carbone et al., 2009; Chaudhary et al., 1999) as well as KSHV K15 (Brinkmann et al., 2003). Of note, the EBV latency membrane protein (LMP)-1 can also activate NFκB (Laherty et al., 1992). Thus it seems consistent with the biology of EBV and PEL that IKBKB, a cellular activator of NFκB was amplified in 5 of 7 EBV-negative cells. ITPR1 is involved in regulating calcium homeostasis in the ER, inducing Ca^{2+} release into the cytosol (Berridge, 1993). Normal B-cells undergoing activation and blastic transformation show elevated levels of cytosolic Ca^{2+} (Feske, 2007). It was recently shown by Dellis et. al. that EBV LMP-1 can down-regulate ER-associated enzymes to increase levels of cytosolic Ca^{2+} and promote cellular transformation(Dellis et al., 2009). Therefore, it can be hypothesized that amplification of ITPR1 in EBV-negative PEL compensates for the absence of EBV to drive B-cell transformation.

Last but not the least, it was very exciting to note that one of the genes deleted in EBV-negative PEL, GRID2, is also a fragile site gene. Deletion of GRID2 in 5 of 7 EBV-negative PEL was observed while remaining unaltered in EBV-positive PEL. This further speaks to the instability of the host genome in the absence of EBV in PEL. GRID2 is

noted for its role in neurological development (Durkin and Glover, 2007). Ours is the second report suggesting a role for GRID2 in tumorigenesis (Bluteau et al., 2002).

In summary, this represents the first high-resolution CGH analysis of PEL. I found evidence of genomic instability, which was greater in EBV-negative PEL. I verified that the PEL associated genomic signature maps mainly to amplifications in chromosome 7, 8, 12 and q-arm of 1, as previously reported. This is the first report to show association of deletion of the fragile site tumor suppressor genes: FHIT and WWOX with PEL and GRID2 with EBV-negative PEL.

Acknowledgements

This work was funded in part by NIH grants DE018304, CA121935, CA112217 to DD, CA096500 and DE018281 to BD, the Centers for AIDS research (CfAR), the AIDS malignancy consortium (CA121947), the University Cancer Research Fund (UCRF) and the Leukemia & Lymphoma Society of America (R6169-10). BD is a scholar of the Leukemia & Lymphoma Society and a Burrows Welcome trust investigator.

The authors would like to thank K. L. Richards for critical reading of the manuscript.

Author Contribution

Roy, D: Designed and conducted experiments, analyzed data and wrote manuscript; Sin, SH: Conducted experiments; Damania, B: Designed experiments and analyzed data; Dittmer, DP: Designed experiments, analyzed data and wrote manuscript

FIGURES

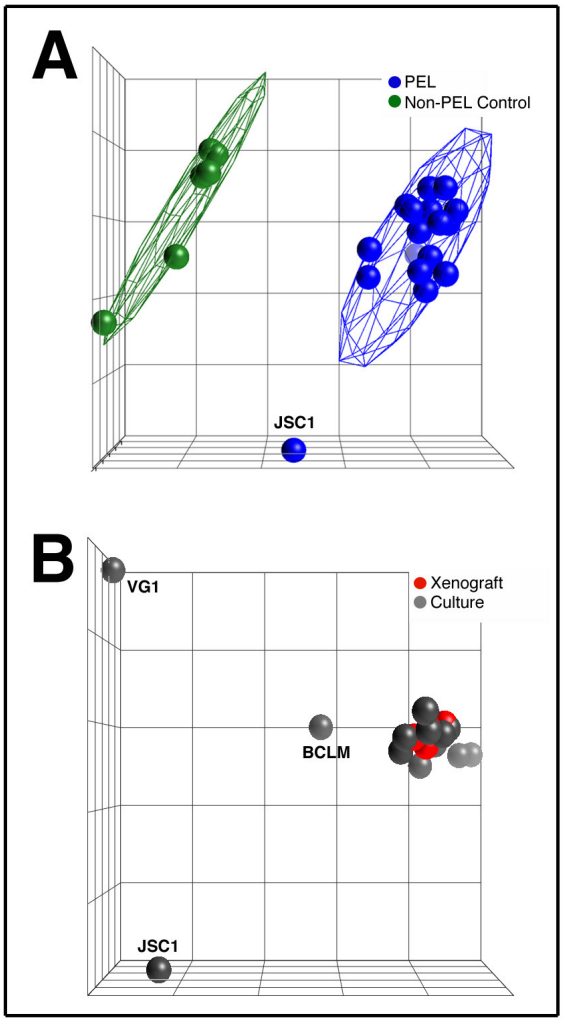

Figure III.1: Principle Component Analysis of PEL

Panel A represents the two distinct clusters formed by endothelial cells in green and all the 17 (excluding JSC1) PEL / B-cells in red, irrespective of whether they were from culture or xenograft. Panel B demonstrates that PEL cells from culture (in grey) and xenograft (in red) co- cluster with the exceptions of JSC1, VG1 and BCLM.

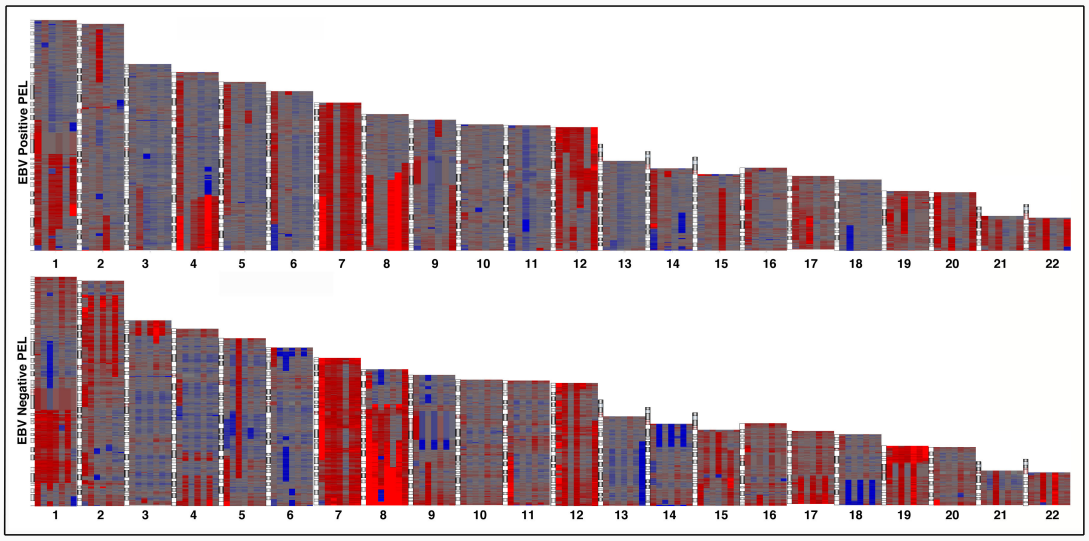

Figure III.2: Heat map representation of CNV in PEL, separated by EBV status. The top panel includes all the EBV positive cells and the bottom panel all the EBV negative cells in culture. Where red represents amplification, blue denotes deletion, with the grey range in between. Each heat map is accompanied with its respective chromosome represented as a cytoband to the left.

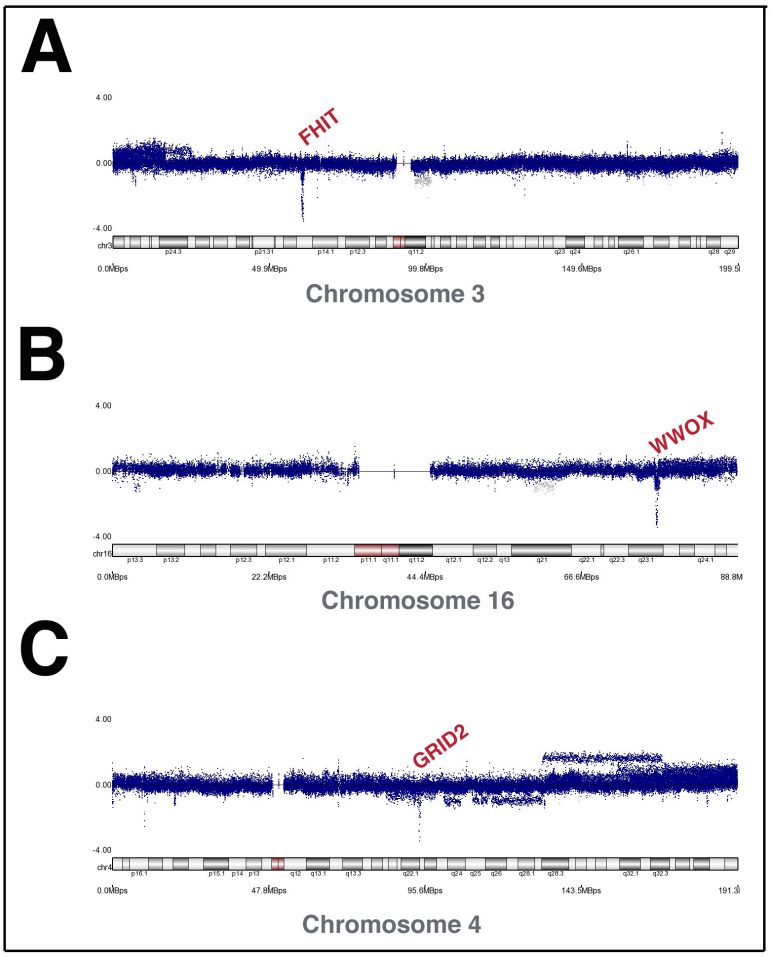

Figure III.3: CFS Tumor Suppressor Genes: FHIT, WWOX and GRID Dot Plot in PEL

Dot Plot representation of markers distributed along the chromosome. Panels A, B and C show the loss of FHIT, WWOX and GRID2 from chromosomes 3, 16 and 4, respectively. The markers (from each of the 14 PEL cell lines) are represented by blue dots $\log_2$ scale with the cytoband at the base of each dot plot. The grey dots represent alterations that only occurred in 1/13 PEL cell lines and were thus considered exceptions.

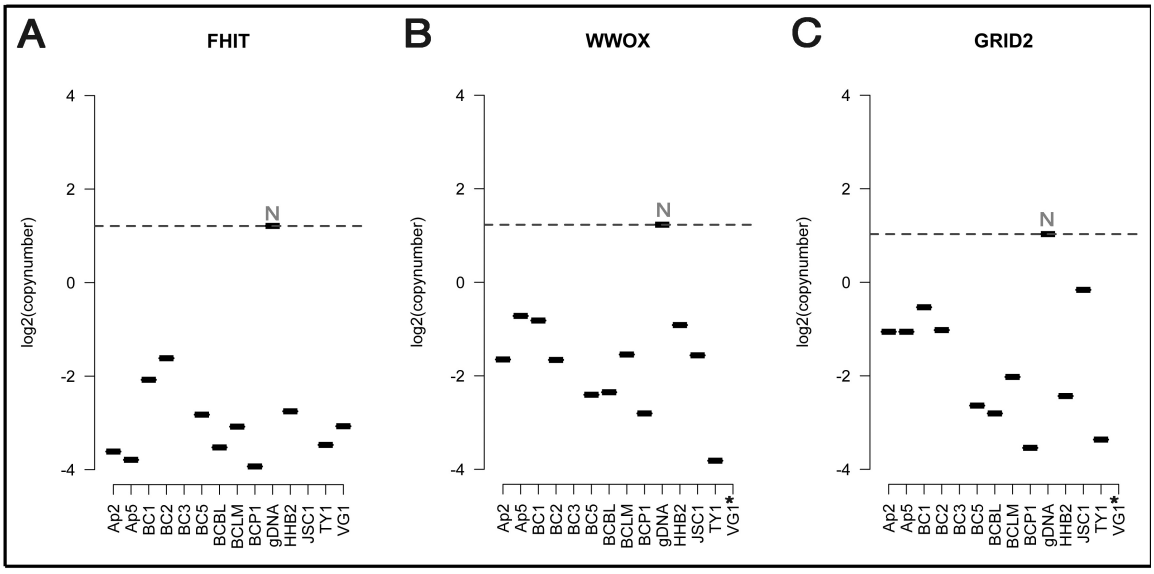

Figure III.4: q-PCR Verification of CFS Tumor Suppressor Gene Loss in PEL Panels A, B and C show the qPCR data for FHIT, WWOX and GRID2 respectively. The cell lines are arranged along the X-axis while the relative copy number is represented along the Y-axis on a $\log_2$ scale. The dotted line represents normal copy number and genomic DNA control sample is labeled N. GRID2 qPCR data was not available for VG1 cells marked with an asterisk.

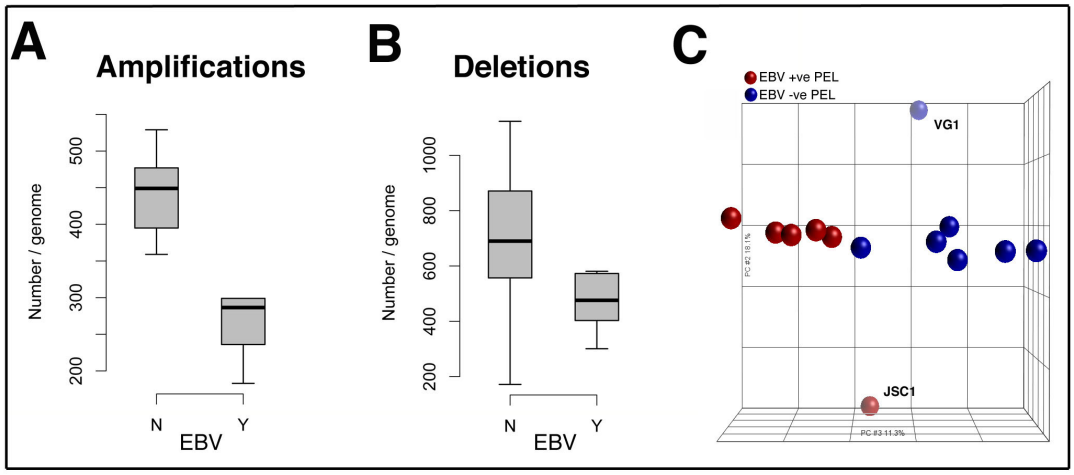

Figure III.5: Quantification of CNV in PEL, separated by EBV status. Panel A demonstrates that there are significantly more amplifications in EBV negative PEL compared to EBV positive. Panel B shows that although there is increased deletion of markers in the EBV negative population, there difference is less conclusive. Panel C is PCA to illustrate that PEL cells in culture form two distinct groups correlative with their EBV infection status: blue indiciates EBV(-) and brown EBV(+) samples.

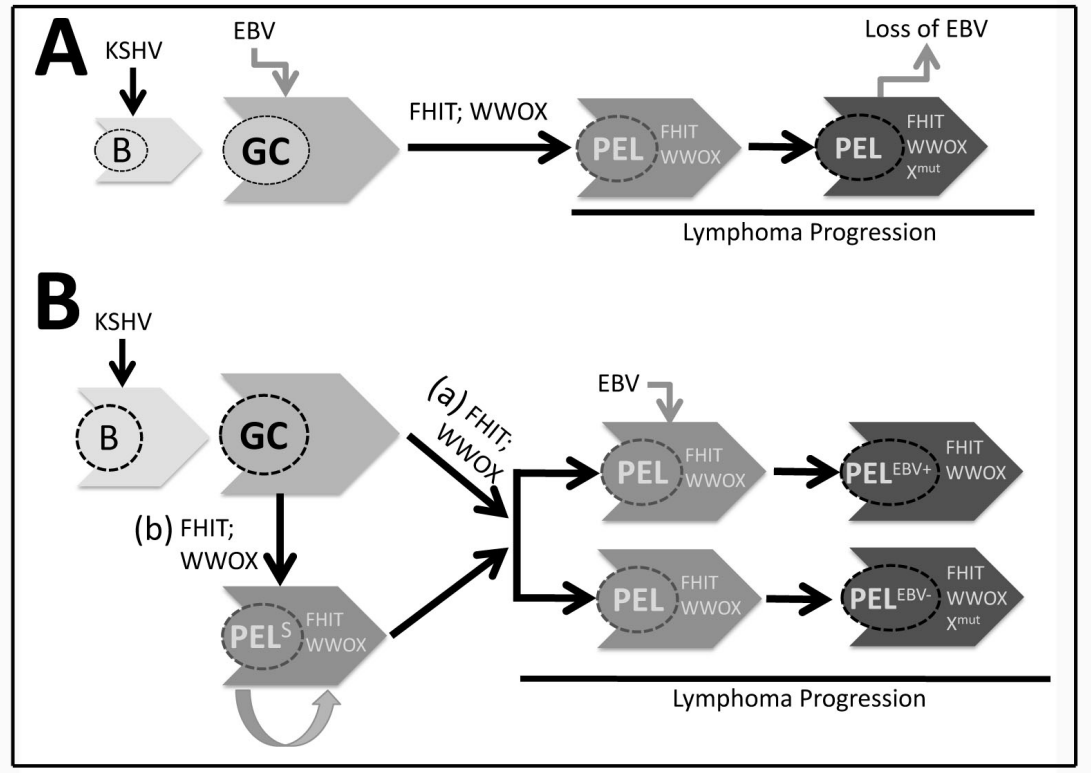

Figure III.6: Role of EBV in PEL pathogenesis: Model. Panel A represents the classical scenario where naïve B-cells (B) entering the germinal center (GC) are infected with EBV. They further lose FHIT and WWOX as they mature through the GC to form PEL and in a subset of cases they can acquire genomic instability (X^{mut}) along with losing EBV as the lymphoma progresses. Panel B represents 2 hypothetical scenarios: (a) Parallel and (b) Stem-cell guided. In the Parallel model, analogous to Sequential model, the GC B-cells first lose FHIT and WWOX to proceed to PEL and then are either infected with EBV or acquire genomic aberrations (X^{mut}) as the lymphoma progresses. In the Stem-cell guided model it can be speculated that a sub-population of GC B-cells acquire stem cell properties to form a renewal source of proliferating cells that are either infected with EBV or become chromosomally unstable (X^{mut}), analogous to the Parallel model.

Table III.1: Summary of PEL Cell Lines used in SNP Sequencing

Sample Name	KSHV	EBV	p53 Status	Sample Type	Isolated from	Original Description
AP2	+	+	K139E;	Culture	Pleural effusion of HIV+ male	Carbone, A., et. al. Int J Cancer, 1997
AP5	+	+	R181P	Culture	Pleural effusion of HIV+ male	Carbone, A., et. al. Br J Haematol, 1998
BC1	+	+	wild type	Culture	Ascitic fluid from HIV+ male	Cesarman, E., et. al. Blood, 1995
BC2	+	+	wild type	Culture	HIV+ male	Cesarman, E., et. al. Blood, 1995
BC3	+	-	wild type	Culture	Pleural effusion of HIV+ male	Arvanitakis, L., et. al. Blood, 1996

BC5	+	+	wild type	Culture	HIV+ male	Guasparri, I., et. al. J Exp Med, 2004
BCBL1	+	-	S262 insertion	Culture	HIV+ patient	Komanduri, K.V., et. al. J AIDS Hum Retrovirol, 1996
BCLM	+	-	wild type	Culture	Pleural effusion of HIV+ male	Ghosh, S.K., et. al. Blood, 2003
BCP1	+	-	M246I	Culture	PBMCs from HIV- male	Boshoff, C., et. al. Blood, 1998
HHB2	+	-	wild type	Culture	Pleural effusion of HIV+ male	Gradoville, L., et. al. J Virol, 2000
JSC1	+	+	wild type	Culture	Ascitic fluid HIV+ male	Cannon, J.S., et. al. J Virol, 2000
TY1	+	-	S262 insertion; M246I	Culture	Pericardial fluid HIV+ male	Katano, H., et. al. J Med Virol, 1999
VG1	+	-	wild type	Culture	Pleural fluid from HIV- male	Brander, C., et. al. J Immunol,

						2000
mBC1.1	+	+	wild type	Xenograft	Xenograft tumor in SCID mice using cultured BC1 cells	Sin, SH., et. al. Blood 2007
mBC1.1	+	+	wild type	Xenograft		
mBC2.1	+	+	wild type	Xenograft	Xenograft tumor in SCID mice using cultured BC2 cells	Sin, SH., et. al. Blood 2007
mBC2.1	+	+	wild type	Xenograft		

Table III.2: Genes deregulated in majority of PEL cell lines

Gene ID	Gene Name	Location	Amplification	Deletion	EBV Dependent
DERL1	DER-1 Like domain family, member 1	8q24.13	AP2, AP5, BC1, BC2, BC3, BCBL, BCLM, BCP1, HHB2, JSC1, TY1, VG1	NONE	No
ETV1	ETS Translocation Variant 1	7p21.3	AP5, BC1, BC2, BC3, BC5, BCBL, BCLM, BCP1, HHB2, JSC1, TY1, VG1		
RASA4	RAS p21 protein Activator 4	7q22	AP2, AP5, BC1, BC3, BC5, BCBL, BCLM,		
TPK1	Thiamin Pyrophospho- Kinase 1	7q34			

TRIM56	TRIpartite Motif-containing 56	7q22.1	BCP1, HHB2, JSC1, TY1, VG1		
VPS41	Vacuolar Protein Sorting 41 homolog	7p14			
*WWOX	WW-domain containing OXido-reductase	16q23.3	NONE	AP5, BC1, BC2, BC3, BC5, BCBL, BCLM, BCP1, HHB2, JSC1, TY1, VG1	
*FHIT	Fragile HIstidine Triad	3p14.2	NONE	AP2, AP5, BC1, BC2, BC3, BC5, BCBL, BCLM, BCP1, TY1, VG1	
*GRID2	Glutamate Receptor, Ionotropic, Delta 2	4q22.1	NONE	BC3, BCBL, BCLM, TY1, VG1	Yes

Table III.3: Genes altered only in EBV negative PEL

Gene ID	Gene Name	Location	Category	Amplification	Deletion	Unchanged
ACSBG2	Acyl-CoA synthetase bubblegum family member 2	19p13.3	Metabolism	BC3, BCBL, BCLM, BCP1, HHB2, TY1	_	VG1
FUT3	CD174; Fucosyltransferase 3	19p13.3	Metabolism	BC3, BCBL, BCLM, BCP1, HHB2, TY1	_	VG1
HLA-DRB5	MHC-II, DR-Beta-5	6p21.3	MHC	BCBL, BCLM, BCP1, TY1, VG1	_	BC3, HHB2
IKBKB	IκB Kinase Beta	8p11.2	Cell Signaling	BC3, BCBL, BCLM, BCP1, TY1	_	HHB2, VG1
ITPR1	Inositol-1,4,5-	3p26.1	Cell Signaling	BCBL, BCLM,	_	BC3, HHB2

	triphosphate receptor, type 1			BCP1, TY1, VG1		
RAF1	v-Raf murine leukemia homolog 1	3p25	Oncogene	BCBL, BCLM, BCP1, TY1, VG1	–	BC3, HHB2
RFX2	Regulatory factor X, 2	19p13.3	Transcription	BC3, BCBL, BCLM, BCP1, HHB2	–	TY1, VG1
ARAP2	Arf and RhoGAP Adaptor Protein 2	4p14	Cytoskeleton	–	BC3, BCBL, BCP1, HHB2, TY1	BCLM, VG1
BRCA2	Breast Cancer 2, early onset	13q12.3	Tumor Suppressor	–	BC3, BCBL, BCLM, HHB2, TY1	BCP1, VG1
CADM2	Cell Adhesion Molecule 2	3p11.1	Cell Adhesion	–	BC3, BCBL, BCP1, HHB2, TY1	BCLM, VG1
CDH9	Cadherin 9, type 2	5p14.1	Cell Adhesion	HHB2	BC3, BCBL, BCLM, BCP1, TY1	VG1

CDYL	Chromodomain protein, Y-like	6p25.1	Transcription	VG1	BCBL, BCLM, BCP1, HHB2, TY1	BC3
CHD1	Chromodomain Helicase DNA binding protein 1	5q21.1	Transcription	HHB2	BCBL, BCLM, BCP1, TY1, VG1	BC3
EPHA3	Ephrin Receptor A3	3p11.2	Development	–	BC3, BCBL, BCLM, BCP1, TY1	HHB2, VG1
EPHA5	Ephrin Receptor A5	4q13.1	Development	VG1	BC3, BCBL, BCLM, BCP1, HHB2, TY1	
EDIL3	EGF-like repeats and discoidin-I like domain 3	5q14.3	Cell Adhesion	HHB2	BC3, BCBL, BCLM, BCP1, TY1	VG1
GRID2	Glutamate receptor, ionotropic, delta 2	4q22.1	Development	–	BC3, BCBL, BCLM, TY1, VG1	BCP1, HHB2
HBS1L	Hsp70 subfamily B	6q23.3	Development	–	BCBL, BCLM,	BC3, VG1

	suppressor 1-like protein				BCP1, HHB2, TY1	
LRFN5	Leucine rich repeat and fibronectin type III domain containing 5	14q21.1	Cell Adhesion	–	BC3, BCBL, BCLM, BCP1, TY1	HHB2, VG1
MEF2C	Myocyte Enhancer Factor 2	5q14.3	Transcription	HHB2	BC3, BCBL, BCP1, TY1, VG1	BCLM
PCDH9	Protocadherin 9	13q21.32	Cell Adhesion	–	BC3, BCBL, BCLM, BCP1, TY1	HHB2, VG1
RREB1	Ras-Responsive Element Binding protein 1	6p24.3	Transcription	BC3, VG1	BCBL, BCP1, HHB2, TY1	BCLM
ZEB1	Zinc finger E-box binding homeobox 1	10p11.2	Transcription	–	BC3, BCBL, BCLM, BCP1, HHB2	TY1, VG1

REFERENCES

Aqeilan, R.I., Trapasso, F., Hussain, S., Costinean, S., Marshall, D., Pekarsky, Y., Hagan, J.P., Zanesi, N., Kaou, M., Stein, G.S., *et al.* (2007). Targeted deletion of Wwox reveals a tumor suppressor function. Proc Natl Acad Sci U S A *104*, 3949-3954.

Bechtel, D., Kurth, J., Unkel, C., and Kuppers, R. (2005). Transformation of BCR-deficient germinal-center B cells by EBV supports a major role of the virus in the pathogenesis of Hodgkin and posttransplantation lymphomas. Blood *106*, 4345-4350.

Bednarek, A.K., Laflin, K.J., Daniel, R.L., Liao, Q., Hawkins, K.A., and Aldaz, C.M. (2000). WWOX, a novel WW domain-containing protein mapping to human chromosome 16q23.3-24.1, a region frequently affected in breast cancer. Cancer Res *60*, 2140-2145.

Berridge, M.J. (1993). Inositol trisphosphate and calcium signalling. Nature *361*, 315-325.

Bluteau, O., Beaudoin, J.C., Pasturaud, P., Belghiti, J., Franco, D., Bioulac-Sage, P., Laurent-Puig, P., and Zucman-Rossi, J. (2002). Specific association between alcohol intake, high grade of differentiation and 4q34-q35 deletions in hepatocellular carcinomas identified by high resolution allelotyping. Oncogene *21*, 1225-1232.

Boulanger, E., Agbalika, F., Maarek, O., Daniel, M.T., Grollet, L., Molina, J.M., Sigaux, F., and Oksenhendler, E. (2001). A clinical, molecular and cytogenetic study of 12 cases of human herpesvirus 8 associated primary effusion lymphoma in HIV-infected patients. Hematol J *2*, 172-179.

Boulanger, E., Marchio, A., Hong, S.S., and Pineau, P. (2009). Mutational analysis of TP53, PTEN, PIK3CA and CTNNB1/beta-catenin genes in human herpesvirus 8-associated primary effusion lymphoma. Haematologica *94*, 1170-1174.

Brinkmann, M.M., Glenn, M., Rainbow, L., Kieser, A., Henke-Gendo, C., and Schulz, T.F. (2003). Activation of mitogen-activated protein kinase and NF-kappaB pathways by a Kaposi's sarcoma-associated herpesvirus K15 membrane protein. J Virol *77*, 9346-9358.

Bubman, D., Guasparri, I., and Cesarman, E. (2007). Deregulation of c-Myc in primary effusion lymphoma by Kaposi's sarcoma herpesvirus latency-associated nuclear antigen. Oncogene *26*, 4979-4986.

Capello, D., Scandurra, M., Poretti, G., Rancoita, P.M., Mian, M., Gloghini, A., Deambrogi, C., Martini, M., Rossi, D., Greiner, T.C.*, et al.* (2010). Genome wide DNA-profiling of HIV-related B-cell lymphomas. Br J Haematol *148*, 245-255.

Carbone, A., Cesarman, E., Spina, M., Gloghini, A., and Schulz, T.F. (2009). HIV-associated lymphomas and gamma-herpesviruses. Blood *113*, 1213-1224.

Chadburn, A., Hyjek, E., Mathew, S., Cesarman, E., Said, J., and Knowles, D.M. (2004). KSHV-positive solid lymphomas represent an extra-cavitary variant of primary effusion lymphoma. Am J Surg Pathol *28*, 1401-1416.

Chaganti, S., Bell, A.I., Pastor, N.B., Milner, A.E., Drayson, M., Gordon, J., and Rickinson, A.B. (2005). Epstein-Barr virus infection in vitro can rescue germinal center B cells with inactivated immunoglobulin genes. Blood *106*, 4249-4252.

Chang, Y., Cesarman, E., Pessin, M.S., Lee, F., Culpepper, J., Knowles, D.M., and Moore, P.S. (1994). Identification of herpesvirus-like DNA sequences in AIDS-associated Kaposi's sarcoma. Science *266*, 1865-1869.

Chaudhary, P.M., Jasmin, A., Eby, M.T., and Hood, L. (1999). Modulation of the NF-kappa B pathway by virally encoded death effector domains-containing proteins. Oncogene *18*, 5738-5746.

D'Haene, B., Vandesompele, J., and Hellemans, J. (2010). Accurate and objective copy number profiling using real-time quantitative PCR. Methods *50*, 262-270.

Deffenbacher, K.E., Iqbal, J., Liu, Z., Fu, K., and Chan, W.C. (2010). Recurrent chromosomal alterations in molecularly classified AIDS-related lymphomas: an integrated analysis of DNA copy number and gene expression. J Acquir Immune Defic Syndr *54*, 18-26.

Dellis, O., Arbabian, A., Brouland, J.P., Kovacs, T., Rowe, M., Chomienne, C., Joab, I., and Papp, B. (2009). Modulation of B-cell endoplasmic reticulum calcium homeostasis by Epstein-Barr virus latent membrane protein-1. Mol Cancer *8*, 59.

Dumon, K.R., Ishii, H., Fong, L.Y., Zanesi, N., Fidanza, V., Mancini, R., Vecchione, A., Baffa, R., Trapasso, F., During, M.J.*, et al.* (2001). FHIT gene therapy prevents tumor development in Fhit-deficient mice. Proc Natl Acad Sci U S A *98*, 3346-3351.

Durkin, S.G., and Glover, T.W. (2007). Chromosome fragile sites. Annu Rev Genet *41*, 169-192.

Fabbri, M., Iliopoulos, D., Trapasso, F., Aqeilan, R.I., Cimmino, A., Zanesi, N., Yendamuri, S., Han, S.Y., Amadori, D., Huebner, K.*, et al.* (2005). WWOX gene restoration prevents lung cancer growth in vitro and in vivo. Proc Natl Acad Sci U S A *102*, 15611-15616.

Fakhari, F.D., and Dittmer, D.P. (2002). Charting latency transcripts in Kaposi's sarcoma-associated herpesvirus by whole-genome real-time quantitative PCR. J Virol *76*, 6213-6223.

Fan, W., Bubman, D., Chadburn, A., Harrington, W.J., Jr., Cesarman, E., and Knowles, D.M. (2005). Distinct subsets of primary effusion lymphoma can be identified based on their cellular gene expression profile and viral association. J Virol *79*, 1244-1251.

Feske, S. (2007). Calcium signalling in lymphocyte activation and disease. Nat Rev Immunol *7*, 690-702.

Fujishita, T., Doi, Y., Sonoshita, M., Hiai, H., Oshima, M., Huebner, K., Croce, C.M., and Taketo, M.M. (2004). Development of spontaneous tumours and intestinal lesions in Fhit gene knockout mice. Br J Cancer *91*, 1571-1574.

Gaidano, G., Capello, D., Cilia, A.M., Gloghini, A., Perin, T., Quattrone, S., Migliazza, A., Lo Coco, F., Saglio, G., Ascoli, V.*, et al.* (1999). Genetic characterization of HHV-8/KSHV-positive primary effusion lymphoma reveals frequent mutations of BCL6: implications for disease pathogenesis and histogenesis. Genes Chromosomes Cancer *24*, 16-23.

Gaidano, G., Capello, D., Fassone, L., Gloghini, A., Cilia, A.M., Ariatti, C., Buonaiuto, D., Vivenza, D., Gallicchio, M., Avanzi, G.C.*, et al.* (2000). Molecular characterization of HHV-8 positive primary effusion lymphoma reveals pathogenetic and histogenetic features of the disease. J Clin Virol *16*, 215-224.

Godfrey, A., Anderson, J., Papanastasiou, A., Takeuchi, Y., and Boshoff, C. (2005). Inhibiting primary effusion lymphoma by lentiviral vectors encoding short hairpin RNA. Blood *105*, 2510-2518.

Jane-Valbuena, J., Widlund, H.R., Perner, S., Johnson, L.A., Dibner, A.C., Lin, W.M., Baker, A.C., Nazarian, R.M., Vijayendran, K.G., Sellers, W.R., *et al.* (2010). An oncogenic role for ETV1 in melanoma. Cancer Res *70*, 2075-2084.

Ji, L., Fang, B., Yen, N., Fong, K., Minna, J.D., and Roth, J.A. (1999). Induction of apoptosis and inhibition of tumorigenicity and tumor growth by adenovirus vector-mediated fragile histidine triad (FHIT) gene overexpression. Cancer Res *59*, 3333-3339.

Johnson, D.R., Levan, G., Klein, G., Nigida, S.M., Jr., and Wolfe, L.G. (1981). Chromosomes and cell surface markers of marmoset lymphocytes and Epstein-Barr virus-transformed marmoset cell lines. Cancer Genet Cytogenet *3*, 101-108.

Johnson, W.E., Li, W., Meyer, C.A., Gottardo, R., Carroll, J.S., Brown, M., and Liu, X.S. (2006). Model-based analysis of tiling-arrays for ChIP-chip. Proc Natl Acad Sci U S A *103*, 12457-12462.

Kameoka, Y., Tagawa, H., Tsuzuki, S., Karnan, S., Ota, A., Suguro, M., Suzuki, R., Yamaguchi, M., Morishima, Y., Nakamura, S., *et al.* (2004). Contig array CGH at 3p14.2 points to the FRA3B/FHIT common fragile region as the target gene in diffuse large B-cell lymphoma. Oncogene *23*, 9148-9154.

Kawai, H., Suda, T., Aoyagi, Y., Isokawa, O., Mita, Y., Waguri, N., Kuroiwa, T., Igarashi, M., Tsukada, K., Mori, S., *et al.* (2000). Quantitative evaluation of genomic instability as a possible predictor for development of hepatocellular carcinoma: comparison of loss of heterozygosity and replication error. Hepatology *31*, 1246-1250.

Klein, U., Gloghini, A., Gaidano, G., Chadburn, A., Cesarman, E., Dalla-Favera, R., and Carbone, A. (2003). Gene expression profile analysis of AIDS-related primary effusion lymphoma (PEL) suggests a plasmablastic derivation and identifies PEL-specific transcripts. Blood *101*, 4115-4121.

Laherty, C.D., Hu, H.M., Opipari, A.W., Wang, F., and Dixit, V.M. (1992). The Epstein-Barr virus LMP1 gene product induces A20 zinc finger protein expression by activating nuclear factor kappa B. J Biol Chem *267*, 24157-24160.

Lilley, B.N., and Ploegh, H.L. (2004). A membrane protein required for dislocation of misfolded proteins from the ER. Nature *429*, 834-840.

Ludes-Meyers, J.H., Kil, H., Nunez, M.I., Conti, C.J., Parker-Thornburg, J., Bedford, M.T., and Aldaz, C.M. (2007). WWOX hypomorphic mice display a higher incidence of

B-cell lymphomas and develop testicular atrophy. Genes Chromosomes Cancer *46*, 1129-1136.

Mack, A.A., and Sugden, B. (2008). EBV is necessary for proliferation of dually infected primary effusion lymphoma cells. Cancer Res *68*, 6963-6968.

Mancao, C., Altmann, M., Jungnickel, B., and Hammerschmidt, W. (2005). Rescue of "crippled" germinal center B cells from apoptosis by Epstein-Barr virus. Blood *106*, 4339-4344.

Matolcsy, A., Nador, R.G., Cesarman, E., and Knowles, D.M. (1998). Immunoglobulin VH gene mutational analysis suggests that primary effusion lymphomas derive from different stages of B cell maturation. Am J Pathol *153*, 1609-1614.

Mullaney, B.P., Ng, V.L., Herndier, B.G., McGrath, M.S., and Pallavicini, M.G. (2000). Comparative genomic analyses of primary effusion lymphoma. Arch Pathol Lab Med *124*, 824-826.

Nador, R.G., Cesarman, E., Chadburn, A., Dawson, D.B., Ansari, M.Q., Sald, J., and Knowles, D.M. (1996). Primary effusion lymphoma: a distinct clinicopathologic entity associated with the Kaposi's sarcoma-associated herpes virus. Blood *88*, 645-656.

Nair, P., Pan, H., Stallings, R.L., and Gao, S.J. (2006). Recurrent genomic imbalances in primary effusion lymphomas. Cancer Genet Cytogenet *171*, 119-121.

Nunn, J., Scholes, A.G., Liloglou, T., Nagini, S., Jones, A.S., Vaughan, E.D., Gosney, J.R., Rogers, S., Fear, S., and Field, J.K. (1999). Fractional allele loss indicates distinct genetic populations in the development of squamous cell carcinoma of the head and neck (SCCHN). Carcinogenesis *20*, 2219-2228.

O'Hara, A.J., Vahrson, W., and Dittmer, D.P. (2008). Gene alteration and precursor and mature microRNA transcription changes contribute to the miRNA signature of primary effusion lymphoma. Blood *111*, 2347-2353.

O'Hara, A.J., Wang, L., Dezube, B.J., Harrington, W.J., Jr., Damania, B., and Dittmer, D.P. (2009). Tumor suppressor microRNAs are underrepresented in primary effusion lymphoma and Kaposi sarcoma. Blood *113*, 5938-5941.

Ohshima, K., Ishiguro, M., Yamasaki, S., Miyagi, J., Okamura, S., Sugio, Y., Muta, T., Sasaki, H., Tuchiya, T., Kawasaki, C., *et al.* (2002). Chromosomal and comparative genomic analyses of HHV-8-negative primary effusion lymphoma in five HIV-negative Japanese patients. Leuk Lymphoma *43*, 595-601.

Ohta, M., Inoue, H., Cotticelli, M.G., Kastury, K., Baffa, R., Palazzo, J., Siprashvili, Z., Mori, M., McCue, P., Druck, T., *et al.* (1996). The FHIT gene, spanning the chromosome 3p14.2 fragile site and renal carcinoma-associated t(3;8) breakpoint, is abnormal in digestive tract cancers. Cell *84*, 587-597.

Oracki, S.A., Walker, J.A., Hibbs, M.L., Corcoran, L.M., and Tarlinton, D.M. (2010). Plasma cell development and survival. Immunol Rev *237*, 140-159.

Petre, C.E., Sin, S.H., and Dittmer, D.P. (2007). Functional p53 signaling in Kaposi's sarcoma-associated herpesvirus lymphomas: implications for therapy. J Virol *81*, 1912-1922.

Rebhan, M., Chalifa-Caspi, V., Prilusky, J., and Lancet, D. (1997). GeneCards: integrating information about genes, proteins and diseases. Trends Genet *13*, 163.

Reid, A.H., Attard, G., Ambroisine, L., Fisher, G., Kovacs, G., Brewer, D., Clark, J., Flohr, P., Edwards, S., Berney, D.M., *et al.* (2010). Molecular characterisation of ERG, ETV1 and PTEN gene loci identifies patients at low and high risk of death from prostate cancer. Br J Cancer *102*, 678-684.

Rousseeuw P., L.A. (2003). Robust Regression and Outlier Detection (Hoboken, Wiley & Sons).

Rozier, L., El-Achkar, E., Apiou, F., and Debatisse, M. (2004). Characterization of a conserved aphidicolin-sensitive common fragile site at human 4q22 and mouse 6C1: possible association with an inherited disease and cancer. Oncogene *23*, 6872-6880.

Shin, S., Bosc, D.G., Ingle, J.N., Spelsberg, T.C., and Janknecht, R. (2008). Rcl is a novel ETV1/ER81 target gene upregulated in breast tumors. J Cell Biochem *105*, 866-874.

Sin, S.H., Roy, D., Wang, L., Staudt, M.R., Fakhari, F.D., Patel, D.D., Henry, D., Harrington, W.J., Jr., Damania, B.A., and Dittmer, D.P. (2007). Rapamycin is efficacious against primary effusion lymphoma (PEL) cell lines in vivo by inhibiting autocrine signaling. Blood *109*, 2165-2173.

Sogame, N., Kim, M., and Abrams, J.M. (2003). Drosophila p53 preserves genomic stability by regulating cell death. Proc Natl Acad Sci U S A *100*, 4696-4701.

Soulier, J., Grollet, L., Oksenhendler, E., Cacoub, P., Cazals-Hatem, D., Babinet, P., d'Agay, M.F., Clauvel, J.P., Raphael, M., Degos, L.*, et al.* (1995). Kaposi's sarcoma-associated herpesvirus-like DNA sequences in multicentric Castleman's disease. Blood *86*, 1276-1280.

Staudt, M.R., Kanan, Y., Jeong, J.H., Papin, J.F., Hines-Boykin, R., and Dittmer, D.P. (2004). The tumor microenvironment controls primary effusion lymphoma growth in vivo. Cancer Res *64*, 4790-4799.

Storey, J.D., and Tibshirani, R. (2003). Statistical significance for genomewide studies. Proc Natl Acad Sci U S A *100*, 9440-9445.

Vaghefi, P., Martin, A., Prevot, S., Charlotte, F., Camilleri-Broet, S., Barli, E., Davi, F., Gabarre, J., Raphael, M., and Poirel, H.A. (2006). Genomic imbalances in AIDS-related lymphomas: relation with tumoral Epstein-Barr virus status. AIDS *20*, 2285-2291.

Wang, J., Hua, H., Ran, Y., Zhang, H., Liu, W., Yang, Z., and Jiang, Y. (2008). Derlin-1 is overexpressed in human breast carcinoma and protects cancer cells from endoplasmic reticulum stress-induced apoptosis. Breast Cancer Res *10*, R7.

CHAPTER IV

RAPAMYCIN INHIBITS THE GROWTH OF KAPOSI'S SARCOMA TUMOR CELLS *IN VIVO* BY DOWN REGULATING PARACRINE FACTORS SUCH AS VASCULAR ENDOTHELIAL GROWTH FACTOR (VEGF)

Debasmita Roy, Sang-Hoon Sin, Dirk P. Dittmer

This work is being formatted for submission at Cancer Research

ABSTRACT

Kaposi's Sarcoma (KS) is a cancer of endothelial cell origin mainly seen in the immune-compromised setting. KS is caused by Kaposi's Sarcoma-associated Herpes Virus (KSHV), also known as Human Herpes Virus (HHV)-8. This study reports on the use of Rapamycin, an inhibitor of key cellular kinase mammalian Target of Rapamycin (mTOR), as a therapeutic agent against KS. Using a newly developed L1T2 cell line, it has been shown that Rapamycin treatment significantly inhibits cell growth both in culture and in our xenograft model. Rapamycin results in reduced levels of key paracrine and angiogenic factor Vascular Endothelial Growth Factor (VEGF) and defective tumor vasculature to inhibit tumor progression. Further, the effect of combining Rapamycin with Doxorubicin, a common chemotherapeutic agent, has been explored here. Surprisingly, it was observed that Doxorubicin dampens the tumor inhibitory effect of Rapamycin by partially rescuing the tumor vasculature defect. Based on these observations, I propose that the growth inhibitory effect of Rapamycin is mediated by down-regulation of VEGF to create a less optimal tumor microenvironment.

INTRODUCTION

Kaposi's Sarcoma (KS) is an aggressive cancer of the endothelial cell origin afflicting immunocompromised patients, especially those with Acquired Immunodeficiency Syndrome (AIDS). KS was initially identified by the Hungarian dermatologist, Dr Moritz Kaposi as purple, flat skin lesions in older Mediterranean men back in the 19th century(Kaposi, 1872). However, it was not until the early 1990's, nearly a century later, that KS came into the limelight as an AIDS-defining malignancy. Using differential sequence analysis on KS biopsies obtained from HIV-positive patients, Chang et. al. identified the novel Human Herpes Virus-8 (HHV8), also known as Kaposi's Sarcoma-associated Herpes Virus (KSHV)(Chang et al., 1994). In addition to its Classical and AIDS-associated forms, KS has also been seen in HIV-negative transplant patients on immune-suppression, known as iatrogenic KS. (Ganem, 2010)

Upon presentation, KS lesions appear as flat dermal 'patches'. As the lesion progresses from patch to plaque to nodular masses, the initial red color presentation deepens to a purple hue. The characteristic color of KS lesions is indicative of the high degree of vasculogenesis and angiogenesis typical of KS. Unlike other tumors, angiogenesis in KS is believed to begin even before the formation of a visible tumor lesion. Another diagnostically significant observation is the morphological change that the endothelial cells undergo into the unique 'spindle' shape. In addition, infected cells express the major latency protein, Latency-associated Nuclear Antigen (LANA). Upon staining, KS biopsy sections exhibit the distinct punctate nuclear staining that is tightly associated with KSHV infection.(Ballestas et al., 1999; Kedes et al., 1997)

Like all other Herpesviruses, KSHV can exist either in a latent or lytic replicative state. Upon establishing latency, the virus is maintained as an episome tethered to the host chromosome via LANA. Being a rhadinovirus, it maintains a latent reservoir in B-lymphocytes, occasionally switching to a lytic replication cycle to disseminate to healthy cells. Latent KSHV infection of B-cells is also associated with the rare AIDS-related lymphoma, Primary Effusion Lymphoma (PEL)(Cesarman et al., 1995). Although KS is believed to derive from infection of endothelial cells, the exact lineage of these cells is still being investigated.(Damania, 2004; Ganem, 2010)

Latently-infected cells express a small subset of viral genes, including LANA, viral Cyclin (vCyclin), viral Fas-associated with death domain (FADD)-like interleukin-1β-converting enzyme (FLICE)/ caspase-8-inhibitory protein (vFLIP), Kaposin and viral micro-RNAs, all transcribed from the same latency locus. While vCyclin is capable of promoting cell cycle progression, vFLIP can inhibit apoptosis, thus ensuring persistent infection (Guasparri et al., 2004; Laman et al., 2001). In addition to tethering the viral episome, LANA can bind to and functionally inactivate key tumor suppressor genes such as p53 and Rb (An et al., 2005; Friborg et al., 1999). Although the exact roles of the viral miRNAs have not been established, there is evidence in the literature that viral miR-K12-10 shares 100% homology to and can target the same set of messenger RNAs as cellular miR-155. Mir-155 is classified as an oncogenic miRNA and has specifically shown to be over-expressed in lymphomas (Gottwein et al., 2007; Skalsky et al., 2007). Furthermore, the literature suggests that the KSHV viral microRNAs likely play a role in viral persistence and tumorigenesis (Abend et al., 2010; Hansen et al., 2010; Lei et al., 2010; Lu et al., 2010).

Apart from spontaneous reactivation, the lytic replication program can be chemically induced by treatment with phorbolester, calcium ionophores, IFNγ or infection with cytomegalovirus (CMV). This induces expression of the immediate-early signature lytic gene Replication and Transcription Activator (RTA). RTA in turn induces a cascade of other viral genes like viral homologs of cellular Interleukin-6 (vIL6) and G-protein coupled receptor (vGPCR). Work from our lab as well as others have suggested that both latent and lytic viral proteins are capable of deregulating cellular homeostasis to result in disease.

While vIL6 resembles proinflammatory cytokine IL6, vGPCR is homologous to the IL8 receptor(Cesarman et al., 1996; Nicholas et al., 1997). However, unlike IL6, vIL6 can signal independently of the gp80 receptor and vGPCR is activated in the absence of ligand, thus resulting in more constitutive signaling (Arvanitakis et al., 1997; Molden et al., 1997; Wan et al., 1999). vGPCR is a transmembrane protein that has been shown to be able to activate key cellular mediators of signaling like phospho-inositide-3-Kinase (PI3K) and phospho-lipase C (PLC) (Montaner, 2007). vGPCR has also been associated with expression of pro-growth factors like Vascular Endothelial Growth Factor (VEGF) (Bais et al., 1998; Sodhi et al., 2000). Given the highly angiogenic nature of KS, it stands to reason that agents directed against these growth factors may present a robust therapeutic approach.

Given the viral involvement in KS, the treatment modalities range from inhibitors of viral replication to small molecule inhibitors of key cellular proteins. Since LANA can functionally inactivate key cellular regulators, they are genetically intact and can be targeted for therapeutics. It has been shown that small molecule inhibitors like Nutlin that

are capable of inhibiting the p53:LANA interaction or stabilize p53 dimers resulted in growth inhibition of KSHV-infected cells (Sarek et al., 2007). Likewise, Doxorubicin, a chemotherapeutic agent that invokes the DNA damage response resulting in p53-mediated apoptosis has been shown to be effective against PEL cells. Given the prevalence of iatrogenic KS, several reports in the literature discuss treatment modalities against KS in transplant patients. It was initially shown by Stallone et. al. that switching the immuno-suppresive regimen of renal transplant patients from Cyclosporin-A to Rapamycin resulted in a complete regression of iatrogenic KS lesions (Stallone et al., 2005). Since then, various groups have shown that Rapamycin can be used as an effective anti-tumor therapy.

Rapamycin was identified as an anti-fungal drug with immune suppressive properties (Baker et al., 1978). It was subsequently shown to also exhibit strong anti-tumor activity. It targets the key cellular kinase, mTOR, which plays a critical role in mediating translational regulation. Inhibition of mTOR results in reduced phosphorylation of p70-S6-Kinase (p70S6K) and eukaryotic initiation factor-4E (eIF4E) binding protein (4EBP1). It has been well-documented that 4EBP1 is involved in regulating 5'-cap-dependent mRNA translation. Upon phosphorylation, 4EBP1 dissociates from translation initiation factor, eIF4E, thereby activating translation. Thus, Rapamycin leads to a reduction in phospho-4EBP1, resulting in translational inhibition of key mRNAs like Myc, Cyclin D1 and VEGF, all of which have been implicated in cancer. The other arm of the pathway leads to phosphorylation of ribosomal protein S6 (S6R) via phospho-p70S6K, which is again inhibited by Rapamycin treatment. Activated ribosomal S6 protein results in upregulation of 5'-terminal oligopyrimidine tract (TOP)

mRNA translation. Specifically, 5'TOP is present in mRNA encoding ribosomal proteins and other components of the translation machinery, thus up-regulating phospho-S6 results in overall increased cellular translation. (Sabatini, 2006; Vivanco and Sawyers, 2002)

Previous data from our lab has shown that inhibition of mTOR in latently KSHV-infected B-cells results in reduced levels of IL6 and IL10, key cytokines in mediating the pathogenesis of PEL(Sin et al., 2007). There have been other reports demonstrating the inhibition of mTOR and/or upstream mediator, Phospho-inositol-3-Kinase (PI3K), effectively inhibiting growth of KSHV-infected B-cells.(Bhatt et al., 2010; Uddin et al., 2005) However, due to the limitations of studying KS *in vitro*, currently there are no reports comparing the effects of the different immune-suppressants most commonly used in the clinic on latently infected KS-like endothelial cells.

In addition to Rapamycin, FK506, also known as Tacrolimus(Kino et al., 1987), is another popular immunosuppressive used in the clinic. Currently, there are no reports exploring the effect of FK506 on KSHV-infected cells. With the increasing application of transplantation procedures in the clinic, Rapamycin, FK506 and several of their derivatives have also been put to use. In this study, I looked at two Rapamycin derivatives Everolimus (RAD-001) and Temsirolimus (CCI-779), and two of the FK506 derivatives, Ascomycin and Pimecrolimus that are in the clinic today.

Despite the availability of primary KS biopsy samples, both from HIV-positive and –negative patients, there is a dearth of *in vitro* models of the disease. The primary reason for this is that although cells isolated from primary biopsies can be optimally

grown in culture, they often lose LANA expression and the viral episome over time. SLK cells constitute the classic cell line isolated from an oral KS biopsy of an HIV-negative male.(Herndier et al., 1994) At the time of tissue procurement, the biopsy expressed LANA-positive spindle cells. Although the LANA positivity was lost over time in culture, the spindle cells are retained and SLK cells form KS-like tumors in nude mice (ref?). Various groups have successfully been able to show de novo infection of endothelial cells of varied origins by KSHV (table IV.1), but there are just a handful of latently infected cell lines (Flore et al., 1998; Lagunoff et al., 2002; Wang and Damania, 2008). The KSHV-positive KS cell line, k-SLK, was developed upon transfection of the KSHV episome into SLK cells, which were then maintained on Puromycin selection(Grundhoff and Ganem, 2004). However, to our knowledge, An et. al. is the only group to have reported the isolation of two clones--E1 and L1, KSHV-infected telomerase immortalized human vein endothelial cells (TIVE)--that have maintained the KSHV episome and express LANA in the absence of a selective pressure.(An et al., 2006)

In this study, I show the efficacy of Rapamycin against KS *in vivo* and propose that this inhibition is mediated via disruption of the tumor microenvironment. A new cell line L1T2 was used to evaluate the efficacy of Rapamycin and FK506 in our xenograft mouse model. It was shown that Rapamycin effectively inhibits tumor growth whereas FK506 aggravates tumor progression. Molecular analysis showed that Rapamycin mediates this inhibition by reducing phosphorylation of mTOR downstream target ribosomal S6 and does not result in increased apoptosis. I illustrated that reduced VEGF secretion, as noted *in vitro*, translates to immature tumor vasculature *in vivo*. This led to

the speculation that in cancers like KS disrupting the tumor microenvironment has a profound effect on tumor progression. I further evaluated the effect of combination therapy of Rapamycin together with Doxorubicin *in vivo*. While an additive effect was observed with combination therapy over Doxorubicin alone, surprisingly, it was noted that Rapamycin in itself was more effective in restricting tumor growth.

MATERIALS AND METHODS

Cell culture All cell lines were cultured in DMEM supplemented with 100μg/ml streptomycin sulfate, 100U/ml penicillin G (Life Technologies, Carlsbad, CA, USA), and 10% FBS at 37°C in 5% CO_2.

Colony Formation Assay Cells were counted, washed once in ice-cold phosphate-buffered saline (PBS, Cellgro Mediatech, Inc., Herndon, VA) and an optimal number (50-500 cells per well/plate, determined empirically) were plated in growth media (as above) supplemented either with vehicle or drug at the indicated concentrations. Growth was monitored over a period of 2-weeks or 7-days for 10cm dishes and 12-well plates respectively. Media was replaced with fresh media supplemented with fresh drugs every 3-4 days during the growth period. At the end of the assay, colonies were stained with Magic Blue Stain (3g crystal violet and 0.92g of Ammonium oxalate in 20% ethanol) and assessed visually by counting the number of colonies formed.

xCelligence Automated Cell Growth Monitoring System The xCELLigence system (Roche Diagnostics, Indianapolis?, IN) uses electronic readout, termed 'Cell

Index', to monitor growth of adherent cells in real time. Cells are plated on specialized microplates that contain microelectronic sensor arrays at the bottom of the wells. The interaction of the plated cells with these sensors generates cell-electrode impedance that is correlated to the number of live cells. Live cells that adhere to the bottom result in higher impedance, thus a higher Cell Index, and dying cells lose contact thereby lowering the Cell Index. Effect of drug treatment on KS cells was determined by monitoring the electronic impedance every 15-30min over a period of 48hrs. Growth curves and IC50 plots were generated using RTCA Software v1.2 (ACEA Bio. Inc., San Diego, CA)

Quantitative PCR for the KSHV Genome Genomic DNA was extracted using the Wizard SV Genomic DNA Purification System, as per the manufacturer's protocol (Promega, Madison, WI) and quantitative PCR was used to detect the viral genome in the different KS cell lines as per our previous publications(Fakhari et al., 2006).

Immunofluorescence Cells were cultured overnight on glass coverslips in 6-well plates (Falcon-BD Bioscience Inc, San Jose, CA). They were washed in PBS and immune fluorescence was performed using the protocol as previously described(Chen et al., 2010). Mouse anti-LANA (Novocastra Lab Ltd., Newcastle, UK), diluted 1:600 was used. Images were taken on a LEICA DM4000B fluorescence microscope (Leica, Heidelberg, Germany) equipped with a 63/1.4-0.6 numerical aperture (NA) objective and a Q-Imaging Retiga 2000RV camera. Raw, single microscopy images were deconvoluted using Simple PCI™ (Hamamatsu Corp., Sewickley, PA, USA) 2D Blind Deconvolution that iteratively applies the AutoQuant Imaging (Media Cybernetics, Inc. Bethesda, MD) proprietary algorithm to remove blur and generate high clarity images, stored as tiff files.

Tumor formation Cells were counted, washed once in ice-cold phosphate-buffered saline (PBS, Cellgro Mediatech, Inc., Herndon, VA) and indicated cell doses were diluted into 100 µl PBS and mixed with 100 µl growth factor-depleted Matrigel (BD Biosciences, Bedford, MA). $1x10^6$ cells were injected sub-cutaneously into the flank of C.B.-17 SCID mice (Jackson Laboratory, Bar Harbor, MN) following our previously validated procedures (Staudt et al., 2004). The mice were observed every day for the presence of palpable tumors. Drug or vehicle was injected intra-peritoneally at the indicated dosing schedule. Tumor diameters were determined by caliper measurements. Tumor volume was calculated as V = a * b * c, where a, b and c are the three diameters (length, breadth and width) of the tumor. The tumors were excised from the site of injection and fixed in formalin (Fisher Diagnostics, Middletown, VA).

Immunohistochemistry Tumors were removed and processed as per our prior publication(Sin et al., 2007) using the appropriate primary antibody: total S6 ribosomal protein monoclonal antibody (1:100 dil.), phospho-S6 ribosomal protein (S235/236) monoclonal antibody (1:50 dil.) and Cleaved Caspase-3 (D175) polyclonal antibody (1:100 dil.) from Cell Signaling Inc. (Boston, MA). Sections were imaged using a LEICA DM LA histology microscope (Leica, Heidelberg, Germany) equipped with a 10/0.25 numerical aperture (NA) or a 40/0.75 NA N plan objective and Leica DPC 480 camera. Images were stored as TIFF files under Mac OS X10.5.

Tumor Vasculature Staining Tumor vasculature was determined using commercially available Periodic Acid Schiff (PAS) staining system following the manufacturer's recommendations (Sigma Aldrich, St. Louis, MO). Sections were imaged using a LEICA DM LA histology microscope (Leica, Heidelberg, Germany) equipped

with a 10/0.25 numerical aperture (NA) or a 40/0.75 NA N plan objective and Leica DPC 480 camera. Images were stored as TIFF files under Mac OS X10.5.

VEGF Quantification VEGF levels in the culture supernatant was determined using a commercial VEGF ELISA assay as per the manufacturer's recommendations (PeproTech, Rocky Hill, NJ).

RESULTS

Development of L1T2 cell line and xenograft model

The L1T2 cell line was established by explanting cells from xenograft tumors formed by injecting L1-TIVE cells subcutaneously into SCID mice. Tumor masses were disaggregated in DMEM containing 10% FBS, 100 μg/mL streptomycin sulfate, 100 U/mL penicillin G, 2 mM L-glutamine, and 50ug/mL Nystatin (Sigma). Cells that grew from the explant and adhered to the culture dish to continue to proliferate were designated L1T2.

The L1T2 cells were assessed for LANA expression using immunofluorescence staining to show that these cells maintain latent infection analogous to the previously characterized L1- and E1-TIVE cells. I was able to detect the classic punctate LANA staining in the nuclei indicative of the presence of the viral episome, figure IV.1, panel A. The top panel represents DAPI (blue) staining the nucleus, LANA (green) and the merge, in the presence of LANA-specific primary antibody, at 63X magnification. The bottom panel shows the no antibody control where no green (LANA) staining is detected. Upon

quantification, I noted that the L1T2 cells showed a moderate increase in the number of latently infected cells compared to the precursor L1-TIVE cells. Where An et. al. reported less than 10% LANA positivity after 4 weeks in culture, comparatively nearly 40% (100/256) L1T2 cells stained positive for LANA.

Using the KSHV array that was previously designed in our lab, I evaluated the integrity of the KSHV genome. Figure IV.1, panel B shows the heat map comparing the quantitative PCR data generated from L1T2 genomic DNA compared to other current *in vitro* models of KS. As our positive control, I used DNA from BCBL1: a well characterized latently infected PEL cell line, and for negative control: SLK cells. It was noted that where BCBL-1 shows presence of high levels of viral DNA (indicated by red), SLK is distinctly negative (represented by the dark blue color). K-SLK cells showed viral DNA at comparable levels to the BCBL-1 positive control, verifying that the viral episome is successfully maintained through *in vitro* culturing. E1- and L1-TIVE, along with L1T2 represent the spectrum in between our positive and negative controls. Of specific note is the expression of LANA, marked with a black asterisk, in figure IV.1, panel B. As expected, no LANA was detected in SLK cells and very high levels were found in K-SLK and BCBL1 cells. Interestingly, more LANA expression was detected in L1T2 cells compared to E1- and L1-TIVE.

The tumor-forming potential of the L1T2 cells was assessed following our standard xenograft protocol in SCID mice. $1x10^6$ cells were injected subcutaneously and tumor progression was monitored over a period of 2 weeks post-injection. As shown in figure IV.1, panel C, all mice (n=9), males (grey line) and females (black line), injected

with L1T2 cells developed solid, palpable tumors within 2 days of injection and continued to grow up to 2 weeks post-injection?.

Rapamycin and FK506 are effective against KS cell line *in vitro*

I further compared the effects of different immunosuppressants used in transplant patients in our cell culture and xenograft models of KS. I evaluated Rapamycin, two of its derivatives, FK506 along with two of its derivatives and Doxorubicin (Dox), as shown in table IV.1. FK506 and Rapamycin share the same intermediate binding partner, FK506 Binding Protein (FKBP) -12, but target different signaling pathways. Biochemically, the Rapamycin:FKBP12 complex has been shown to directly bind to and inhibit mTORC1, whereas FK506:FKBP12 interacts with Cyclophilin to inhibit Calcineurin-mediated signaling. In our *in vitro* studies, I also assessed the effects of Cyclosporin A (CsA), a common immunosuppressant in the clinic, and LY-294002, an inhibitor of PI3K, a kinase that acts upstream of Rapamycin/mTOR.

Using an *in vitro* plating assay, it was shown that colony formation is unaffected by treatment with any of the drugs compared to their respective vehicle controls, with the exception of Dox and CsA (Figure IV.2). Panel A represents Rapamycin (500uM) treatment of E1- and L1-TIVE cells compared to vehicle control and panels B and C show SLK and L1T2 cells treated with the panel of drugs as listed in table IV.2. Where both Dox and CsA have been documented as cytotoxic drugs in the literature, Rapamycin is classified as a cytostatic drug. Further, using the xCelligence system, an automated cell counter that measures growth of adherent cells based on changes in electrical conductance (designated 'Cell Index'), I was able to demonstrate growth inhibition in

SLK and L1T2 cells. While the *in vitro* colony formation assay measures end-point proliferation, xCelligence measures growth every 30 min, over a period of 48hrs or longer, to generate growth curves and determine IC_{50} values as shown in table IV.2. Therefore, the xCelligence system provides greater sensitivity in assaying for cytostatic drugs like Rapamycin, FK506 and their derivatives.

Figure IV.2 shows the growth curves and IC_{50} values obtained for the highest (in grey) and lowest (in black) concentrations of Doxorubicin, Rapamycin and FK506 in subpanels (i), (ii) and (iii) respectively. Panel D represents drug treatment of SLK cells whereas panel E shows treatment of L1T2 cells. Different growth patterns were observed in the two cell lines, where L1T2 seems to have a bi-phasic growth curve. Nonetheless, both cell lines show susceptibility *in vitro* to Doxorubicin, Rapamycin and FK506 alike. The IC_{50} values were generated by the xCelligence software taking into account all six drug concentrations (10-fold dilutions), that were used to treat each individual cell line over a period of 48 hours. Again, comparing the type of IC_{50} plots for Doxorubicin vs. Rapamycin/FK506, there was a difference in the nature of the sigmoidal curves, confirming the cytotoxic vs. cytostatic nature of these agents.

Rapamycin, not FK506, is effective against KS cell lines *in vivo*

Previous reports in the literature had shown that treatment of mice with CsA resulted in more aggravated tumors. The same response was observed in our PEL xenograft tumors, where treatment with CsA resulted in larger tumors compared to the vehicle control (data not shown). Thus, CsA was not used for any further studies.

Given that the L1 and E1-TIVE cells have been established as viable model systems to study KS pathogenesis, I initially used these cell lines to examine the effect of Rapamycin treatment on tumor growth. L1- and E1-TIVE cells were injected subcutaneously as noted above and tumor growth was monitored. Upon formation of palpable tumors in all experimental animals, they were injected with either Rapamycin (3mg/kg/day: 3 times a week) or mock treatment. Progression of the tumor was further monitored over a period of approximately 10 days to determine drug effect. Figure IV.3, panels A and B show the plot for all animals injected with L1- and E1-TIVE cells, respectively, where the green arrow indicates the time of start of treatment. In each cohort, the drug-treated animals showed significantly smaller tumors than the mock-treated ones. It was noted that despite the E1-TIVE tumors being substantially larger in volume than the L1-TIVE cells, both were similarly inhibited by Rapamycin treatment. For our subsequent experiments, I used the newly developed L1T2 cells that exhibited a more robust tumor uptake within ~2 days post-injection.

In the clinic, Rapamycin dosing presents to be a significant challenge. There is evidence in the literature that different *in vitro* effects of Rapamycin require doses that vary by more than 1000-fold.(Foster and Toschi, 2009) Therefore, before proceeding with further studies, I sought to investigate the dosing regimen required to obtain therapeutic drug trough levels, while minimizing the adverse effects of Rapamycin treatment on the overall health of the animals. For our dosing studies L1-TIVE and SLK cell lines were used.

In our initial xenograft experiments, it was noted that the animals on high (3-5mg/kg) doses of Rapamycin exhibited health concerns (weight loss and lethargy) and

had to be sacrificed early on in the study. Upon reducing the dose to 1.5mg/kg, I observed significant improvement in the survival curve, but a minimal effect on tumor progression. Accordingly, the dose was slightly increased to 2mg/kg Rapamycin and it seemed to be more effective at tumor inhibition, without adversely affecting overall survival, than 1.5mg/kg dose although still not statistically significant (data not shown).

I further clarified the dosing scheme using SLK cells as they exhibit a quicker tumor onset. Figure IV.4 shows SLK-tumors in SCID mice that were mock-treated (panel A) or treated with 2.25mg/kg Rapamycin (panel B) or 5mg/kg Rapamycin (panel C). While 5mg/kg Rapamycin was very effective, it adversely affected overall health. In contrast, 2.25mg/kg of Rapamycin, while being nearly equally effective, resulted in an improved survival plot. In Figure IV.4, panel D, the Kaplan-Meir curve illustrates the significant improvement of the animals when treated with 2.25mg/kg of Rapamycin compared to 5mg/kg (p-value = 0.008). In fact, 5mg/kg of Rapamycin generated a poorer survival curve than the mock treatment, further emphasizing the importance of an optimal dosing scheme in the clinic. Thus, considering both sets of L1-TIVE and SLK experiments, 2.5mg/kg of Rapamycin, injected intra-peritoneally 3 times a week, was determined as an optimal dose to inhibit tumor formation without affecting overall health.

As mentioned previously, the L1T2 cell line was generated by explanting an L1-TIVE tumor and selecting for proliferative advantage in culture and in mice. SCID mice were injected with L1T2 cells and compared the tumor growth upon treatment with 2.5mg/kg Rapamycin or 2.5mg/kg FK506. While treatment with Rapamycin was effective in inhibiting tumor growth, treatment with FK506 in fact further aggravated tumor progression. Figure IV.5, panel A, compares the average growth of L1T2 tumors in

different animals, illustrating that the difference between Rapamycin and FK506 is significant.

The effect of Rapamycin vs. FK506 treatment was independently verified in SLK cells (Figure IV.5). SLK xenograft tumors in SCID mice were subject to either 2.5mg/kg Rapamycin, 2.5mg/kg FK506 or mock treatment. Analogous to L1T2 cells, a significant inhibition was observed with Rapamycin treatment but tumor growth was aggravated with FK506 treatment over mock (figure IV.5, panel B). Of further note was the difference in overall tumor sizes. L1T2 cells formed tumors nearly twice the size of SLK cells, leading us to speculate that although SLK cells form KS-like tumors without the viral episome, the presence of KSHV in the L1T2 cells might provide a proliferative advantage that results in larger tumors.

To further investigate some of the nuances of Rapamycin-mediated inhibition of tumor growth, I wanted to determine whether Rapamycin truly acted as a cytostatic drug in mice. Figure IV.5, panel C illustrates the experiment where the animals were treated either with 2.5mg/kg Rapamycin or FK506 for a period of time (green arrow indicating the start of treatment) followed by drug withdrawal (indicated by the red arrow). Upon drug withdrawal, tumor growth resumed in the Rapamycin treatment group to the point that the tumor volumes were equivalent and even greater than the FK506 treatment group. This led to the hypothesis that being a cytostatic agent, Rapamycin is not able to completely eliminate the tumor cells and a subset of them remain growth arrested. Thus, as Rapamycin is withdrawn, these cells recover and proceed to proliferate, resulting in larger tumor volumes. This further suggested that combining cytotoxic chemotherapeutic drugs, like Doxorubicin, together with cytostatic agents, like Rapamycin, might constitute

a better therapeutic approach. Specifically in the case of a tumor like KS that harbors wild type, inducible p53, using agents like Doxorubicin and Nutlin has been shown to be therapeutically viable.

The fact that both Rapamycin and FK506 were equally effective in inhibiting cell growth *in vitro*, but *in vivo* had opposing effects is an interesting observation. It highlights the importance of the tumor microenvironment and its impact on tumor growth.

Rapamycin inhibits phosphorylation of ribosomal S6 protein without affecting total S6 levels in xenograft tumors

The tumors were stained with Hematoxylin and Eosin to determine the overall tumor histology. Rapamycin and FK506-treated tumors were similar in that the interior of the tumor mainly consisted of necrotic tissue. Spindle cells that are characteristic of KS lesions were seen to be dispersed throughout the tumor sections. Figure IV.6, panel A is a representative panel showing L1T2 tumors obtained from individual mice treated with Rapamycin, FK506 and vehicle control, where the spindle cells are marked with asterisks.

Phosphorylation of ribosomal S6 protein is considered a robust readout for mTOR activation. Immunohistochemical staining of tumors for phosphorylated ribosomal S6 at Serine 235/236 residues (pS6R (S235/236)) showed that treatment with Rapamycin resulted in dramatically reduced levels of pS6R (S235/236). Figure IV.6 shows representative images demonstrating that all L1T2 tumors expressed comparable levels of total S6 (panel B) and the Rapamycin-treated tumors are the only ones that completely

lack pS6R (S235/236) staining (panel C). This indicated that Rapamycin is successfully in inhibiting endogenous mTOR target to mediate tumor inhibition.

I also assayed for apoptosis using immunohistochemical staining for cleaved Caspase-3 that identified cells undergoing both FAS-ligand and mitochondrial-mediated apoptosis. Figure IV.6, panel D, shows the complete lack of apoptotic cells in vehicle-treated cells and a minimal degree of staining in Rapamycin and FK506-treated cells compared to Doxorubicin-treated cells (figure IV.8, panel B) that represent the positive control.

Rapamycin inhibits VEGF *in vitro* and associated vasculature *in vivo*

KS tumors are characterized by their typical purple color indicative of increased vasculature and angiogenesis. Therefore, I hypothesized that in lieu of inhibiting the KSHV-infected endothelial cell growth *in vivo*, Rapamycin inhibits tumor vasculature.

Although ineffective in inhibiting colony formation in culture, Rapamycin led to reduced levels of secreted VEGF, as measured by ELISA (figure IV.7). I conducted a time course followed by a drug washout experiment to assess both the production and accumulation of VEGF in the culture supernatant. The cells were treated for 48hrs with 5uM (4.5ug/ml) Rapamycin and then exchanged the media with fresh drug-free media that was replaced every 24hrs, over 72hrs. I noted that during the initial drug treatment, there was reduced VEGF levels in both E1- and L1-TIVE cells; but, as the drug was withdrawn, the cells gradually recovered and produced more VEGF. Similar results were noted for SLK and L1T2 cells (data not shown). This suggested that the Rapamycin-

mediated inhibition in VEGF levels is not simply a reduced accumulation in the media but an actual reduction in VEGF production.

In culture, the cells are grown in DMEM media containing 10% serum, which constitutes a less nutritionally demanding environment. In contrast, in the xenograft the cells have to establish an optimal microenvironment that promotes tumor growth. Thus, I hypothesized that reduction in growth factors in this environment would have a more pronounced impact on tumor growth via autocrine and paracrine manners. Using PAS staining, which stains for vasculature (pink), it was shown that treatment with Rapamycin indeed results in a tumor vasculature defect. Figure IV.6, panel E shows that the Rapamycin-treated tumors have less mature vessel formation compared to the vehicle. Rapamycin-treated tumors have significantly reduced branching, indicative of immature vasculature.

Rapamycin alone is more effective in inhibiting tumor growth compared to Rapamycin-Doxorubicin combination therapy

Doxorubicin is a chemotherapeutic agent that has been shown to be effective in inhibiting growth of PEL cells and KSHV-infected B-cells. Given our observation that Rapamycin is capable of inhibiting tumor cell growth but unable to eliminate them, led us to speculate the effectiveness of combining a cytostatic agent like Rapamycin with a cytotoxic agent like Doxorubicin. Treatment of both SLK and L1T2 cells with Doxorubicin in culture, in contrast to Rapamycin treatment, resulted in 100% inhibition of colony formation (figure IV.2, panels B and C). Likewise, in our cell growth

monitoring experiment, distinctly different inhibitory curves were noted for treatment with Doxorubicin compared to Rapamycin (figure IV.2, panels D(i) and E(i)).

In our *in vivo* studies, L1T2 tumors in SCID mice were treated with 4 different regimens: 2.5mg/kg Rapamycin i.p. 3x weekly, 4mg/kg Doxorubicin i.p. 5x weekly, 2.5mg/kg Rapamycin (i.p. 3x weekly) + 4mg/kg Doxorubicin (i.p. 5x weekly) or mock treatment (figure IV.8, panel A). I observed that both Rapamycin and Doxorubicin were effective individually in inhibiting tumor progression, although Rapamycin was more effective than Doxorubicin. Surprisingly, the combination treatment did not show synergy or an additive effect in inhibiting tumor growth over Rapamycin alone. On the contrary, Rapamycin alone was more effective in tumor inhibition. However, I did show that combination therapy was more effective than Doxorubicin alone.

Reports in the literature have shown that Doxorubicin activates the DNA damage response to inhibit tumor progression and results in apoptosis of tumor cells. Immunohistochemical staining for cleaved Caspase-3 marks cells undergoing apoptosis, both Fas-ligand as well as mitochondria mediated. Figure IV.8, panel B shows representative staining for cleaved Caspase-3 in the different treatment groups. Doxorubicin-treated tumors showed significant staining, as expected, compared to the vehicle control. Rapamycin treatment on the other hand showed minimal staining and in fact adding Rapamycin treatment to the Doxorubicin regimen resulted in fewer apoptotic cells.

On the contrary, staining for tumor vasculature revealed that while Rapamycin significantly inhibited vessel branching, Doxorubicin left it unaltered (figure IV.8, panel

D). Histologically, it appeared that Doxorubicin-treated sections maintained tumor vasculature even better than vehicle treatment. Quantification of vessel branch points (figure IV.8, panel C) denotes the significant loss of branching upon Rapamycin treatment compared to Doxorubicin, (p-value ≤ 0.005). Looking at the reduced number of branch points in combination treatment compared to Doxorubicin alone (p-value ≤ 0.001) suggests that Rapamycin treatment overshadows the effect of Doxorubicin to disrupt the tumor vasculature.

Overall, it was interesting to note the inverse relationship between the degree of vascular branching and apoptotic cells in Rapamycin and Doxorubicin-treated tumors compared to mock. Correlating the tumor response to drug treatment to the above-mentioned apoptosis and vasculature phenotypes led us to further emphasize the importance of vasculogenesis and angiogenesis in the progression of KS. It led us to speculate that the virus-mediated modulation of the tumor microenvironment as opposed to alteration of the growth cycle of the infected cells constitutes primary KSHV oncogenesis.

DISCUSSION

This study investigated the effect of mTOR inhibition on KSHV-induced tumorigenesis of endothelial cells *in vitro* and *in vivo*. Given the prevalence of KS in transplant patients on immunosuppressants, I examined the effects of both FK506 (or Tacrolimus) and Rapamycin (or Sirolimus), the primary mTOR inhibitor. In culture, both Rapamycin and FK506 along with their derivatives are effective in inhibiting growth. It

was further demonstrated that growth inhibition mediated by cytotoxic drugs like Doxorubicin and Cyclosporin-A is distinct from that mediated by Rapamycin, FK506 and their derivatives, which are classified as cytostatic agents.

However, *in vivo* there were some very different and interesting observations. I showed independently in two cell lines, SLK (KSHV-negative) and L1T2 (KSHV-positive), that treatment with Rapamycin resulted in tumor inhibition whereas treatment with FK506 further aggravated tumor progression. This was a particularly interesting observation since FK506 forms FK506:FKBP12 to inhibit the Calcineurin signaling cascade that is also inhibited by CsA, also shown to aggravate tumor phenotype and increase angiogenesis.

Looking at the molecular signature of mTOR inhibition I showed, as expected, that treatment with Rapamycin resulted in reduced levels of phospho-S6R (S235/236). Further, it was shown that treatment with Rapamycin disrupted vasculature in the tumor microenvironment but did not result in increased apoptosis, as determined by the PAS and cleaved Caspase-3 staining, respectively. It has been suggested in the literature that angiogenesis and vasculogenesis begin in KS patients even before the formation of a visible lesion. This, together with our *in vivo* data, led to the hypothesis that for tumors like KS, which are particularly dependent on angiogenesis and thrive in an optimal microenvironment, disrupting this tumor niche may provide for a very effective therapeutic option.

Considering the different modes of action of cytotoxic versus cytostatic drugs like Doxorubicin and Rapamycin, respectively, I sought to explore their effects on tumor

progression *in vivo*. Using our KSHV-positive L1T2 cells, the outcomes of treatment with Rapamycin and Doxorubicin alone or in combination was explored. It was very interesting to note that while the combination treatment was better than Doxorubicin alone, it was in fact worse than Rapamycin alone. Looking at the vasculature and apoptosis in the tumor, I noted that contrary to Rapamycin, Doxorubicin resulted in increased apoptosis, as would be expected from a DNA damage response-inducing agent, but had no effect on vasculature. In fact, comparing the different drug treatments it almost seemed that sections from the combination-treated tumors exhibited more Rapamycin-like rather than Doxorubicin-like phenotypes.

These observations led us to propose a model for KS pathogenesis, as illustrated in figure IV.9. It can be hypothesized that following de novo infection, as the virus is preparing to go into latency, it activates the PI3K-mTOR signaling cascade via lytic proteins like vGPCR and K1. Once in its latent state, the LANA protein together with vCyclin and vFLIP further disrupt the normal progression of the cell cycle and apoptosis. Previous reports from our lab and others have shown that inhibiting mTOR by Rapamycin results in reduced levels of IL6 and IL10 in infected B-cells. This suggested that via activation of the PI3K-mTOR signaling cascade, the virus induces expression of these pro-growth factors to serve as both autocrine and paracrine effectors. Likewise, in the context of KSHV-infected endothelial cells, VEGF, which is a pro-angiogenic factor, can induce vasculogenesis to create a microenvironment optimal for tumor growth.

As outlined in figure IV.9, four possible nodes for intervention were postulated to inhibit KSHV tumorigenesis in this mouse model. The upregulated growth factors can induce growth in an autocrine, (option #1) or paracrine (option #2) fashion in the host or

neighboring cells. A subset of these factors, such as VEGF, can also induce vessel formation and in the xenograft setting, specifically mouse blood vessel formation (option #3). Upon formation of the initial mouse vessel, the mouse endothelial cells lining these vessels can in turn produce mouse-specific VEGF to induce branching and maturation of the vasculature (option #4).

As a general translational inhibitor, Rapamycin can inhibit mTOR activity that in turn results in inhibition of VEGF. VEGF mRNA possesses a highly structured 5'-cap, making it ideal for eIF4E-mediated regulation. The *in vitro* observation of reduced VEGF levels in cell supernatants can further be extrapolated to the tumor setting to argue that Rapamycin can intervene at the autocrine and paracrine growth stages (options #1 and #2) as well as the initial vessel induction stage (option #3). However, further studies need to be conducted to determine the effect of Rapamycin treatment on the localized levels of mouse VEGF in the tumor microenvironment.

Doxorubicin, on the other hand, is a chemotherapeutic agent that acts by activating the p53 apoptotic response by mimicking DNA damage. Thus, it is only effective against replicating cells and can be hypothesized to be capable of interfering with the autocrine and paracrine factor mediated growth (options #1 and #2) of the tumor cells themselves. This is indeed what was observed *in vivo* where Doxorubicin induced significant apoptosis throughout the tumor section, including the edges.

Considering the postulations and *in vivo* pilot study, I speculate a therapeutic scheme where Rapamycin is administered in transplant patients and for the subset that may still develop KS, use of Doxorubicin or other such inhibitors can be used to target

replicating cells. The basis for this approach is the speculation that the cells forming the KS lesion have acquired a proliferative advantage that allow them to grow in a suboptimal microenvironment, thus constituting a Rapamycin-resistant type. This speculation is also supported by our observation that growth-arrested tumor cells (L1T2) retain their proliferative capacity and continue to grow upon drug withdrawal (figure IV.5, panel C).

Recently, it was shown by Gilbert and Hemann that treatment with a genotoxic agent such as Doxorubicin results in increased expression of IL-6 from the thymus, which provides a protective niche for residual tumor cells.(Gilbert and Hemann, 2010) This led us to speculate whether Doxorubicin-induced IL-6 was responsible for the Rapamycin alone faring better than Rapamycin-Doxorubicin combination treatment. To further verify whether increased IL-6 production by the thymus is providing protection to the tumor cells, a combination therapy xenograft experiment can be conducted in the athymic nude mice where no such protection would be expected.

In the context of KSHV infection, the protective effect of IL-6 can be particularly beneficial. Previous data from our lab has shown in the context of KSHV-infected B-cells that adding exogenous IL-6 concomitantly with Rapamycin rescues the growth inhibition mediated by mTOR. Applying this to KS, I conclude that simultaneous administration of Doxorubicin (or other genotoxic chemotherapeutic) and Rapamycin (or other mTOR/VEGF inhibitors) would not constitute a suitable therapeutic approach. From a more clinical perspective, perhaps cycling the two classes of drugs targeting both the microenvironment dependent and independent tumor cells could provide for an improved therapy against KS.

FIGURES

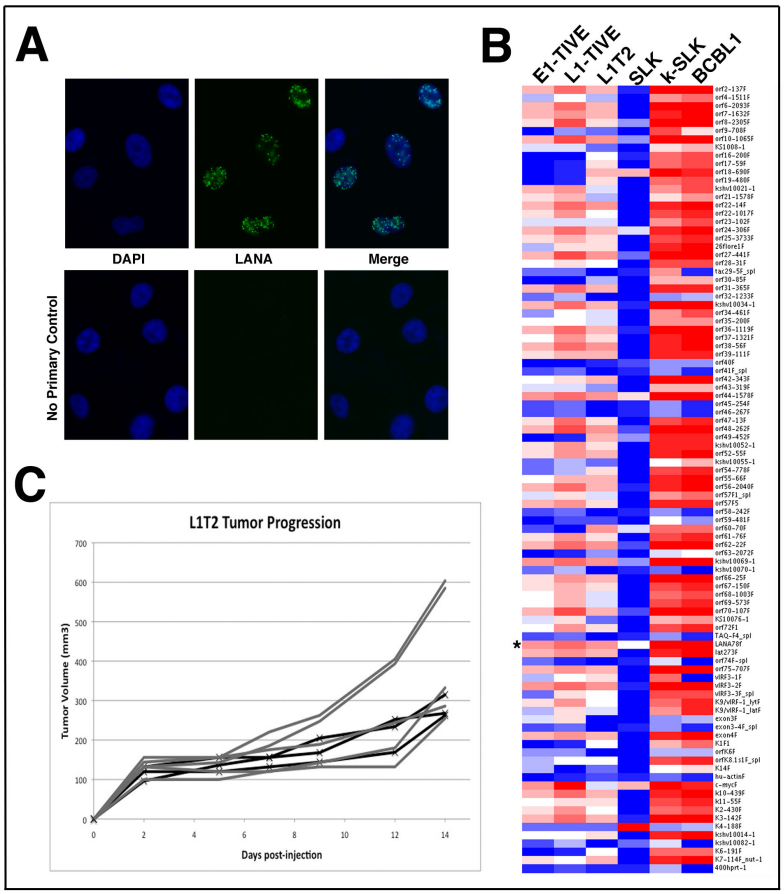

Figure IV.1: Establishment of L1T2 Cells in culture and xenograft model

Panel A represents immunofluorescence staining for LANA showing that the L1T2 harbor latent KSHV infection as indicated by the punctate green dots present only with LANA-specific antibody but not in the no primary antibody control (panel A, lower panel). Panel B represents the heat map showing the presence of the KSHV genome in the various *in vitro* KS cell lines by qPCR. BCBL1 is the positive control (indicated by red) and SLK is the negative control (indicated by blue). Panel C indicates the formation of tumors in both male and female SCID mice upon s.c. injection of L1T2 cells in 1:1 PBS:Matrigel™ mix.

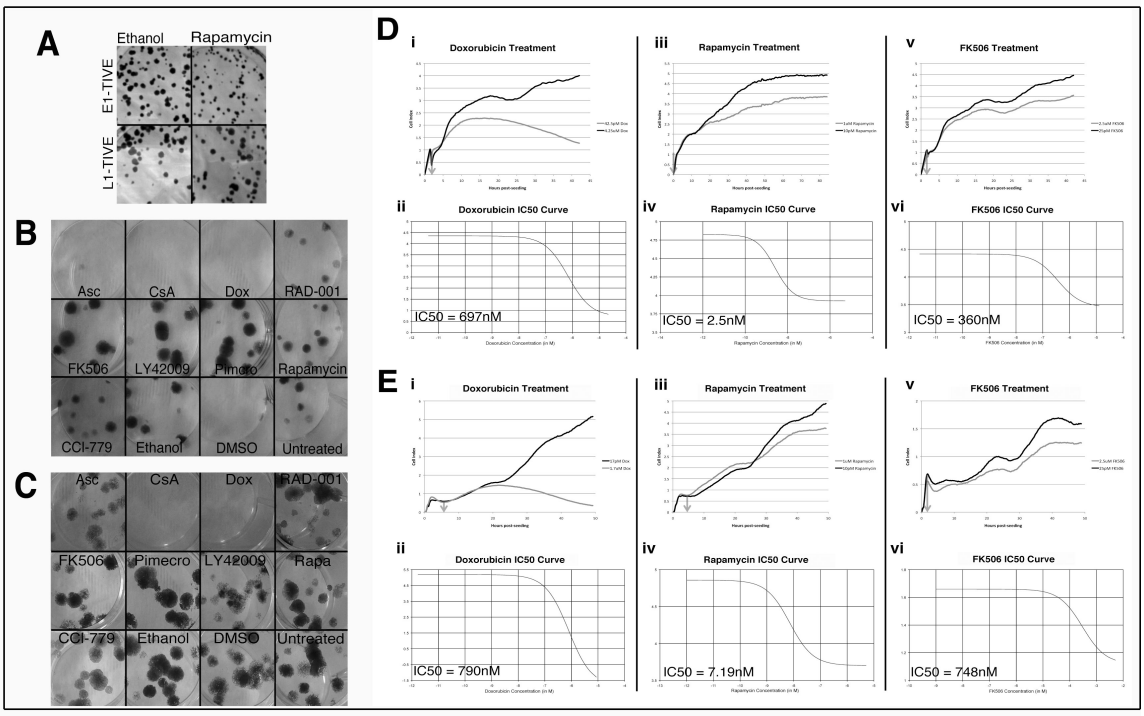

Figure IV.2: Effect of Doxorubicin, Rapamycin and FK506 treatment *in vitro*

Panels A, B and C show the colony formation assay. Panel A shows E1- and L1-TIVE colonies (top and bottom respectively) formed either with 5uM Rapamycin or mock (Ethanol) treatment. Panels B and C indicate colony formed by SLK and L1T2 cells respectively upon treatment with 5uM each of: Ascomycin(Asc), CyclosporinA (CsA), Doxorubicin (Dox), Everolimus (RAD-001), FK506, LY42009, Pimecrolimus (Pimecro), Rapamycin, Temsirolimus (CCI-779), and Controls (Ethanol, DMSO and Untreated). Panels D and E represent the growth monitoring plots for SLK and L1T2, respectively, generated using the xCelligence automated cell monitoring system. Subpanels (i), (iii) and (v) show the growth curves for the highest (grey) and lowest (black) drug concentrations. Subpanels (ii), (iv) and (vi) are the growth inhibitory plots used to determine (IC50) values for the individual drugs in the respective cell lines.

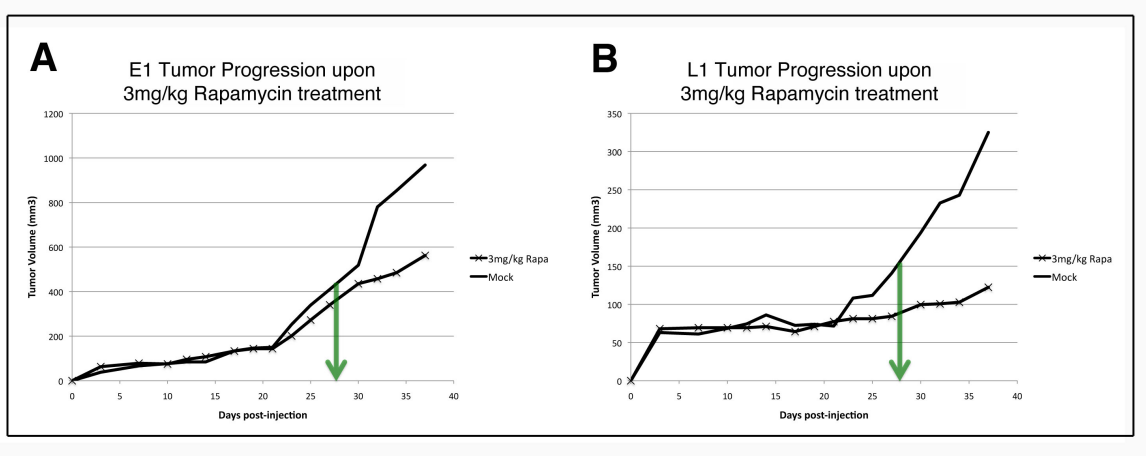

Figure IV.3: Effect of Rapamycin treatment on L1- and E1-TIVE *in vivo*

Panels A and B show E1- and L1-TIVE tumors that were treated either with 3mg/kg Rapamycin (i.p. 3x weekly) or vehicle control. Treatment was started at day 27 post-injection, as indicated by the green arrow and growth was monitored for 10 days following treatment.

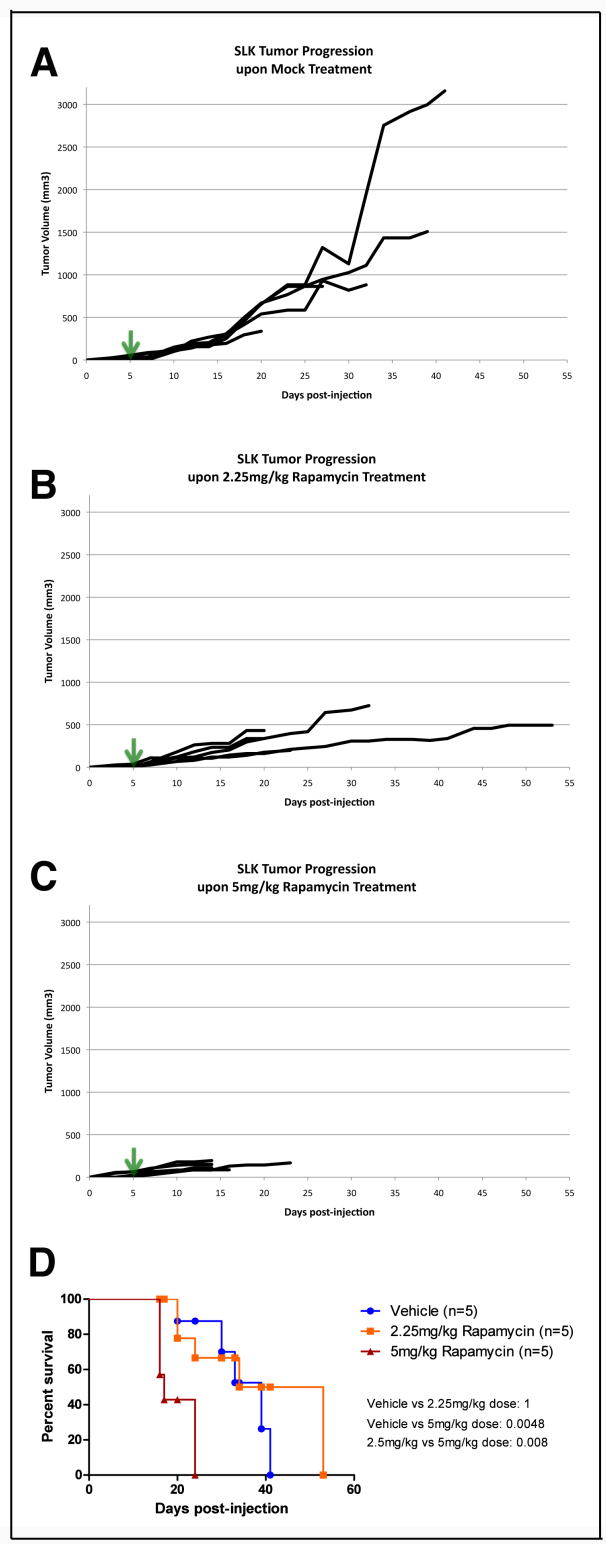

Figure IV.4: Rapamycin dosing regimen in SLK cells

Panels A, B and C are growth curves of all SLK-tumors treated with vehicle control, 2.25mg/kg or 5mg/kg of Rapamycin respectively. Panel D is the Kaplan-Meir curve generated comparing the survival rates of the different treatment groups.

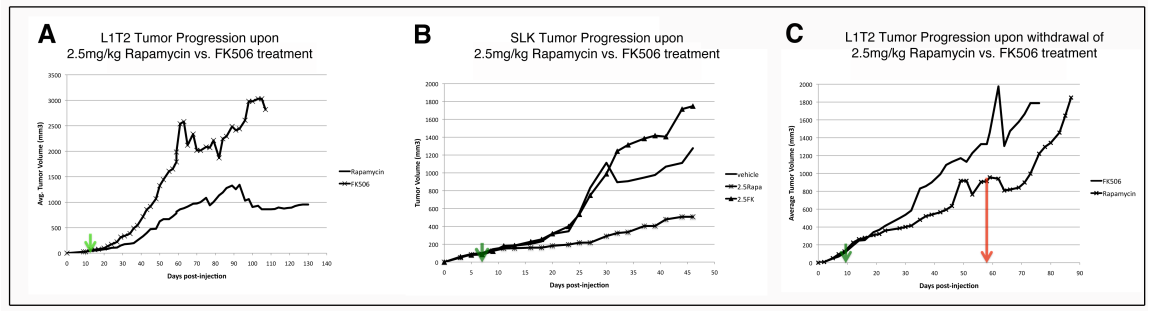

Figure IV.5: Effect of Rapamycin and FK506 treatment on L1T2 and SLK cells *in vivo*

Panels A and B show L1T2 and SLK tumors that were treated either with 2.5mg/kg Rapamycin (i.p. 3x weekly) or 2.5mg/kg FK506 (i.p. 3x weekly). Treatment was started at: day 6 for L1T2 and day 7 for SLK, post-injection as indicated by the green arrow and growth was monitored for several weeks following treatment, as indicated on the X-axes. Panel C illustrates the drug withdrawal regimen where L1T2 tumors were treated with 2.5mg/kg Rapamycin or FK506 starting at day 9 post-injection (as indicated by the green arrow) and treated for ~45 days and drug was withdrawn (as indicated by the red arrow) at which time tumor growth resumed.

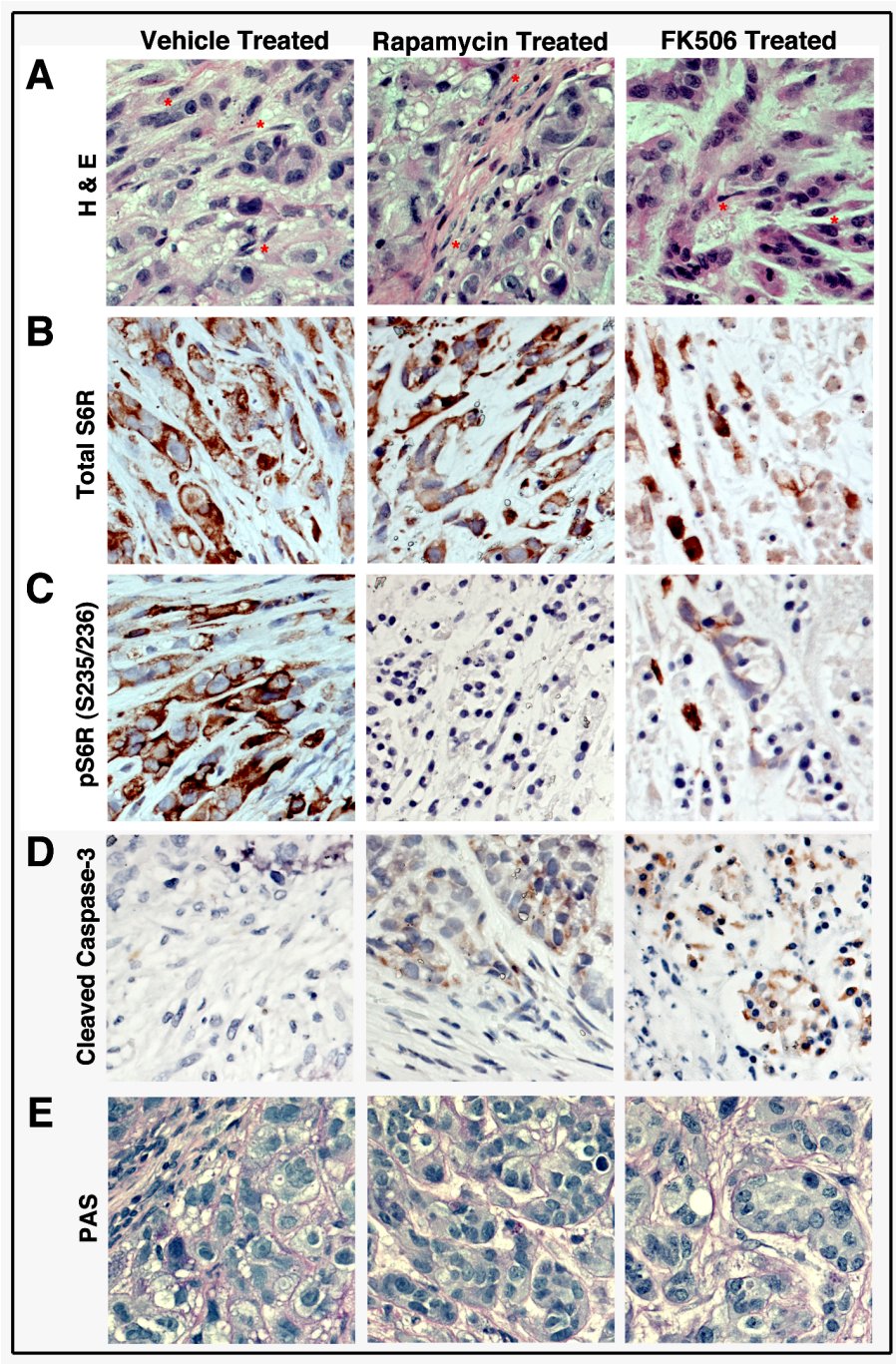

Figure IV.6: Immunohisto-chemical analysis of L1T2 tumors treated with vehicle, Rapamycin or FK506

Panels A, B, C, D and E represent 400X images of tumor sections stained with Hematoxylin-Eosin (H&E), total S6 ribosomal protein, phospho-S6 ribosomal protein at residue S235 and S236 (pS6R(S235/236)), cleaved Caspase-3 and PAS respectively. H&E mark the overall histology of tumors, pS6R(S235/236) indicates mTOR activity, cleaved Caspase-3 marks apoptotic cells and PAS stains for tumor vasculature.

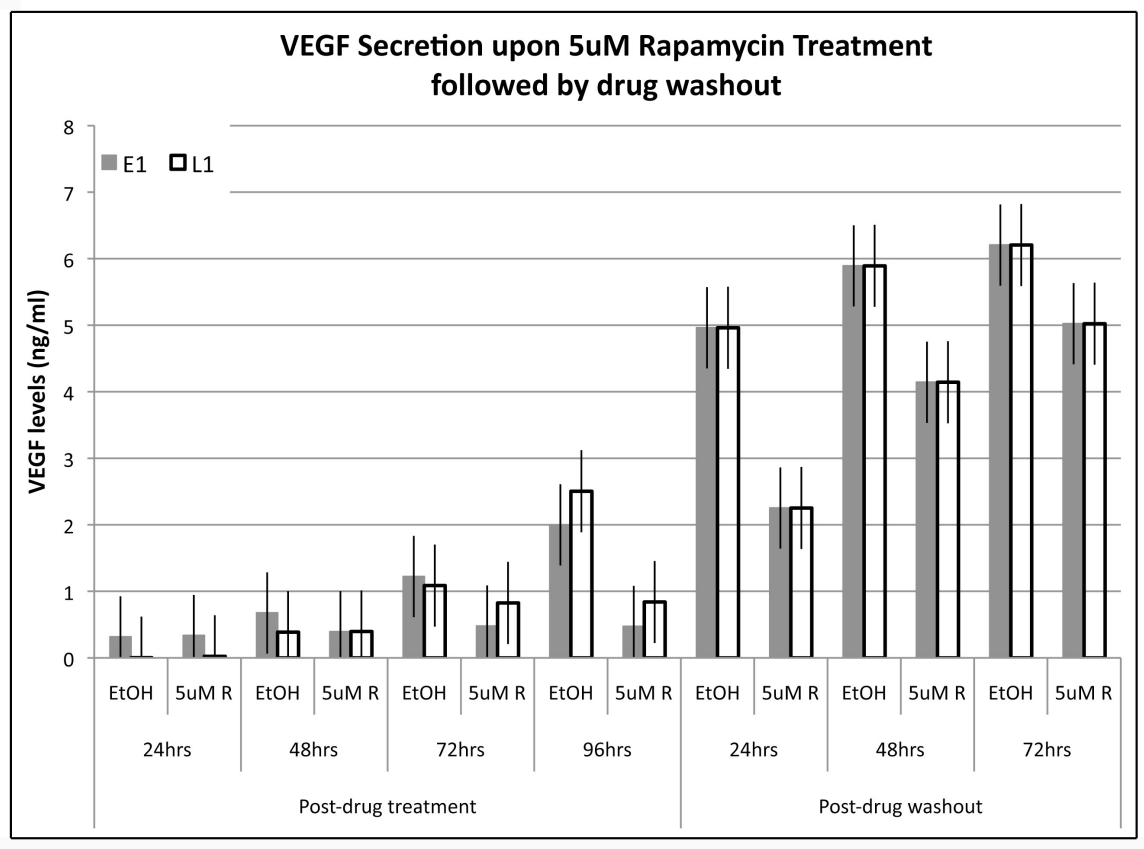

Figure IV.7: Quantification of secreted levels of VEGF *in vitro*

Secreted levels of VEGF were determined using a commercially available human VEGF-specific ELISA using the supernatant of E1- and L1-TIVE cells. Cells were grown in media containing 5uM drug or vehicle control followed by drug washout, wherein the media was replaced with fresh drug/vehicle media every 24hrs. VEGF levels were assessed at 24 and 48hrs post-seeding and 24, 48 and 72hrs post-washout.

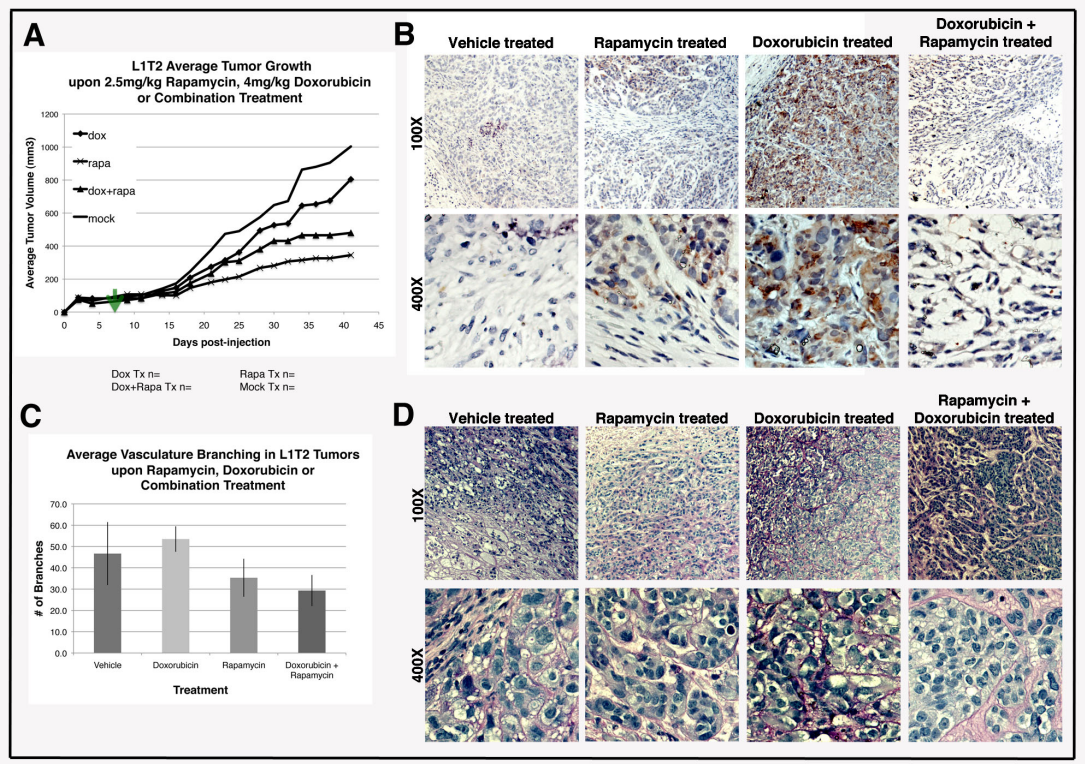

Figure IV.8: Effect of Rapamycin-Doxorubicin combination treatment on L1T2 xenograft tumor

Panel A shows L1T2 tumors that were treated either with: (i) 2.5mg/kg Rapamycin (i.p. 3x weekly); (ii) 4mg/kg Doxorubicin (i.p. 5x weekly); (iii) 4mg/kg Doxorubicin (i.p. 5x weekly) + 2.5mg/kg Rapamycin (i.p. 3x weekly) (iv) Vehicle control. Treatment was started at day 4 post-injection as indicated by the green arrow and growth was monitored for several weeks following treatment, as indicated on the X-axis. Panels B and C represent immunohistochemical staining for apoptotic marker, Caspase-3, and tumor vasculature, PAS staining in vehicle, Rapamycin, Doxorubicin and combination treatment at 100X and 400X magnification. Panel D shows the significant reduction in the number of vessel branch points in Rapamycin vs. Doxorubicin treatment, as determined by visual counting.

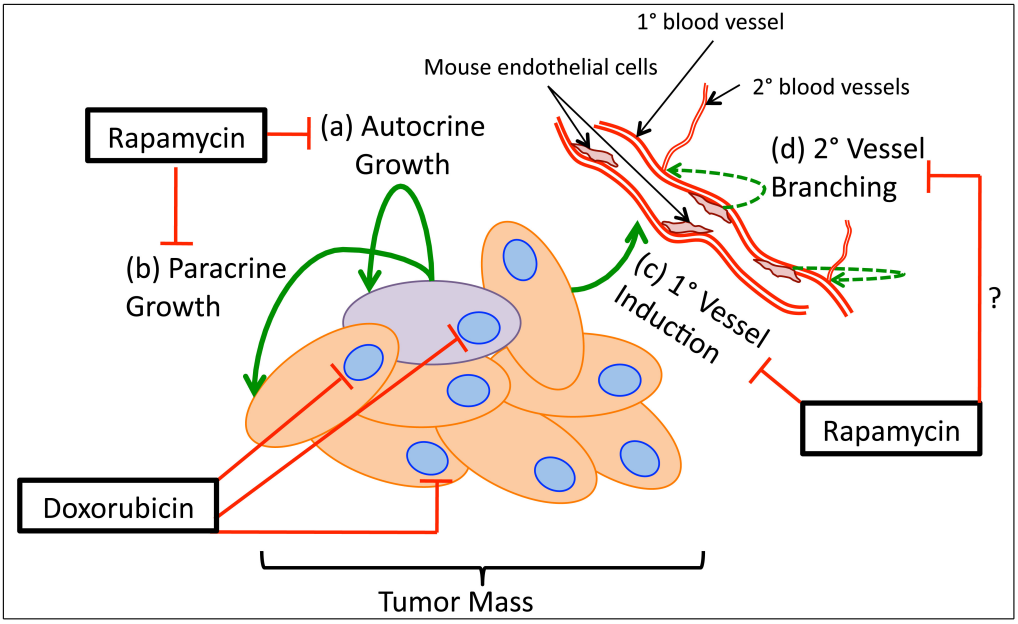

Figure IV.9: Paracrine growth factor mediated angiogenic model of KS

Hypothetical model for KS tumorigenesis representing the interplay between the tumor cells and surrounding vasculature. The tumor cell in purple marks a unique cell in the tumor mass secreting factors like IL-6 and VEGF that can act as autocrine and paracrine growth-inducing factors for itself and the neighboring cells (options (a) and (b)), which may or may not be KSHV-infected. Additionally, the secreted VEGF can act as an angiogenic cue to attract mouse endothelial cells to form blood vessels to supply the tumor nutrients (option (c)). Upon formation of this primary vessel, either the tumor-secreted human VEGF or mouse VEGF secreted by the vessel lining endothelial cells (option (d)) can induce vessel branching and vasculature maturation. I propose that Rapamycin can affect the production of growth-inducing factors, thus affecting all the nodes, but Doxorubicin exclusively acts on dividing cells and thus counteracts only (a) and (b).

Table IV.1: Summary of Current *in vitro* KS cell lines

Cell Line	Source	Selection	KSHV	HIV	Tumor in mice	Reference
SLK	Oral mucosal biopsy of male patient	None	No	-	Yes	Herndier et. al. AIDS 1994
KSHV-SLK	SLK cells transfected with KSHV episome	Puromycin	Yes	-	Yes	Grundoff and Ganem; JCI 2004
Primary endothelial cell KSHV	Primary bone marrow microvascular endothelial cells infected with KSHV	None	Yes	-	?	Flore et. al. Nature 1998
E1- and L1-TIVE	Tert-immortalized vein endothelial cells infected with KSHV	None	Yes	-	Yes	An et. al. JVI 2006

HUVEC-KSHV	Tert-immortalized primary vein endothelial cells infected with KSHV	Puromycin	Yes	-	No	Wang and Damania; Cancer Research 2008
KS-IMM	Biopsy from renal transplant male patient	None	Yes		Yes	Albini et. al. AIDS 1997
KS-TIME	Tert-immortalized dermal microvascular endothelial cells infected with KSHV	None	Yes	-	?	Lagunoff et. al. JVI 2002
mECK36	Mouse bone marrow endothelial cell transfect-ed with KSHV-BAC	Hygromycin	Yes	-	Yes	Mutlu et. al. Cancer Cell 2007

Table IV.2: mTOR-PI3K Inhibitors against KS-like Cell lines

Drug	Molecular Target	Clinical Use	IC50 Values	
			L1T2	SLK
Ascomycin (Asc)	FK506 derivative	Autoimmune and skin diseases	435 nM	87 nM
Cyclosporin A (CsA)	Calcineurin inhibitor	Transplant immunosuppressant	-	-
Doxorubicin (Dox)	Genotoxic agent	Chemotherapeutic	790 nM	398 nM
Everolimus (RAD-001)	Rapamycin derivative	Advanced Kidney Cancer	-	1.7 nM
LY42009	PI3K inhibitor	-	-	-
Pimecrolimus (Pimecro)	FK506 derivative	Atopic dermatitis	-	2.08 nM

Sirolimus (Rapamycin)	mTORC1 inhibitor	Immunosuppressant in renal transplant	7.19 nM	214 nM
Tacrolimus (FK506)	Calcineurin inhibitor	Transplant immunosuppressant	748 nM	365 nM
Temsirolimus (CCl-779)	Rapamycin derivative	Renal Cell Carcinoma	-	570 nM

REFERENCES

Abend, J.R., Uldrick, T., and Ziegelbauer, J.M. (2010). Regulation of tumor necrosis factor-like weak inducer of apoptosis receptor protein (TWEAKR) expression by Kaposi's sarcoma-associated herpesvirus microRNA prevents TWEAK-induced apoptosis and inflammatory cytokine expression. J Virol *84*, 12139-12151.

An, F.Q., Compitello, N., Horwitz, E., Sramkoski, M., Knudsen, E.S., and Renne, R. (2005). The latency-associated nuclear antigen of Kaposi's sarcoma-associated herpesvirus modulates cellular gene expression and protects lymphoid cells from p16 INK4A-induced cell cycle arrest. J Biol Chem *280*, 3862-3874.

An, F.Q., Folarin, H.M., Compitello, N., Roth, J., Gerson, S.L., McCrae, K.R., Fakhari, F.D., Dittmer, D.P., and Renne, R. (2006). Long-Term-Infected Telomerase-Immortalized Endothelial Cells: a Model for Kaposi's Sarcoma-Associated Herpesvirus Latency In Vitro and In Vivo. J Virol *80*, 4833-4846.

Arvanitakis, L., Geras-Raaka, E., Varma, A., Gershengorn, M.C., and Cesarman, E. (1997). Human herpesvirus KSHV encodes a constitutively active G-protein-coupled receptor linked to cell proliferation. Nature *385*, 347-350.

Bais, C., Santomasso, B., Coso, O., Arvanitakis, L., Raaka, E.G., Gutkind, J.S., Asch, A.S., Cesarman, E., Gershengorn, M.C., Mesri, E.A.*, et al.* (1998). G-protein-coupled receptor of Kaposi's sarcoma-associated herpesvirus is a viral oncogene and angiogenesis activator [see comments] [published erratum appears in Nature 1998 Mar 12;392(6672):210]. Nature *391*, 86-89.

Baker, H., Sidorowicz, A., Sehgal, S.N., and Vezina, C. (1978). Rapamycin (AY-22,989), a new antifungal antibiotic. III. In vitro and in vivo evaluation. J Antibiot (Tokyo) *31*, 539-545.

Ballestas, M.E., Chatis, P.A., and Kaye, K.M. (1999). Efficient persistence of extrachromosomal KSHV DNA mediated by latency- associated nuclear antigen. Science *284*, 641-644.

Bhatt, A.P., Bhende, P.M., Sin, S.H., Roy, D., Dittmer, D.P., and Damania, B. (2010). Dual inhibition of PI3K and mTOR inhibits autocrine and paracrine proliferative loops in PI3K/Akt/mTOR-addicted lymphomas. Blood *115*, 4455-4463.

Cesarman, E., Chang, Y., Moore, P.S., Said, J.W., and Knowles, D.M. (1995). Kaposi's sarcoma-associated herpesvirus-like DNA sequences in AIDS-related body-cavity-based lymphomas. N Engl J Med *332*, 1186-1191.

Cesarman, E., Nador, R.G., Bai, F., Bohenzky, R.A., Russo, J.J., Moore, P.S., Chang, Y., and Knowles, D.M. (1996). Kaposi's sarcoma-associated herpesvirus contains G protein-coupled receptor and cyclin D homologs which are expressed in Kaposi's sarcoma and malignant lymphoma. J Virol *70*, 8218-8223.

Chang, Y., Cesarman, E., Pessin, M.S., Lee, F., Culpepper, J., Knowles, D.M., and Moore, P.S. (1994). Identification of herpesvirus-like DNA sequences in AIDS-associated Kaposi's sarcoma. Science *266*, 1865-1869.

Chen, W., Hilton, I.B., Staudt, M.R., Burd, C.E., and Dittmer, D.P. (2010). Distinct p53, p53:LANA, and LANA complexes in Kaposi's Sarcoma--associated Herpesvirus Lymphomas. J Virol *84*, 3898-3908.

Damania, B. (2004). Oncogenic gamma-herpesviruses: comparison of viral proteins involved in tumorigenesis. Nat Rev Microbiol *2*, 656-668.

Fakhari, F.D., Jeong, J.H., Kanan, Y., and Dittmer, D.P. (2006). The latency-associated nuclear antigen of Kaposi sarcoma-associated herpesvirus induces B cell hyperplasia and lymphoma. J Clin Invest *116*, 735-742.

Flore, O., Rafii, S., Ely, S., O'Leary, J.J., Hyjek, E.M., and Cesarman, E. (1998). Transformation of primary human endothelial cells by Kaposi's sarcoma- associated herpesvirus. Nature *394*, 588-592.

Foster, D.A., and Toschi, A. (2009). Targeting mTOR with rapamycin: one dose does not fit all. Cell Cycle *8*, 1026-1029.

Friborg, J., Jr., Kong, W., Hottiger, M.O., and Nabel, G.J. (1999). p53 inhibition by the LANA protein of KSHV protects against cell death. Nature *402*, 889-894.

Ganem, D. (2010). KSHV and the pathogenesis of Kaposi sarcoma: listening to human biology and medicine. J Clin Invest *120*, 939-949.

Gilbert, L.A., and Hemann, M.T. (2010). DNA damage-mediated induction of a chemoresistant niche. Cell *143*, 355-366.

Gottwein, E., Mukherjee, N., Sachse, C., Frenzel, C., Majoros, W.H., Chi, J.T., Braich, R., Manoharan, M., Soutschek, J., Ohler, U.*, et al.* (2007). A viral microRNA functions as an orthologue of cellular miR-155. Nature *450*, 1096-1099.

Grundhoff, A., and Ganem, D. (2004). Inefficient establishment of KSHV latency suggests an additional role for continued lytic replication in Kaposi sarcoma pathogenesis. J Clin Invest *113*, 124-136.

Guasparri, I., Keller, S.A., and Cesarman, E. (2004). KSHV vFLIP is essential for the survival of infected lymphoma cells. J Exp Med *199*, 993-1003.

Hansen, A., Henderson, S., Lagos, D., Nikitenko, L., Coulter, E., Roberts, S., Gratrix, F., Plaisance, K., Renne, R., Bower, M.*, et al.* (2010). KSHV-encoded miRNAs target MAF to induce endothelial cell reprogramming. Genes Dev *24*, 195-205.

Herndier, B.G., Werner, A., Arnstein, P., Abbey, N.W., Demartis, F., Cohen, R.L., Shuman, M.A., and Levy, J.A. (1994). Characterization of a human Kaposi's sarcoma cell line that induces angiogenic tumors in animals. Aids *8*, 575-581.

Kaposi, M. (1872). Idiopathisches multiples Pigmentsarkom der Haut. Arch Dermatol Syph *4*, 265–273.

Kedes, D., H. , Lagunoff, M., Renne, R., and Ganem, D. (1997). Identification of the gene encoding the major latency-associated nuclear antigen of the Kaposi's sarcoma-associated herpesvirus. Journal of Clinical Investigation *100*, 2606-2610.

Kino, T., Hatanaka, H., Miyata, S., Inamura, N., Nishiyama, M., Yajima, T., Goto, T., Okuhara, M., Kohsaka, M., Aoki, H.*, et al.* (1987). FK-506, a novel immunosuppressant isolated from a Streptomyces. II. Immunosuppressive effect of FK-506 in vitro. J Antibiot (Tokyo) *40*, 1256-1265.

Lagunoff, M., Bechtel, J., Venetsanakos, E., Roy, A.M., Abbey, N., Herndier, B., McMahon, M., and Ganem, D. (2002). De novo infection and serial transmission of Kaposi's sarcoma-associated herpesvirus in cultured endothelial cells. J Virol *76*, 2440-2448.

Laman, H., Coverley, D., Krude, T., Laskey, R., and Jones, N. (2001). Viral cyclin-cyclin-dependent kinase 6 complexes initiate nuclear DNA replication. Mol Cell Biol *21*, 624-635.

Lei, X., Bai, Z., Ye, F., Xie, J., Kim, C.G., Huang, Y., and Gao, S.J. (2010). Regulation of NF-kappaB inhibitor IkappaBalpha and viral replication by a KSHV microRNA. Nat Cell Biol *12*, 193-199.

Lu, F., Stedman, W., Yousef, M., Renne, R., and Lieberman, P.M. (2010). Epigenetic regulation of Kaposi's sarcoma-associated herpesvirus latency by virus-encoded microRNAs that target Rta and the cellular Rbl2-DNMT pathway. J Virol *84*, 2697-2706.

Molden, J., Chang, Y., You, Y., Moore, P.S., and Goldsmith, M.A. (1997). A Kaposi's sarcoma-associated herpesvirus-encoded cytokine homolog (vIL- 6) activates signaling through the shared gp130 receptor subunit. J Biol Chem *272*, 19625-19631.

Montaner, S. (2007). Akt/TSC/mTOR activation by the KSHV G protein-coupled receptor: emerging insights into the molecular oncogenesis and treatment of Kaposi's sarcoma. Cell Cycle *6*, 438-443.

Nicholas, J., Ruvolo, V.R., Burns, W.H., Sandford, G., Wan, X., Ciufo, D., Hendrickson, S.B., Guo, H.G., Hayward, G.S., and Reitz, M.S. (1997). Kaposi's sarcoma-associated human herpesvirus-8 encodes homologues of macrophage inflammatory protein-1 and interleukin-6. Nat Med *3*, 287-292.

Sabatini, D.M. (2006). mTOR and cancer: insights into a complex relationship. Nat Rev Cancer *6*, 729-734.

Sarek, G., Kurki, S., Enback, J., Iotzova, G., Haas, J., Laakkonen, P., Laiho, M., and Ojala, P.M. (2007). Reactivation of the p53 pathway as a treatment modality for KSHV-induced lymphomas. J Clin Invest *117*, 1019-1028.

Sin, S.H., Roy, D., Wang, L., Staudt, M.R., Fakhari, F.D., Patel, D.D., Henry, D., Harrington, W.J., Jr., Damania, B.A., and Dittmer, D.P. (2007). Rapamycin is efficacious against primary effusion lymphoma (PEL) cell lines in vivo by inhibiting autocrine signaling. Blood *109*, 2165-2173.

Skalsky, R.L., Samols, M.A., Plaisance, K.B., Boss, I.W., Riva, A., Lopez, M.C., Baker, H.V., and Renne, R. (2007). Kaposi's Sarcoma-associated Herpesvirus Encodes an Ortholog of miR-155. J Virol.

Sodhi, A., Montaner, S., Patel, V., Zohar, M., Bais, C., Mesri, E.A., and Gutkind, J.S. (2000). The Kaposi's sarcoma-associated herpes virus G protein-coupled receptor up-regulates vascular endothelial growth factor expression and secretion through mitogen-

activated protein kinase and p38 pathways acting on hypoxia-inducible factor 1alpha. Cancer Res *60*, 4873-4880.

Stallone, G., Schena, A., Infante, B., Di Paolo, S., Loverre, A., Maggio, G., Ranieri, E., Gesualdo, L., Schena, F.P., and Grandaliano, G. (2005). Sirolimus for Kaposi's sarcoma in renal-transplant recipients. N Engl J Med *352*, 1317-1323.

Staudt, M.R., Kanan, Y., Jeong, J.H., Papin, J.F., Hines-Boykin, R., and Dittmer, D.P. (2004). The tumor microenvironment controls primary effusion lymphoma growth in vivo. Cancer Res *64*, 4790-4799.

Uddin, S., Hussain, A.R., Al-Hussein, K.A., Manogaran, P.S., Wickrema, A., Gutierrez, M.I., and Bhatia, K.G. (2005). Inhibition of phosphatidylinositol 3'-kinase/AKT signaling promotes apoptosis of primary effusion lymphoma cells. Clin Cancer Res *11*, 3102-3108.

Vivanco, I., and Sawyers, C.L. (2002). The phosphatidylinositol 3-Kinase AKT pathway in human cancer. Nat Rev Cancer *2*, 489-501.

Wan, X., Wang, H., and Nicholas, J. (1999). Human herpesvirus 8 interleukin-6 (vIL-6) signals through gp130 but has structural and receptor-binding properties distinct from those of human IL-6. J Virol *73*, 8268-8278.

Wang, L., and Damania, B. (2008). Kaposi's sarcoma-associated herpesvirus confers a survival advantage to endothelial cells. Cancer Res *68*, 4640-4648.

CHAPTER V

DISCUSSION

mTOR is dysregulated in a vast majority of cancers. Thus, there is an increasing advent in the discovery and use of anti-mTOR therapeutics in both solid cancers as well as lymphomas, and viral-associated cancers are no exception (Reviewed in (Cloughesy et al., 2008; Hay, 2005; Johnston et al., 2010; Sabatini, 2006; Sawyers, 2003). In the context of KSHV-infected B- and endothelial lineage cancers, treatment with Rapamycin, the primary mTOR inhibitor, results in growth inhibition. It was further noted that both PEL cells and KS biopsies post-translationally inactivate PTEN. This was evidenced by phosphorylation of the PTEN protein. This results in addiction to the mTOR pathway in the presence of genetically wild type PTEN and provides a favorable background for the use of pharmacological agents targeting this signaling cascade (interestingly other tumor suppressor genes p53, Rb, p16Ink4 that were investigated in these tumors also retained wild-type sequence and protein expression). Using the Affymetrix 6.0 SNP array, a tight correlation was shown between EBV-infection and the extent of genomic alterations in PEL. EBV co-infected PEL exhibited substantially fewer gross genomic alterations compared to EBV negative PEL. Additionally, deletions were detected in three common

fragile site tumor suppressor genes (WWOX, FHIT, GRID2) in PEL that warrant further investigation. These laboratory data translated into an AIDS-Malignancy Consortium (AMC) clinical trial to conclude that Rapamycin is well tolerated by AIDS patients. Molecular analysis determined that treatment with Rapamycin resulted in a marked reduction of S6 phosphorylation at late times (> 50 days) in the patients. These data suggest that mTOR inhibitors may constitute viable therapeutics for both transplant- and AIDS- associated KS.

PTEN in PEL and KS

Various cellular and viral proteins have been shown to stimulate the PI3K-Akt-mTOR signaling cascade in KSHV-infected cells (Damania, 2004; Montaner, 2007; Sodhi et al., 2004; Tomlinson and Damania, 2004). Addiction to the PI3K-mTOR signaling cascade is often accompanied with loss of major tumor suppressor PTEN: the most commonly deleted tumor suppressor that negatively regulates the PI3K signaling cascade (Cully et al., 2006; Neshat et al., 2001). In Roy and Dittmer, it was reported that PTEN is genetically intact in PEL. There was detectable mRNA and protein present in all of the tested cell lines. In addition to total, phosphorylated PTEN, specifically at residue S380, was detected. Previous biochemical reports in the literature had shown that upon phosphorylation at S380, PTEN undergoes a conformational change that renders it functionally inactive (Tamguney and Stokoe, 2007). Assessment of the PI3K signaling cascade in primary KS biopsies showed the presence of total and phospho-PTEN along with phosphorylated Akt (indicative of activated PI3K). This led to the hypothesis that unlike other Rapamycin-sensitive solid tumors (Cloughesy et al., 2008), PTEN is post-translationally silenced in PEL and KS.

The identity of the kinase that phosphorylates PTEN resulting in its inactivation in PEL and KS is not yet known. Although currently there is no experimental evidence, a viral kinase can be speculated to be responsible for phosphorylating PTEN. Considering that overexpression of PTEN in latently infected B-cells resulted in growth inhibition, suggesting that latent genes are not involved in phosphorylating and therefore silencing PTEN. It can further be speculated that upon *de novo* infection, viral lytic genes like K1 and vGPCR can activate PI3K while the hypothetical viral lytic kinase inactivates PTEN concomitantly, resulting in a hyperactive PI3K-mTOR signaling cascade. This scenario presents an almost ideal setup for initiation of tumorigenesis. Initially, the virus hijacks the cellular signaling cascade with virally encoded gene products to initiate an autocrine growth loop which continues to sustain cellular products like IL6, IL10 and VEGF, even after the virus goes into hiding and establishing latency. Data from our lab and others have shown that treatment with Rapamycin results in reduced expression of the above-mentioned pro-growth factors not only in KSHV-associated cancers but in other tumor types as well, further supporting our speculation.

It can also be hypothesized that the virus does not directly phosphorylate PTEN, but simply upregulates a specific cellular kinase capable of phosphorylating PTEN. Presently, there is a limited number of cellular kinases implicated in phosphorylating PTEN. These include Glycogen Synthase Kinase (GSK)-3β, Caesin Kinase 2 (CK2), Glioma Tumor Suppressor Candidate Region 2 (GLTSCR2), also known as PICT1, and RhoA-associated Kinase (ROCK)(Tamguney and Stokoe, 2007). Review of the KSHV literature indicates that the latency protein LANA is capable of binding and sequestering GSK3β in the nucleus to disrupt β-catenin regulation (Fujimuro and Hayward, 2003).

However, another report showed that while LANA could interact with GSK-3β but could not modulate its function (Hagen, 2009). Thus further studies need to be conducted to shed light on the PTEN-GSK3β in the presence of LANA in the infected cell. Currently, there are no known reports linking CK2, PICT1 and ROCK to KSHV, either in its lytic or latent state, which leaves a wide avenue for further studies to be conducted to identify potential kinases capable of silencing PTEN.

The presence of a genetically normal PTEN provides a mode for therapeutic intervention analogous to activation of p53 by the small molecule Nutlin (Sarek et al., 2007). It can be speculated that PTEN-expressing tumors that show dependence on mTOR signaling can not only be targeted with mTOR inhibitors, but also PTEN activating molecules that may be developed in the future.

Genomics of PEL

Much is known about the viral transcription program in PEL cells, but to date there are no comprehensive studies looking at alterations in the host genome in PEL. Using the Affymetrix 6.0 SNP array in Roy et. al. the first genome-wide study of all available PEL cell lines was reported. Two tumor suppressor genes were identified that map to two individual common fragile sites of the genome: FHIT and WWOX to chromosomes 3p and 16q respectively (Smith et al., 2007). Further, a relatively concise list of genes was shown to be altered in the majority (~90%) of all PEL lines. In addition to the two fragile site genes, amplifications were noted in six other genes: DERL1, ETV1, RASA4, TPK1, TRIM56 and VPS41. To our knowledge, thus far, none of these cellular genes have been studied in terms of a potential role in KSHV pathogenesis.

However, the tumor suppressor roles of WWOX and FHIT have been documented in various tumors, both of solid and lymphatic origin.(Aqeilan et al., 2007; Fujishita et al., 2004; Ludes-Meyers et al., 2007) The non-fragile site genes encompass a RAS related protein (RASA4), a transcription factor (ETV1) and an ER-associated factor involved in regulation of misfolded proteins (DERL1), all of which could be hypothesized to promote tumorigenesis. Among these, DERL1 has been shown to be involved in human Cytomegalovirus (HCMV)-mediated deregulation of the immune system. Thus, majority of the genes identified using bioinformatics present to be interesting candidates for further analysis. Determining a genomic signature profile provides us with greater prognostic power for PEL. Investigating the interplay of these genes with KSHV could provide insight not only into PEL, but KSHV pathogenesis in general.

Despite the long-standing knowledge of association of EBV with PEL, the exact role EBV plays in the viral oncogenesis process remains to be elucidated. Both EBV-positive and -negative PEL grow equally well in culture and xenograft but upon losing the EBV genome, the once EBV-positive cells are unable to proliferate (Mack and Sugden, 2008). In Roy et. al. it was reported that the presence of EBV correlates with reduced chromosomal aberrations. Compared to the EBV-positive population, EBV-negative PEL showed a significantly greater number of amplifications genome-wide. In addition to identifying genes dsyregulated in the majority of PEL, genes specifically altered in EBV-negative PEL were also identified. GRID2 is another common fragile site gene that was deleted, but exclusively in EBV-negative PEL. However, unlike FHIT and WWOX, the association of GRID2 to cancer is not well established. There were 22 other genes that were either amplified or deleted exclusively in EBV-negative PEL ($q \leq 0.001$).

A fair number of transcription factors were included in the list. This would be expected, given the level of regulation amplification or deletion of a single transcription factor provides. Given the role NFκB plays in KSHV-mediated pathogenesis (Brinkmann et al., 2003; Guasparri et al., 2004), it was very exciting to note that NFκB activator, IKBKB, was one of the genes amplified. Known tumor suppressor-like BRCA1 was shown to be deleted and oncogene-like RAF1 amplified in EBV-negative PEL. Other genes included those involved in cell adhesion and the cytoskeleton, metabolism and immunity, all of which could be potential candidates involved in KSHV-mediated tumorigenesis. This led to the hypothesis that in the absence of 'helper' oncogenic cues from EBV, host cells acquire additional genetic mutations that are selected for during the course of KSHV pathogenesis.

Inhibition of mTOR in KS

In chapter 3 I showed that Rapamycin is effective in growth arresting KS-like cells *in vitro* and in our xenograft model. Immunohistochemical analysis showed the presence of spindle cells, verifying their KS-like phenotype. Reduced levels of phospho-S6 (S235/236) protein indicated that Rapamycin was able to target mTOR activity efficiently. The reduction of VEGF levels observed in culture translated into defective tumor vasculature *in vivo*. Previous reports in the literature have shown that treatment with the immunosuppressant Cyclosporin A results in larger, more invasive tumors that express increased VEGF and associated angiogenesis (Guba et al., 2002). Additionally, unpublished data from our lab has shown in the context of KSHV-infected cells, treatment of xenograft PEL tumors with Cyclosporin A resulted in increased tumor volume (Sin and Dittmer, unpublished data). Treatment with Rapamycin did not affect

the overall level of apoptosis in the tumor mass, as would be expected of a cytostatic drug.

Further, it was explored whether treatment with Rapamycin was inhibiting the mTOR pathway while hyper-activating a different proliferative signaling cascade. Flow cytometry-based analysis was used for cells in culture treated with Rapamycin looking at the PI3K-Akt, MAP Kinase and NKκB signaling pathways. As expected, lower levels of phosphorylated Akt and S6 ribosomal protein (S235/236) was detected with Rapamycin treatment but no compensatory upregulation was observed for any of the other pro-proliferative signaling cascades as mentioned above (data not shown).

In addition to Rapamycin, I also looked at FK506, another common immuno-suppressant. Treatment of xenograft tumors with FK506 resulted in aggravated larger tumors instead of regression. This was particularly interestingly since both Rapamycin and FK506 share a common intermediate binding partner, FKBP12, but they target different pathways. While Rapamycin:FKBP12 target mTORC1, FK506:FKBP12 is a Calcineurin inhibitor like CyclosporinA, which also results in an aggravated tumor phenotype. This suggested that Calcineurin inhibitors are excellent immunosuppressants but, unlike mTOR inhibitors, do not show anti-tumor activity against KSHV-mediated cancers.

Lastly, the effect of Doxorubicin, a genotoxic agent, on tumor growth was assessed. Doxorubicin is a popular chemotherapeutic agent and the recommended first line therapy for KS that functions by invoking the DNA damage response to induce p53-mediated apoptosis. This is a particularly viable therapy for cancers like KS that harbor

wild type p53 functionally inactivated by viral proteins. Using the newly developed L1T2 cell line, it was shown that Doxorubicin was partially effective in reducing tumor volume. More interestingly, addition of Rapamycin to Doxorubicin elicited better anti-tumoigenic response than Doxorubicin alone, but a weaker response compared to Rapamycin alone. Immunohistochemical analysis showed that the combination therapy had a more Rapamycin-like (immature tumor vasculature, minimal apoptosis) rather than Doxorubicin-like (stable vasculature, high level of apoptosis) staining pattern.

These data led us to hypothesize that KS tumorigenesis is greatly fueled by the presence of an optimal tumor microenvironment. Hence, agents targeted towards disrupting the tumor niche would constitute a more effective therapeutic option rather than targeting the proliferation of tumor cells. Clinically though, the majority of tumors show relapse, whether they were treated with genotoxic agents or signaling inhibitors. Thus, the ideal therapeutic approach would be to cycle the two classes of drug, cytotoxic and cytostatic, to eliminate both actively replicating and residual tumor cells.

Rapamycin against AIDS-KS

In conjunction with the AIDS-Malignancy Consortium (AMC), a pilot clinical trial was conducted looking into evaluating the potential for using Rapamycin (Sirolimus®) as a therapeutic against systemic AIDS-associated KS. Seven patients: 3 on NNRTI- and 4 on Ritonavir-boosted PI-based Highly Active Anti-Retroviral Therapy (HAART) who had controlled AIDS with relatively high CD4 counts and undetectable HIV viral loads were enrolled in the study. Given that administration of Rapamycin is a well-documented concern in the clinic, oral dosing of Sirolimus® was determined

empirically for the individual patients as noted in table V.1. One of the primary goals of the study was to determine the tolerance of Rapamycin, a systemic immunosuppressant in the HIV-positive setting. The study showed very promising data that Sirolimus® was well tolerated in the patients and did not pose deleterious adverse effects. Given that Rapamycin is metabolized by the CYP450 hepatic enzyme system, which is inhibited by PIs, specifically Ritonavir, (Walubo, 2007), a much lower dose of Sirolimus® was required to achieve drug trough levels in patients on a PI regimen. Although patients on NNRTI required much higher (up to a maximum of 200-fold greater) doses of the drug Sirolimus®, it was very well tolerated. There were no significant changes in CD4 counts or HIV viral loads, indicating that treatment with Sirolimus® did not adversely impact their AIDS.

With regards to therapeutic outcome, all the patients exhibited either partial response or stable disease. Interestingly, all 3 patients with partial response were on PI-based therapy. Reports in the literature have suggested direct anti-cancer effects of PIs (Pajonk et al., 2002; Sgadari et al., 2002) It was specifically shown by Maggiorella et al. that Ritonavir increased sensitivity of head and neck cancer to ionizing radiation that could translate into a better clinical outcome (Maggiorella et al., 2005). Further experiments are required to delineate whether the partial response seen in the PI sub-group is due to off-target, anti-tumor effects of PI or increased bioavailability of Rapamycin resulting from PI-mediated inhibition of CYP450.

Finally, looking at the molecular signature of Rapamycin treatment of AIDS patients revealed some interesting points. Phosphorylation of S6 ribosomal protein at Serine 235/236 is used as a robust indicator of mTOR activity. There was a range of

staining that was detected at the baseline in the different patients. However, over the course of the treatment there was a reduction in levels of phospho-S6R (S235/236) both within the tumor cells and within skin epithelial cells. Given that Rapamycin only inhibits the mTOR Complex 1, there has been speculation whether Rapamycin treatment results in upregulation of mTOR Complex 2 that constitutes a feedback loop and hyperactivates Akt. Using phospho-Akt (T308) and phospho-Akt (S473) as markers for PI3K and mTORC2 activity, it was shown that no such hyperactivation of Akt was present in these biopsies. While there were changes in IL-6 and VEGF upon Rapamycin treatment in culture, no such changes were detected at the systemic level. Last but not least, no significant changes were detected in KSHV viral loads of patients on Sirolimus®.

Overall, the AMC study showed that mTOR inhibition can be a viable therapeutic in AIDS- associated KS. AIDS-associated KS required higher doses of Rapamycin to reach the same drug trough levels (5-10ng/ml) (Stallone et al., 2005) compared to transplant-associated KS. However, it was well tolerated in HIV-positive patients on HAART and did not shown any dose-limiting toxicity warranting future, larger studies.

Table V.1: Summary of AMC 051 Rapamycin Trial against AIDS-KS

Patient	ART Regimen	Best Response	Duration (months)	Peak Rapamycin Level (ng/mL)
001	PI/r	Partial Response	10+	172
002	PI/r	Partial Response	9+	64.4
003	PI/r	Stable	4	16.8
005	PI/r	Partial Response	8.5+	19.2
004	NNRTI	Progression	-	13.1
006	NNRTI	Stable	3+	7.4
007	NNRTI	Stable	3	11.9

REFERENCES

Aqeilan, R.I., Trapasso, F., Hussain, S., Costinean, S., Marshall, D., Pekarsky, Y., Hagan, J.P., Zanesi, N., Kaou, M., Stein, G.S., *et al.* (2007). Targeted deletion of Wwox reveals a tumor suppressor function. Proc Natl Acad Sci U S A *104*, 3949-3954.

Brinkmann, M.M., Glenn, M., Rainbow, L., Kieser, A., Henke-Gendo, C., and Schulz, T.F. (2003). Activation of mitogen-activated protein kinase and NF-kappaB pathways by a Kaposi's sarcoma-associated herpesvirus K15 membrane protein. J Virol *77*, 9346-9358.

Cloughesy, T.F., Yoshimoto, K., Nghiemphu, P., Brown, K., Dang, J., Zhu, S., Hsueh, T., Chen, Y., Wang, W., Youngkin, D., *et al.* (2008). Antitumor activity of rapamycin in a Phase I trial for patients with recurrent PTEN-deficient glioblastoma. PLoS Med *5*, e8.

Cully, M., You, H., Levine, A.J., and Mak, T.W. (2006). Beyond PTEN mutations: the PI3K pathway as an integrator of multiple inputs during tumorigenesis. Nat Rev Cancer *6*, 184-192.

Damania, B. (2004). Modulation of Cell Signaling Pathways by Kaposi's Sarcoma-Associated Herpesvirus (KSHVHHV-8). Cell Biochem Biophys *40*, 305-322.

Fujimuro, M., and Hayward, S.D. (2003). The latency-associated nuclear antigen of Kaposi's sarcoma-associated herpesvirus manipulates the activity of glycogen synthase kinase-3beta. J Virol *77*, 8019-8030.

Fujishita, T., Doi, Y., Sonoshita, M., Hiai, H., Oshima, M., Huebner, K., Croce, C.M., and Taketo, M.M. (2004). Development of spontaneous tumours and intestinal lesions in Fhit gene knockout mice. Br J Cancer *91*, 1571-1574.

Guasparri, I., Keller, S.A., and Cesarman, E. (2004). KSHV vFLIP is essential for the survival of infected lymphoma cells. J Exp Med *199*, 993-1003.

Guba, M., von Breitenbuch, P., Steinbauer, M., Koehl, G., Flegel, S., Hornung, M., Bruns, C.J., Zuelke, C., Farkas, S., Anthuber, M., *et al.* (2002). Rapamycin inhibits primary and metastatic tumor growth by antiangiogenesis: involvement of vascular endothelial growth factor. Nat Med *8*, 128-135.

Hagen, T. (2009). Characterization of the interaction between latency-associated nuclear antigen and glycogen synthase kinase 3beta. J Virol *83*, 6312-6317.

Hay, N. (2005). The Akt-mTOR tango and its relevance to cancer. Cancer Cell *8*, 179-183.

Johnston, P.B., Yuan, R., Cavalli, F., and Witzig, T.E. (2010). Targeted therapy in lymphoma. J Hematol Oncol *3*, 45.

Ludes-Meyers, J.H., Kil, H., Nunez, M.I., Conti, C.J., Parker-Thornburg, J., Bedford, M.T., and Aldaz, C.M. (2007). WWOX hypomorphic mice display a higher incidence of B-cell lymphomas and develop testicular atrophy. Genes Chromosomes Cancer *46*, 1129-1136.

Mack, A.A., and Sugden, B. (2008). EBV is necessary for proliferation of dually infected primary effusion lymphoma cells. Cancer Res *68*, 6963-6968.

Maggiorella, L., Wen, B., Frascogna, V., Opolon, P., Bourhis, J., and Deutsch, E. (2005). Combined radiation sensitizing and anti-angiogenic effects of ionizing radiation and the protease inhibitor ritonavir in a head and neck carcinoma model. Anticancer Res *25*, 4357-4362.

Montaner, S. (2007). Akt/TSC/mTOR activation by the KSHV G protein-coupled receptor: emerging insights into the molecular oncogenesis and treatment of Kaposi's sarcoma. Cell Cycle *6*, 438-443.

Neshat, M.S., Mellinghoff, I.K., Tran, C., Stiles, B., Thomas, G., Petersen, R., Frost, P., Gibbons, J.J., Wu, H., and Sawyers, C.L. (2001). Enhanced sensitivity of PTEN-deficient tumors to inhibition of FRAP/mTOR. Proc Natl Acad Sci U S A *98*, 10314-10319.

Pajonk, F., Himmelsbach, J., Riess, K., Sommer, A., and McBride, W.H. (2002). The human immunodeficiency virus (HIV)-1 protease inhibitor saquinavir inhibits proteasome function and causes apoptosis and radiosensitization in non-HIV-associated human cancer cells. Cancer Res *62*, 5230-5235.

Sabatini, D.M. (2006). mTOR and cancer: insights into a complex relationship. Nat Rev Cancer *6*, 729-734.

Sarek, G., Kurki, S., Enback, J., Iotzova, G., Haas, J., Laakkonen, P., Laiho, M., and Ojala, P.M. (2007). Reactivation of the p53 pathway as a treatment modality for KSHV-induced lymphomas. J Clin Invest *117*, 1019-1028.

Sawyers, C.L. (2003). Will mTOR inhibitors make it as cancer drugs? Cancer Cell *4*, 343-348.

Sgadari, C., Barillari, G., Toschi, E., Carlei, D., Bacigalupo, I., Baccarini, S., Palladino, C., Leone, P., Bugarini, R., Malavasi, L.*, et al.* (2002). HIV protease inhibitors are potent anti-angiogenic molecules and promote regression of Kaposi sarcoma. Nat Med *8*, 225-232.

Smith, D.I., McAvoy, S., Zhu, Y., and Perez, D.S. (2007). Large common fragile site genes and cancer. Semin Cancer Biol *17*, 31-41.

Sodhi, A., Montaner, S., Patel, V., Gomez-Roman, J.J., Li, Y., Sausville, E.A., Sawai, E.T., and Gutkind, J.S. (2004). Akt plays a central role in sarcomagenesis induced by Kaposi's sarcoma herpesvirus-encoded G protein-coupled receptor. Proc Natl Acad Sci U S A *101*, 4821-4826.

Stallone, G., Schena, A., Infante, B., Di Paolo, S., Loverre, A., Maggio, G., Ranieri, E., Gesualdo, L., Schena, F.P., and Grandaliano, G. (2005). Sirolimus for Kaposi's sarcoma in renal-transplant recipients. N Engl J Med *352*, 1317-1323.

Tamguney, T., and Stokoe, D. (2007). New insights into PTEN. J Cell Sci *120*, 4071-4079.

Tomlinson, C.C., and Damania, B. (2004). The K1 protein of Kaposi's sarcoma-associated herpesvirus activates the Akt signaling pathway. J Virol *78*, 1918-1927.

Walubo, A. (2007). The role of cytochrome P450 in antiretroviral drug interactions. Expert Opin Drug Metab Toxicol *3*, 583-598.